REVIEW ARTICLE

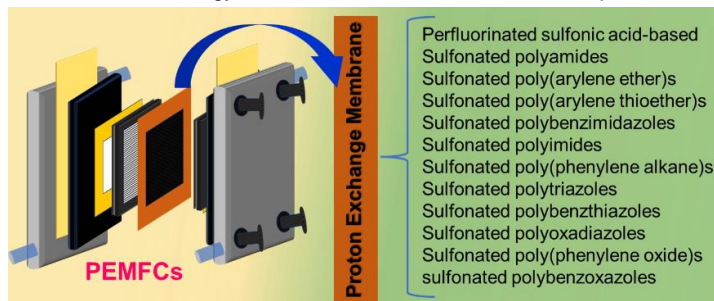# Proton Exchange Membrane Fuel Cells: A Sustainable Approach Towards Energy Generation

Bholanath Ghanti , and Susanta Banerjee *

Materials Science Centre, Indian Institute of Technology Kharagpur, Kharagpur 721302, India.
*Correspondence: susanta@matsc.iitkgp.ac.in

Abstract: Fuel cell technologies are on the verge of creating new milestones in energy conversion devices in the automobile, portable, and transportation sectors. This review article summarizes all types of fuel cells. Proton exchange membrane fuel cells (PEMFCs) have earned massive attention due to their high efficiency, light weight, rapid startup ability, low noise, and net-zero carbon emissions. The perfluorinated sulfonic acid-based membranes are the most utilized proton exchange membrane (PEM) materials; however, they have severe disadvantages. Henceforth, there is a noteworthy urge to develop alternative PEMs for PEMFC applications. The current research aims to design and develop alternative hydrocarbon-based membranes with improved properties and performance for PEMFC applications. This review starts with the essential components and the working principle of the PEMFC. Then, it explores the

recent advances in various alternative sulfonated PEM materials for PEMFC applications, highlighting their synthetic process, PEM properties, and single-cell performances. Unlike a particular PEMFC-related topics review, this literature review emphasizes a comprehensive review of recent advances in the field of various types of hydrocarbon-based alternative sulfonated PEM materials, such as sulfonated polyamides, sulfonated poly(arylene ether)s, sulfonated poly(arylene thioether)s, sulfonated polybenzimidazoles, sulfonated polyimides, sulfonated poly(phenylene alkane)s, sulfonated polytriazoles, sulfonated polybenzothiazoles, sulfonated polyoxadiazoles, etc.

Keywords: *Fuel cell, ion exchange capacity, membrane, proton exchange membrane, sulfonated, sustainable, proton conductivity.*

Contents

1. Introduction

There is a never-ending need to develop eco-friendly energy conversion and storage technologies to fulfill the overwhelming demands of global energy.[1-3] Fossil fuels such as oils, coal, and natural gases are the primary sources of global energy, contributing 84% of the total consumed global energies as of 2019.[3,4] The contribution of the different energy sources in total global energy consumption is depicted in **Figure 1a**. With the exponentially growing world population

Abbreviations

AFC: alkaline fuel cell; AEM: anion exchange membrane; AEMFC: anion exchange membrane fuel cell; CL: catalyst layer; CuAAC: Cu(I)-catalyzed azide-alkyne cycloaddition; DS: degree of sulfonation; DMFC: direct methanol fuel cell; DPP: diphenyl phosphite; EV: electrical vehicle; EW: equivalent weight; FC: fuel cell; GDL: gas-diffusive layer; GHG: greenhouse gas; GPC: gel permeation chromatography; HOR: hydrogen oxidation reaction; ICE: internal combustion engine; IEC: ion exchange capacity; MCFC: molten carbonate fuel cell; MEA: membrane electrode assembly; MOF: metal organic framework; ORR: oxygen reduction reaction; OCV: open circuit voltage; PC: proton conductivity; PDI: polydispersity index; PEM: proton exchange membrane; PEMFC: proton exchange membrane fuel cell; PA: phosphoric acid; PPA: polyphosphoric acid; PAFC: phosphoric acid fuel cell; PEFC: polymer electrolyte membrane fuel cell; PFSA: perfluorinated sulfonic acid; PPD: peak power density; PTFE: polytetrafluoroethylene; PY: pyridine; RH: relative humidity; ROS: reactive oxygen species; RW: residual weight; SACFC: super acid-catalyzed Friedel-Craft; SOFC: solid oxide fuel cell; SPA: sulfonated polyamide; SPAE: sulfonated poly(arylene ether); SPATE: sulfonated poly(arylene thioether); SPBI: sulfonated polybenzimidazole; SPI: sulfonated polyimide; SPPA: sulfonated poly(phenylene alkane); SPT: sulfonated polytriazole; SPBT: sulfonated polybenzthiazole; SPOD: sulfonated polyoxadiazole; SR: swelling ratio; TPP: triphenyl phosphite; WU: water uptake.

and industrialization, the rapid consumption of natural fossil fuels has led to the emission of harmful greenhouse gases
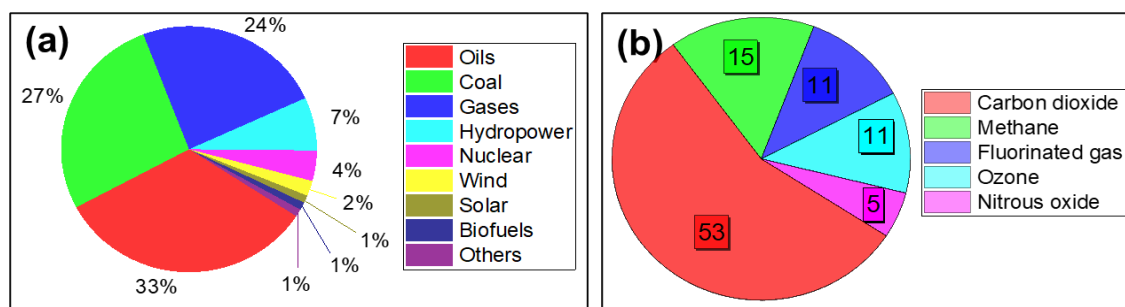
Figure 1. (a) Contribution of various energy sources in total global energy consumption,[3] and (b) Contribution of the different GHGs in global warming.[15]

(GHGs), including CO_x, SO_x, and NO_x, which play an important role in global warming, air pollution, and climate change.[5-8] Carbon dioxide (CO_2) emissions have increased by more than 40% since the Industrial Revolution.[9,10] In this decade, the rate of CO_2 emissions on the planet is 50 billion tons per year.[11,12] Since 1880, the rate of global warming increase was 0.08 ℃ per decade, but recently, it has been 0.18 ℃ per decade.[13] The Intergovernmental Panel on Climate Change (IPCC) reported that the global temperature has climbed by 1.5 °C since the Industrial Revolution.[14] So, the CO_2 emissions rate must be reduced before reaching the 2 °C mark this decade. The global warming caused by the various GHGs is shown in **Figure 1b**.[15] Thus, it is mandatory to focus on alternative renewable and sustainable energy production technology due to the high price, detrimental environmental impacts, and depletable nature of fossil fuel resources.[16-18]

Therefore, an alternative power generation source is essential to fulfill the global energy demand and solve the energy crisis issues, which causes less environmental pollution and has high efficiency and power supply capacity. Over time, internal combustion engines (ICEs) have been considered the most popular energy conversion technology in all sectors, from transportation to power suppliers.[19] However, the ICEs also have various disadvantages, such as the emission of GHGs, relatively low energy conversion efficiency, high noise, and usage of non-renewable fuels for energy conversions.[20-22] So, it is noteworthy to develop alternative green, sustainable, and renewable energy conversion technology to safeguard our society and environment by fulfilling the overwhelming social, industrial, and economic demands. In this direction, the most utilized sustainable and renewable energy conversion technologies are wind power, solar energy, biofuel, hydrothermal, geothermal, and many more.[23,24] These types of energy sources efficiently produce energy with net zero air pollution and GHGs emissions.[24,25] In the 21st century, renewable and sustainable energy production technologies have gained remarkable attention as a mainstream contributor owing to their reliability, affordability, and sustainability, but most of these technologies are in the developing stage.[24,26,27] Among these renewable and sustainable energy production technologies, fuel cell (FC) is the most demanding and promising because of its high efficiency, silent nature, rapid start-up abilities, and net-zero carbon emission.[28-31] FC technology has achieved notable interest in energy conversion technology to serve future energy demands sustainably.

This review article provides a brief history and recent advancements in FC technology. The different types of FCs and their essential components, efficiency, limitations, and applicability are discussed. This review article emphasized the working principle, essential components, basic requirements, and commercially available proton exchange membrane (PEM) materials and mainly focused on the recent developments and endeavors in the field of alternative sulfonated proton exchange membrane fuel cells (PEMFCs), precisely, the synthesis, characterization, PEM properties, and single fuel cell applications of the recently developed hydrocarbon-based alternative sulfonated copolymer backbones [polyamides, poly(arylene ether)s, poly(arylene thioether)s, polybenzimidazoles, polyimides, poly(phenylene alkane)s, polytriazoles, polybenzothiazoles, polyoxadiazoles, etc.].

2. Fuel Cells (FCs)
2.1 Brief History

Fuel cells are electrochemical devices that directly convert the chemical energy of fuels and oxygen into electrical energy without any direct combustion reaction or emission of harmful GHGs.[32,33] It has a long history before flourishing in several applications of the current scenario. Humphry Davy laid the scientific foundation of the FC in 1801, who discovered several new metals (sodium, potassium, and alkali earth) by splitting the common compounds using a voltaic pile electrolysis.[32,34] Then, it was first designed by Christian Friedrich Schönbein in 1838.[32,35] In 1839, Sir William Robert Grove generated electricity for the first time by the electrochemical reaction between hydrogen (H_2) and oxygen (O_2) in a gas voltaic battery.[36-38] Then, the term "fuel cell" was
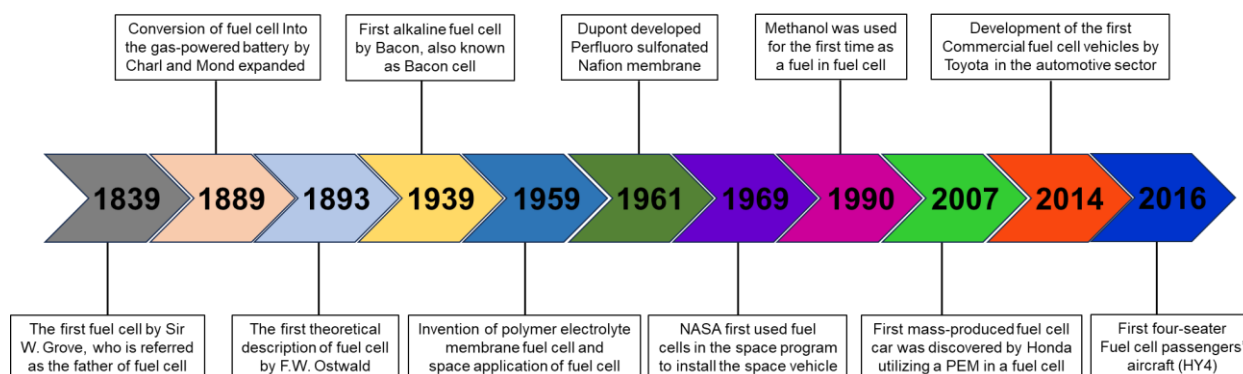

Figure 2. Chronological illustration of the significant developments in the field of FCs.[19,47]

Banerjee and Ghanti

Innov. Chem. Mater. Sustain. **2025**, 2(1), 032-073

Table 1. *Comparison of all types of FC along with their related applications.*[3,45,47,51,52]

| Characteristics	PEFCs	DMFCs	AFCs	PAFCs	MCFCs	SOFCs
Operating temperature (℃)	60-100	70-130	60-250	150-210	500-700	500-1000
Primary fuel	H_2	CH_3OH	H_2	H_2	H_2, CO, CH_4	H_2, CO, CH_4
Electrolyte	Polymer membrane	Polymer membrane	30-50% of KOH solution in water	Phosphoric acid	Molten carbonate ceramic matrix	Solid oxide ceramic matrix
Catalyst	Pt and Pt/Ru	Pt and Pt/Ru	Pt	Pt	Ni	Ni, Perovskites
Conductive ion by electrolyte	H^+/HO^-	H^+	HO^-	H^+	CO_3^{2-}	O^{2-}
Efficiency (%)	40-55	40	60-70	40-50	50-60	40-60
Production power (kW)	≤25	<10	≤20	>50	>1	>200
Advantages	Low operating temperature, small size, lightweight, rapid startup	Low operating temperature, low primary fuel cost, high power density	Less expensive, rapid startup ability, and a wide range of applications	Suitable for combined heat and power (CHP), high impurity tolerance capability	Fuel variety and high-efficiency	High efficiency, fuel flexibility, suitable for CHP and hybrid/gas turbine cycle
Disadvantages	Highly sensitive to temperature, humidity, salinity, and fuel impurities	Low reaction kinetics, the fuel gas is highly toxic and flammable	Highly sensitive to CO_2 in air and fuel gas, electrolyte management (leakage issue), and electrolyte conductivity	Expensive, high startup time, and highly sensitive to sulfur	Slow response time, low gas-crossover resistivity, and low power density	High temperature, long startup time, intensive heat, and limited number of shutdowns
Applications	Vehicles and power plants	Portable applications	Submarine and space	Power plants	Power plants	Power plants

introduced for the first time by Ludwig Mond and Charles Langer in 1889, as they used coal as a fuel and obtained a current density value of 20 A/m² at 0.73 V.[39,40] Francis T. Bacon developed the first alkaline fuel cell (AFC) in 1932, which also known as a "Bacon cell."[41] In 1959, Willard Thomas Grubb and Leonard Niedrach designed and developed the PEMFC for the first time, which was used by NASA in the Gemini space program to provide power and drinking water to the astronauts.[42,43] Then, the interest in incorporating FC in electrical vehicles (EVs) has arisen since 1970, and finally, it was commercialized in 2007.[44-46] In this scenario, worldwide research is ongoing to commercialize the FC to fulfill global energy requirements. The major developments achieved in FC history are shown in **Figure 2**. Since 2008, FC technology has been commercialized for various types of applications.[40,47,48]

2.2 Classification, Applications, Advantages, and Disadvantages

The core components of FCs are an electrolyte, an anode (negative electrode), and a cathode (positive electrode). Depending on the electrolytes and operating temperatures, FCs are classified as alkaline fuel cells (AFCs), direct methanol fuel cells (DMFCs), molten carbonate fuel cells (MCFCs), phosphoric acid fuel cells (PAFCs), polymer electrolyte fuel cells (PEFCs), and solid oxide fuel cells (SOFCs).[3,32,44,49-50] The essential characteristics (operating temperature, electrolyte, life span, efficiency, and required fuels), limitations (advantages and disadvantages), and applications of all types of FC are compiled in **Table 1**.

In light of the aforementioned overview of FCs, it can be concluded that FC technologies will benefit from fulfilling the global energy demand and the energy crisis. FCs have various applications, advantages, and disadvantages depending on the operating temperature, efficiency, and types of electrolytes; those are illustrated as a general overview in **Figure 3**.[1,3]
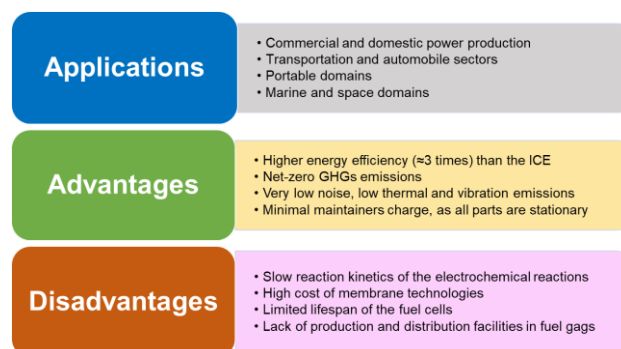
Figure 3. Vertical schematic illustration of applications, advantages, and disadvantages of fuel cell technologies.[1,3]

3. Proton Exchange Membrane Fuel Cells (PEMFCs)

3.1 Comparison and Preference

Among all types of FCs, PEFCs are the most popular, demanding, and favorable type of FC due to their high theoretical (83%) and practical (~50%) efficiencies, low processing temperature range, rapid startup capability, and minimal maintenance charge.[53,54] PEFCs are also classified as proton exchange membrane fuel cells (PEMFCs) and anion exchange membrane fuel cells (AEMFCs), depending on the
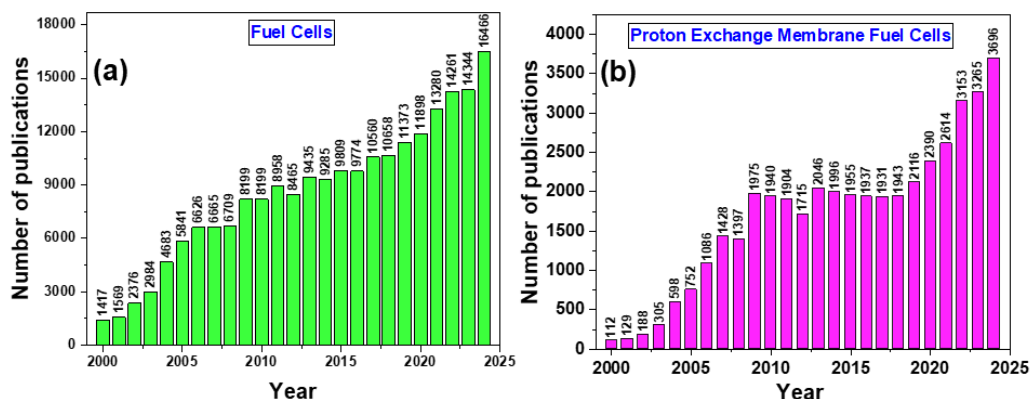
Figure 4. A figure of the year-wise number of publications in (a) FCs and (b) PEMFCs since 2000 (data obtained from Scopus by searching "Fuel Cells" and "Proton Exchange Membrane Fuel Cells").

Banerjee and Ghanti

Innov. Chem. Mater. Sustain. **2025**, 2(1), 032-073
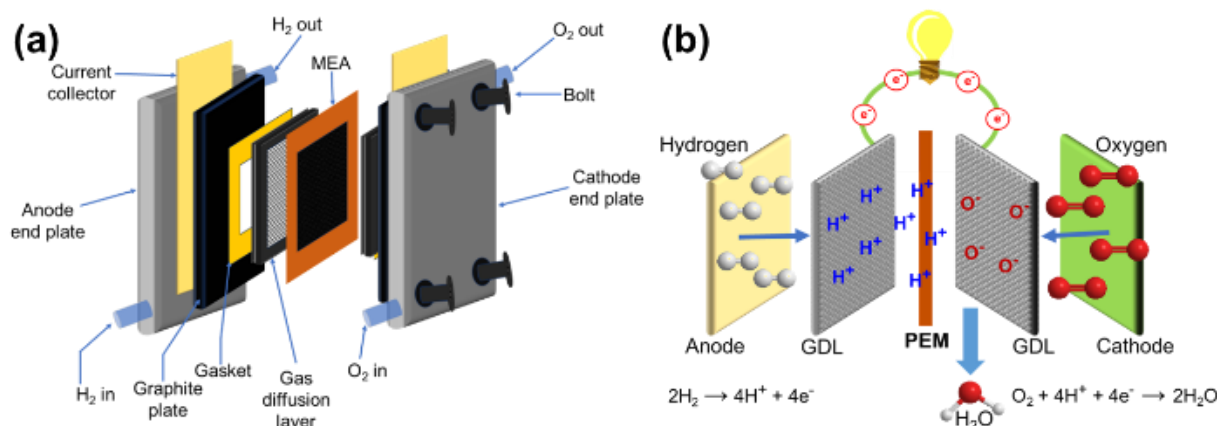
Figure 5. Schematic illustration of (a) structure and (b) working principle of PEMFCs.[81,82]

types of polymeric backbone (electrolyte).[54-57] There are some distinct differences between PEMFCs and AEMFCs. In the case of PEMFCs, the solid polymeric backbone is a cation-exchangeable negatively charged polymer backbone, whereas that of the AEMFCs is an anion-exchangeable positively charged polymeric backbone.[58-64] The basic comparison between the PEMFCs and AEMFCs is shown in **Table 2**.[58] The conductive ions are also different for PEMFCs and AEMFCs; specifically, protons (H^+ ions) are transported between the electrodes for the earlier one, in contract hydroxides (HO^- ions) are transported between the electrodes for the later one.[55] Additionally, water (H_2O) molecules are produced as a product in the cathode for PEMFCs, whereas H_2O is formed at the anode and consumed at the cathode for AEMFCs (**Table 2**).[28,55,65,66] Usually, the polymer electrolyte membranes or proton exchange membranes (PEMs) exhibited higher ionic conductivity values compared to that of the anion exchange membrane (AEM), which can be ascribed due to the intrinsic higher mobility of the protons than the hydroxide ions.[58,67] So, a high ion exchange capacity (IEC) value of the AEM is required to achieve high ionic conductivity values as exhibited by a PEM, but this may cause deterioration of the AEM's mechanical properties and dimensional stability.[58,68,69]

Table 2. *The essential components and characteristics of PEMFCs and AEMFCs.*[55,65,66]

Characteristics	PEMFCs	AEMFCs
Polymer electrolytes	Anionic polymer backbone	Cationic polymer backbone
Conductive ion	H^+	HO^-
Catalyst	Pt, Pt/C, PtCo/C, PtNi/C	Pt, PtRu, Ni alloy
Electrodes reaction	Anode: $2H_2 \rightarrow 4H^+ + 4e^-$	Anode: $2H_2 + 4HO^- \rightarrow 4H_2O + 4e^-$
	Cathode: $O_2 + 4H^+ + 4e^- \rightarrow 2H_2O$	Cathode: $O_2 + 2H_2O + 4e^- \rightarrow 4HO^-$
Availability	Readily available	Limited availability

Furthermore, AEMs may lose some of the quaternary charge-carrier sites in the AEM's backbone due to hydrolysis or elimination reactions of the hydroxide ion during the AEMFC operations that lead to the potential reduction of the IEC value and consequently, reduction in ionic conductivity value and durability of the AEMs.[58,70-73]
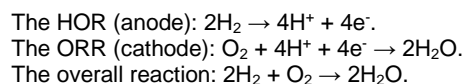
The PEMFCs gained remarkable global recognition as sustainable and renewable energy-producing sources because of their higher ionic conductivity and better durability

than the AEMFCs.[55,74-76] That is due to their high energy efficiency, rapid startup ability, low operating temperature, high power density, and net-zero environmental impacts.[19,28,77-80] A significant number of research on FCs and PEMFCs is ongoing in this decade, and the number of publications on FCs and PEMFCs since 2000 is depicted in **Figure 4**. **Figure 4b** shows that the research activity in the field of PEMFCs has increased substantially since 2022, which indicates the rapid growth of PEMFC-based research interest in sustainable and renewable energy generation.[81]

3.2 Structure and Working Principle

The schematic representation of a PEMFC is shown in **Figure 5a**. The essential components of a PEMFC are end plates, current collectors, graphite plates, gas diffusion plates/layers, gaskets, and membrane electrode assembly (MEA), respectively.[82,83] Among these, the MEA is the heart of the PEMFC, where electrochemical reactions occur.[84] The MEA comprises porous carbon papers, catalyst layers (CL), and PEM.[84-86] The porous carbon paper acts as a gas-diffusive layer (GDL), which helps to diffuse the fuel gases into the CLs.[84-86] The CL generally contains platinum on carbon (Pt/C), in which the hydrogen oxidation reaction (HOR) and oxygen reduction reaction (ORR) take place.[84-86] The PEM is the most vital component of the MEA, which acts as a semipermeable layer.[80,87,88] The PEM conducts the protons from the anode to the cathode, where the ORR occurs, and it resists the movement of electrons and fuel gases through it.[80,84-89] The PEM is sandwiched between the two electrodes and functions as a separator between them by preventing the crossover of the fuels.[80,84-90]

In PEMFCs, electricity is produced from the chemical energy of a fuel (H_2) via the electrochemical reaction with oxygen.[91] The schematic illustration of the working principle of a PEMFC is provided in **Figure 5b**. Initially, the anode's fuel gas (H_2) undergoes electrochemical oxidation in the CL's metal surface (Pt), producing H^+ ions and electrons.[91,92] Then, the PEM conducts these protons to the cathode via the Grotthuss and Vehicular mechanism.[28,55,93,94] The electrons flow towards the cathode through an external wire, producing electricity that powers external devices.[91,93] Finally, the electrochemical reduction reaction of O_2 occurs on the anode's CL in the presence of those received protons and electrons, and water is obtained as the product.[91,95] The electrochemical reactions, along with the overall reaction of the PEMFC, are shown below:

The HOR (anode): $2H_2 \rightarrow 4H^+ + 4e^-$.
The ORR (cathode): $O_2 + 4H^+ + 4e^- \rightarrow 2H_2O$.
The overall reaction: $2H_2 + O_2 \rightarrow 2H_2O$.

4. Proton Exchange Membrane (PEM)

4.1 Role and Criteria

The PEM is the most vital component of a PEMFC.[91,94,95] It functions as a positively charged-carrier solid electrolyte by blocking the crossover of the fuel gases between the electrodes in a PEMFC.[28,93-95] The PEM must possess the following characteristics for fruitful and efficient PEMFC operations.

❖ *Proton conductivity* (PC): A PEM must possess a high proton conductivity (σ) value for the facile H$^+$ ions transportation between the electrodes, reducing the internal resistance in the PEMFC.[82,96] Consequently, the PEM leads to a high efficiency and power density during the PEMFC operations.

❖ *Fuel gas resistivity*: The PEM should exhibit a high fuel resistivity for efficient PEMFC applications. If the fuel gases cross through the PEM, then this also leads to a loss of fuel and reduction of the cell voltages, and hence, the efficiency of PEMFC reduces.[82,97]

❖ *Chemical/oxidative stability*: PEMs should have high chemical or oxidative stability for long-term, durable, and efficient PEMFC applications.[82] During the real-time fuel cell operating conditions, peroxide radicals are formed due to the partial reduction of the oxygen molecules, and these reactive oxygen species (ROSs) may degrade the PEM backbone.[98,99] Therefore, the PEM should withstand a high oxidative resistance for durable and efficient PEMFC applications.

❖ *Dimensional stability*: PEMs must exhibit high dimensional stability under the PEMFC operating conditions for better water management properties and to maintain a fixed and tight interface with the CL of the MEA.[82,99]

❖ *Thermal and mechanical stabilities*: The PEM should have high thermal and mechanical stabilities to endure its durability and remain resilient during the manufacturing process of MEA.[82]

❖ *Processability and cost-effectiveness*: The PEM materials should be highly processable and cost-effective for their successful integration as a PEM in this competitive market.

4.2 Sulfonated PEMs

The PEM plays the most significant role in the proton migration process from the anode to the cathode during the PEMFC operating conditions and ensures the high power density and efficiency of the PEMFC.[3,28,45,82] The PEM usually comprises a hard hydrophobic segment and a soft hydrophilic segment[96,99,100] The hard hydrophobic part ensures its high mechanical and dimensional stabilities.[96,99,100] It also helps to form a well-segregated and interconnected hydrophobic-hydrophilic phase morphology, which is beneficial for achieving an appropriate proton conductivity value.[96,99,100] On the contrary, the hydrophilic part ensures the high proton conductivity and appropriate water absorption values of the PEM.[96,99,100] The soft hydrophilic segment of the PEM generally contains acidic functionalities or protogenic groups in the solid polymeric backbone.[101,102] The PEMs mainly contain two types of acidic groups in the PEM's backbone: sulfonic acid (-SO$_3$H) and phosphonic acid (-PO$_3$H) groups.[96,99,100,101-104] However, the sulfonic acid-containing PEMs are more employed and analyzed than the phosphonic acid-containing PEMs for the PEMFC applications.[101,102] This is mainly due to the higher acidity of the sulfonic acid-containing PEMs compared to the phosphonic acid-containing PEMs, which resulted in a higher proton conductivity value for the earlier one.[105-107] Additionally, the simplistic synthetic procedure of the sulfonic acid-containing PEMs makes them more popular and commercialized than the phosphonic acid-containing PEMs.[101,102] So, the recent studies on the sulfonic acid-containing PEMs are discussed in this review article.

4.2.1 Commercial and State-of-the-Art

The most widely used commercially available PEM material is perfluorinated sulfonic acid (PFSA) ionomer membranes, which are well-known for their outstanding ionic conductivity value and chemical and mechanical stability.[93,108-110] These PFSA-based ionomer membranes are extensively used as a solid-electrolyte separator in PEFCs and chloro-alakli electrolyzer (sodium-ion separator) since 1970.[93] The chemical structures of the commercially available PFSA-based ionomer membranes are depicted in **Figure 6**.[93,110] Generally, these PFSA-based ionomers are classified based on their equivalent weights (EW; grams of polymers per ionic group) and the side-chain length (**Figure 6**).[93,110] In 1960, DuPont developed a PFSA-based Nafion membrane as a solid separator for the chloro-alkali electrolyzer.[93,108,111,112] Nafion is an electronically neutral semicrystalline random copolymer, having a polytetrafluoroethylene (PTFE) backbone and randomly ordered with a pendant perfluorosulfonyl fluoride vinyl ether ionic side chain (**Figure 6**).[93,110] The chemical structures of a few other short side chains (Nafion is considered as a long side chain) PFSA-based ionomers, such as 3M, Aquivion (DOW SSC ionomer or Solvey specialty Polymers), Flemion (Asahi Glass), along with the reinforced composite PFSAs (W. L. Gore & Associates, Inc.) are depicted in **Figure 6**.[93,110] Among these PFSA-based ionomer membranes, DuPont Nafion membrane is considered as the state-of-the-art PEM materials.[3,28,93,94,110] Nafion membrane showed exceptionally high mechanical and dimensional stabilities due to the presence of the hydrophobic PTFE backbone.[93,110,113] The PTFE backbone and pendant perfluorosulfonyl fluoride vinyl ether group in Nafion creates a well-separated and interconnected hydrophobic and hydrophilic phase morphology.[93,110,113] As a result, the PFSA-based Nafion membrane exhibited a high PC value.[93,110,113,114] Additionally, the Nafion membranes endured high chemical stability under the PEMFC operating conditions, mainly associated with the presence of the PTFE backbone and the strong C-F bonds in Nafion's repeat unit.[93,110,113-116]
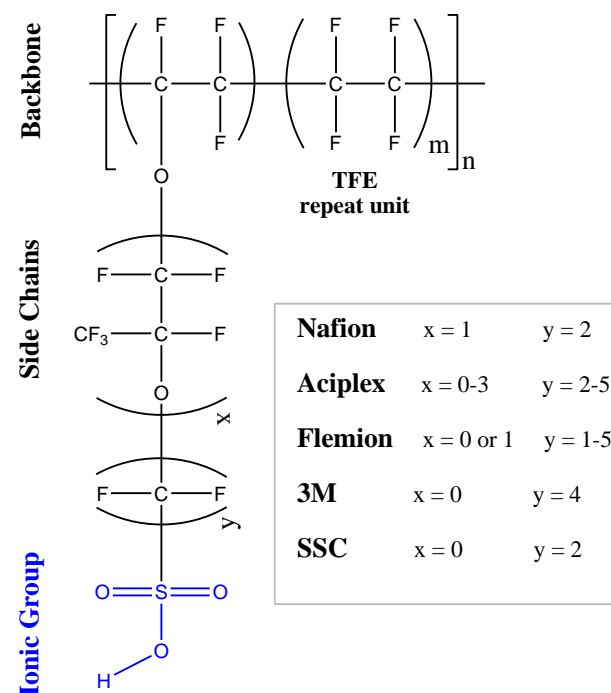

Figure 6. Chemical structures of the commercially available PFSA-based PEM materials [93,110]

Despite the aforementioned superior properties, the Nafion membrane has a few drawbacks, such as its complicated synthetic procedure, high fuel gas permeability, low operating temperature limits, deterioration of mechanical

Banerjee and Ghanti

Innov. Chem. Mater. Sustain. **2025**, 2(1), 032-073
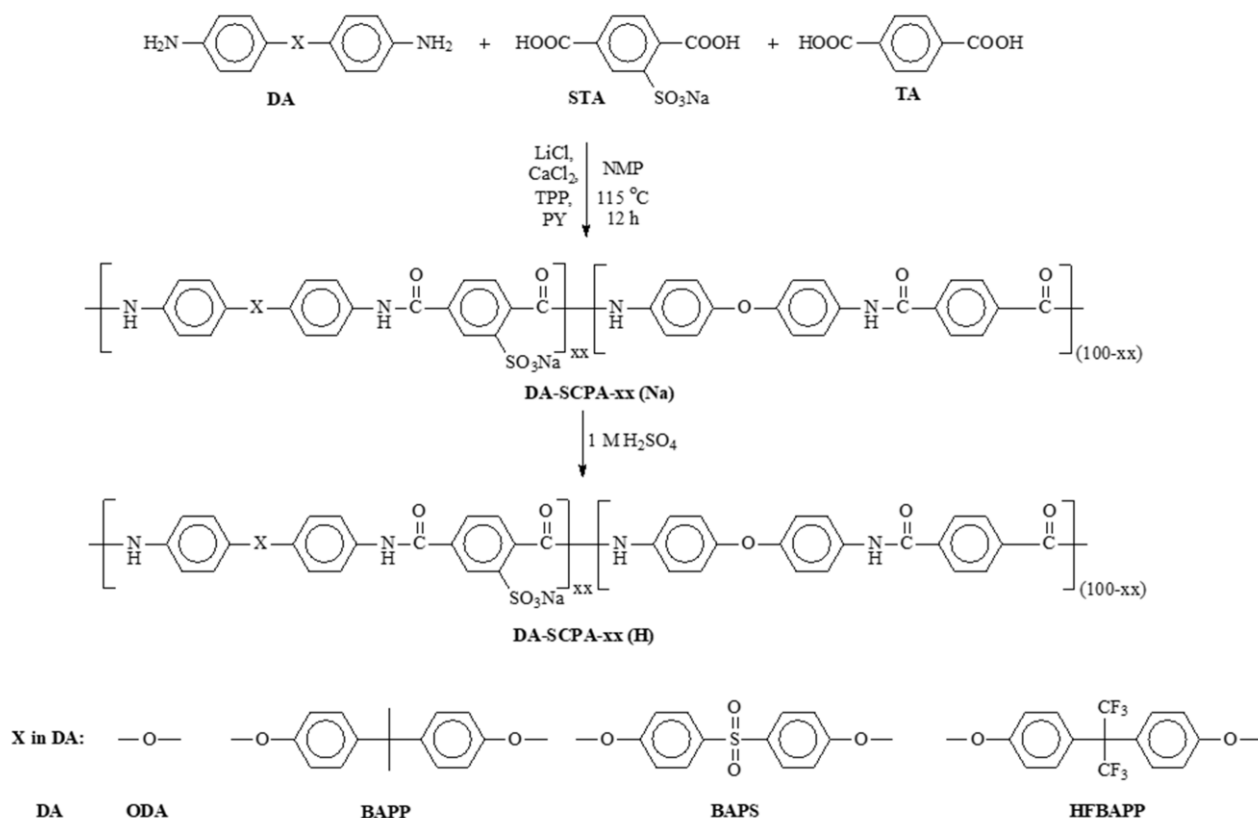
Scheme 1. The synthesis scheme of ether-containing SPAs (DA-SCPA-xx).[140]
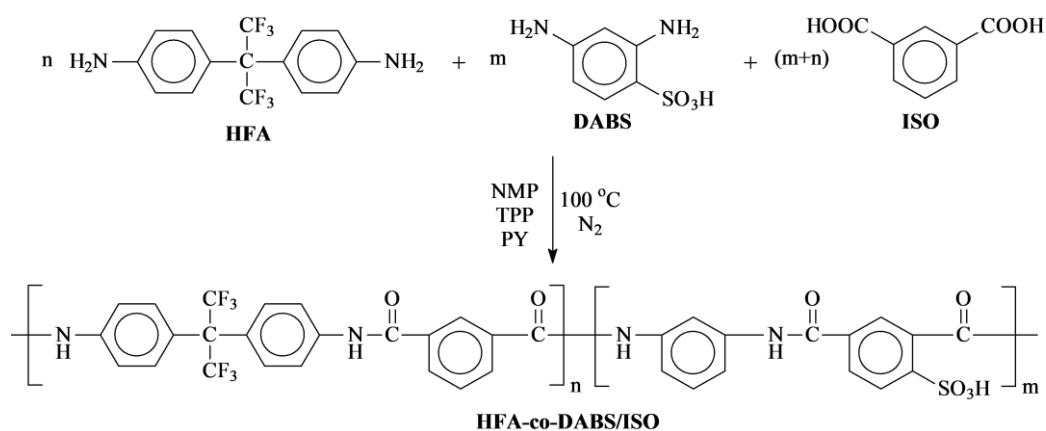
Scheme 2. The synthesis scheme of the semi-fluorinated SPAs (HFA-coDABS/ISO).[142]

stability above 80 ℃, reduction of proton conductivity values at higher temperatures and low humidity levels, and being highly expensive, simulated a golden opportunity for the global researchers to design and develop alternative PEM materials for the PEMFC applications.[28,93,110-117] Recently, aromatic hydrocarbon-based sulfonated PEM materials emerged as a promising alternative to PFSA materials due to their ease of the synthetic procedure and versatility in their structural design.[28,118-121] Recent studies revealed that the various types of aromatic hydrocarbon-based sulfonated PEMs, including polyamides, poly(arylene ether)s, polybenzimidazoles, polyimides, polyphenylenes, polytriazoles, etc., have significant PEM properties.[96,122-130]

4.2.2   Polyamides, PAs

Hydrocarbon-based aromatic sulfonated polyamides (SPAs) are a special type of high-performing engineering polymers because of their high thermal and mechanical stabilities, appropriate stability under acidic conditions, low flammability,

and excellent oxidative stability.[131-136] However, the hydrocarbon-based SPAs have very low processability due to the rigid aromatic backbone and strong interchain hydrogen bonding interactions of the SPA architecture, making them insoluble in many organic solvents.[137,138] Generally, hydrocarbon-based aromatic SPAs are synthesized by the phosphorylation polycondensation reaction between the aromatic diamines and diacids or diacid chloride in the presence of triphenyl phosphite (TPP) or diphenyl phosphite (DPP), pyridine (PY), lithium chloride (LiCl) or calcium dichloride (CaCl₂) in N-methyl-2-pyrrolidone (NMP).[137-139] Herein, the TPP/DPP and PY were used as a condensing agent by forming N-phosphonium pyridinium salts.[139] Hydrocarbon-based aromatic SPAs gained remarkable interest in PEMFC applications due to their high thermal, mechanical, and dimensional stabilities.[140,141] Here, some of the hydrocarbon-based aromatic SPAs are discussed.

JO *et al.* synthesized a set of hydrocarbon-based fluorinated and non-fluorinated SPAs with different degrees of sulfonation (DS) on the dicarbonyl aromatic ring via the phosphorylation polycondensation reaction of terephthalic acid (TA) and sulfonated terephthalic acid (STA) with different aromatic

acid-containing HFAS55 copolymer demonstrated the highest σ value of 3.3 mS/cm at 25 ℃.[142] However, the accelerated Fenton test did not explore the oxidative stability of these SPAs.

Wang *et al.* designed and synthesized a series of pendant

Table 3. *The ion exchange capacity (IEC), weight-average molecular weight (M_w), inherent viscosity (η_{inh}), water uptake (WU), oxidative stability (τ), and proton conductivity (σ) values of the SPAs.*

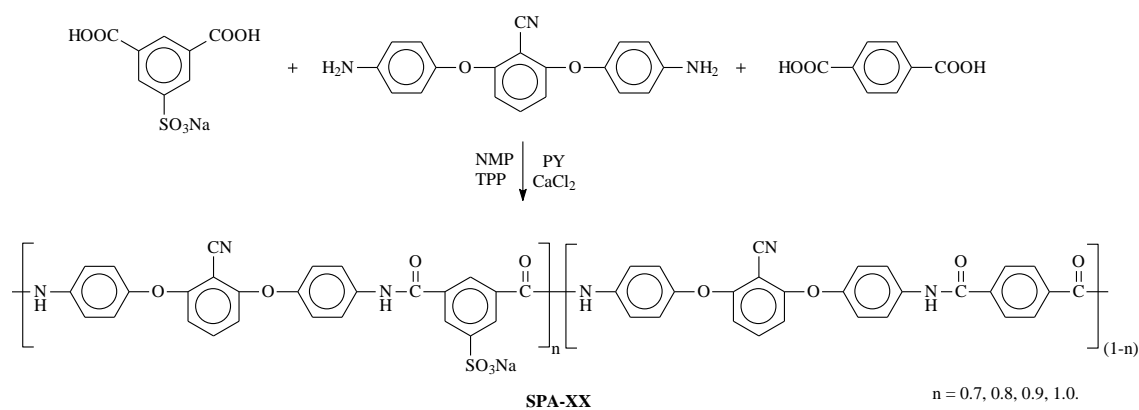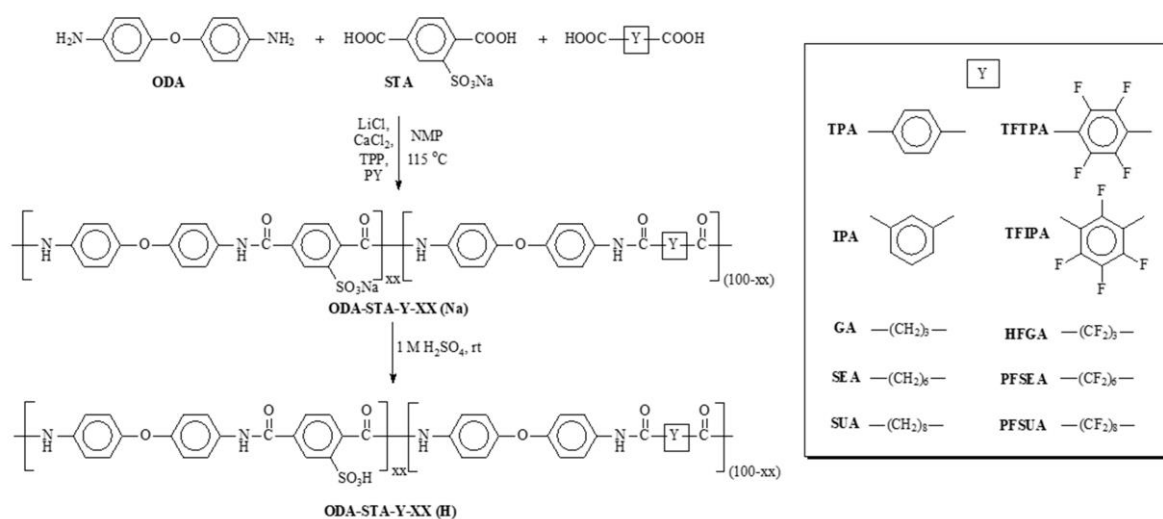| Polymer	IEC (meq/g)[a]	M_w (kDa)[b]	η_{inh} (dL/g)[c]	WU (%)[d]	τ (h)[e,f]	σ (mS/cm)[g]	Ref.
ODA-SPEA-40 (H)	1.05	80.8	-	17	1.8[e]	6.7	140
ODA-SPEA-50 (H)	1.33	45.5	-	23	1.7[e]	46.7	140
ODA-SPEA-60 (H)	1.56	53.2	-	24	1.6[e]	52.5	140
ODA-SPEA-70 (H)	1.83	60.3	-	32	2.0[e]	105	140
BAPP-SPEA-70 (H)	1.06	102.1	-	17	2.5[e]	8.7	140
BAPS-SPEA-70 (H)	1.11	110.4	-	10	2.8[e]	21.4	140
HFBAPP-SPEA-70 (H)	0.64	119.7	-	13	4.3[e]	1.5	140
HFAS82	0.59	-	0.27	8.5[h]	-	<0.04[i]	142
HFAS73	0.87	-	0.25	16[h]	-	0.04[i]	142
HFAS64	1.02	-	0.18	22[h]	-	0.09[i]	142
HFAS55	1.39	-	0.19	25[h]	-	3.3[i]	142
ODA-STA-TPA-90	2.22	-	1.83	65	-	158	143
ODA-STA-TPA-80	2.05	-	1.78	53	-	129	143
ODA-STA-IPA-90	2.15	-	0.79	67	-	142	143
ODA-STA-TFTPA-90	2.10	-	0.97	55	-	140	143
ODA-STA-TFTPA-80	1.94	-	0.81	48	-	117	143
ODA-STA-TFIPA-90	2.13	-	0.64	50	-	110	143
ODA-STA-GA-90	2.01	-	1.93	42	-	166	143
ODA-STA-GA-80	1.71	-	1.48	40	-	104	143
ODA-STA-SEA-90	1.85	-	0.98	42	-	100	143
ODA-STA-SEA-80	1.75	-	1.97	38	-	41	143
ODA-STA-SUA-90	1.90	-	0.91	38	-	126	143
ODA-STA-SUA-80	1.84	-	1.31	35	-	78	143
ODA-STA-HFGA-90	2.02	-	0.89	36	-	114	143
ODA-STA-HFGA-80	1.75	-	0.53	33	-	94	143
ODA-STA-PFSEA-90	1.91	-	0.82	34	-	125	143
ODA-STA-PFSEA-80	1.78	-	0.64	32	-	103	143
ODA-STA-PFSUA-90	1.90	-	0.60	37	-	111	143
ODA-STA-PFSUA-80	1.65	-	0.53	33	-	91	143
SPA-70	1.39	-	1.23	33	8.0[f]	62	144
SPA-80	1.56	-	1.61	37	6.5[f]	96	144
SPA-90	1.73	-	1.85	44	5.0[f]	127	144
SPA-100	1.89	-	2.16	52	4.5[f]	141	144
CP-1	0.79	-	0.28	9[h]	-	0.053[j]	145
CP-2	0.97	-	0.26	12[h]	-	0.054[j]	145
CP-3	1.11	-	0.24	15[h]	-	0.057[j]	145
CP-4	1.19	-	0.23	20[h]	-	0.113[j]	145
CP-5	1.30	-	0.20	27[h]	-	0.29[j]	145

[a]Theoretical IEC value, [b] weight-average molecular weight, [c] inherent viscosity values, [d] water uptake at 80 ℃, [e] starting dissolution time in Fenton's reagent at 80 ℃, [f] complete dissolution time in Fenton's reagent at 80 ℃, [g] σ values at 80 ℃, [h] WU values at 75 ℃, [i] σ values under fully hydrated state at 25 ℃, [j] proton conductivity in dry conditions.

diamines (DAs) in NMP as depicted in **Scheme 1**.[140] The calculated and titrimetric experimental IEC values of the SPAs were 0.94-1.83 and 0.99-1.80 meq/g (**Table 3**). The flexible ether-linkage containing SPAs showed good solubility in polar aprotic solvents. The weight-average molecular weight (M_w) and polydispersity index (PDI) were obtained between 45-120 kg/mol (**Table 3**) and 2.9-4.4, respectively.[140] Among all the fabricated membranes, the ODA-SPEA-70 (H) exhibited the highest water uptake (WU) value of 32% at 80 ℃ (**Table 3**).[140] The bulky trifluoromethyl (-CF₃) groups containing HFBAPP-SPEA-70 (H) demonstrated enhanced oxidative stability in Fenton's reagent due to the electronegative fluorine atoms in the copolymer architecture.[93,113,116] Among the SPA series, the ODA-SPEA-70 (H) membrane exhibited the highest σ value (105.1 mS/cm) at 80 ℃ under 100% relative humidity (RH), as tabulated in **Table 3**.

Aguilar-Vega *et al.* synthesized a series of semi-fluorinated SPAs with increasing DS value by the direct polycondensation reaction of isophthalic diacid (ISO) with two different aromatic diamines [4,4′-(hexafluoroisopropylidene)dianiline (HFA) and 2,4-diaminobenzenosulfonic acid (DABS)] as shown in **Scheme 2**.[142] The synthesized SPAs showed moderate inherent viscosity (η_{inh}) values between 0.18-0.27 dL/g in DMAc (**Table 3**). The SPAs (HFA-co-DABS/ISO) demonstrated high thermal stability (onset temperature was 320 ℃) and mechanical properties (tensile strength, TS: 20-34 MPa; Young's modulus, YM: 280-428 MPa, and elongation at break, EB: 9-12%).[144] The semifluoro-sulfonated copolyamides HFAS64 and HFAS55 exhibited the best water absorption properties at 75 ℃ (**Table 3**). The highest sulfonic

nitrile (-CN) group-based SPAs for the first time by the phosphorylation polyamidation reaction of 2,6-bis(4-aminophenoxy)benzonitrile with two different aromatic dicarboxylic acids (5-sulfoisophthalic acid sodium salt and terephthalic acid) as shown in **Scheme 4**.[144] The η_{inh} values of the SPA-XX copolymers were found between 1.39-2.16 dL/g, as tabulated in **Table 3**. The SPA-XX membranes exhibited the WU and swelling ratio (SR) values in the 32-52% range and 7-18% at 80 ℃, respectively (**Table 3**). The SPA-100 membrane showed the highest σ value of 141 mS/cm at 80 ℃ under fully hydrated conditions (**Table 3**). All the nitrile group bearing SPA-XX membranes demonstrated better oxidative stability values (τ ≥ 4 h, **Table 3**) in Fenton's reagent at 80 ℃, which is even higher than literature-reported SPAs having identical IEC_w values.[140] Thus, the presence of the polar -CN group in the SPA-XX backbone improved the solubility, water absorption properties, and proton conductivity values.[144]

Sulub-Sulub *et al.* prepared a series of block SPAs by the polycondensation reaction of a hydrophobic block [4,4′-(hexafluoroisopropylidene)bis(p-phenyleneoxy)-dianiline, HFD] and a hydrophilic block [4,4′-Diaminobiphenyl-2,2′-disulfonic acid, DFS], as provided in **Scheme 5**.[145] The DS values of the block copolyimides were controlled by varying the mole proportion of the HFD/DFS blocks.[145] The calculated IEC and η_{inh} values of the sulfonated block copolyamides (CP-1 to -5) were between 0.6-1.38 meq/g and 0.20-0.28 dL/g, as illustrated in **Table 3**. The 10% thermal decomposition temperature ($T_{d10\%}$) of CP-1 to CP-5 block copolymers was found between 240-320 ℃.[145] Among all the sulfonated block

Scheme 3. The synthesis scheme of the various SPAs (ODA-STA-Y-XX).[143]

Scheme 4. The synthesis scheme of the pendant nitrile group-containing SPAs (SPA-XX).[144]

copolyamides, the CP-5 membrane demonstrated the highest water absorption value (WU: 27%) at 75 °C (**Table 3**). The sulfonated block copolyamides (CP-1 to CP-5) showed σ values between 0.053-0.29 mS/cm in dry conditions (**Table 3**),

Scheme 5. Synthesis scheme of the block SPAs (HFD-b-DSF).[145]
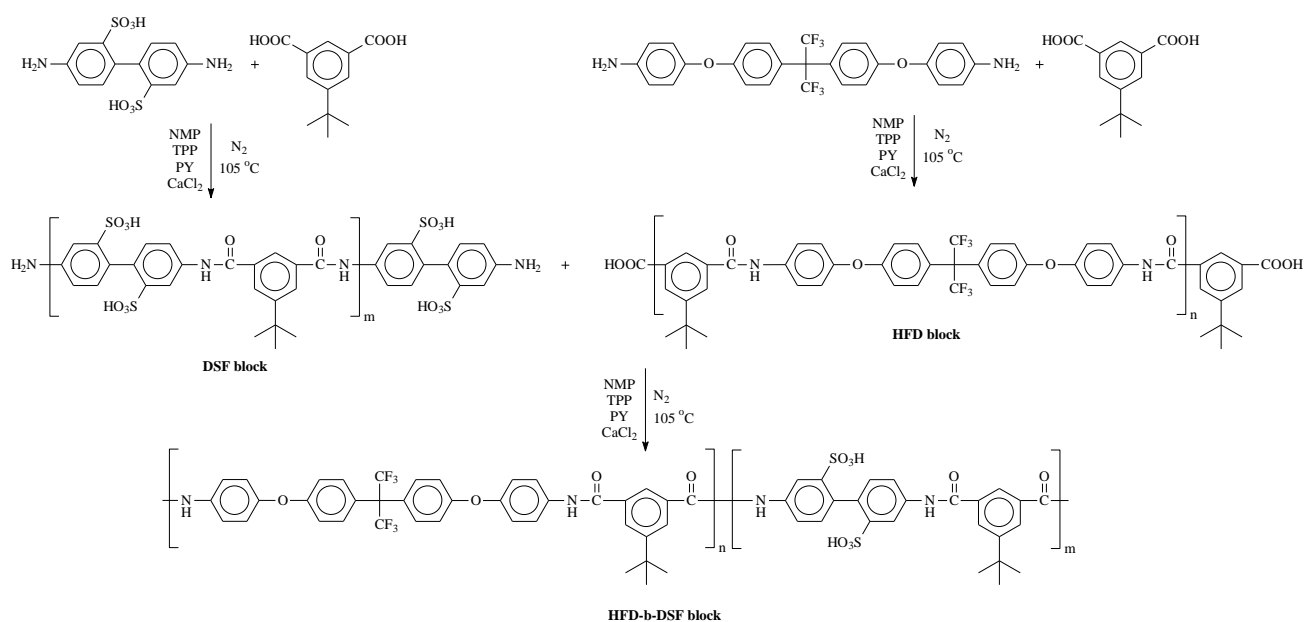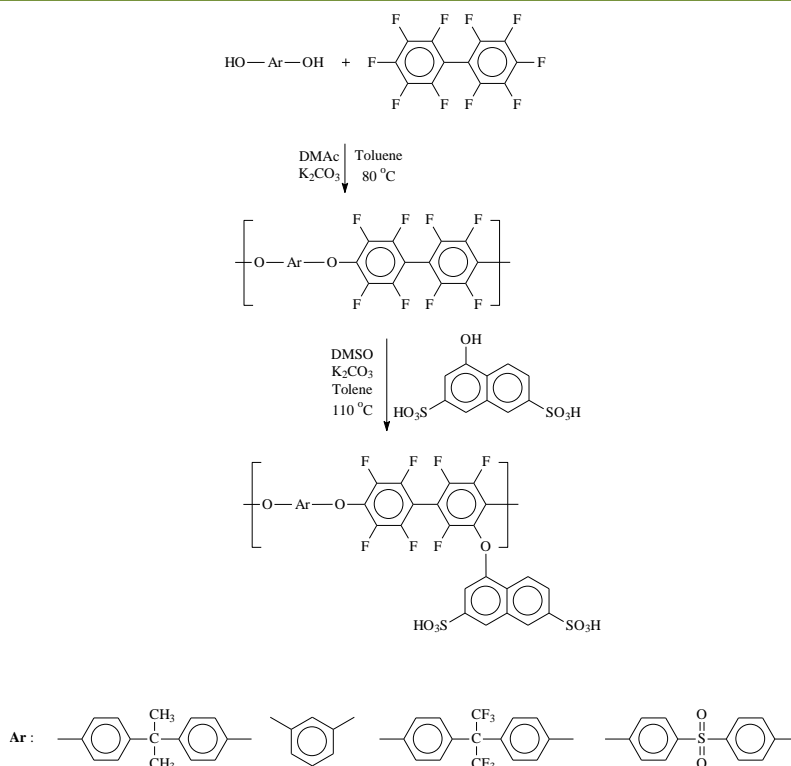
Scheme 6. The synthesis scheme of the pendant disulfonated naphthol-based SPAEs.[153]

which is lower than that of Nafion-115 under similar testing conditions.[145]

4.2.3   Poly(arylene ether)s, PAEs

Sulfonated poly(arylene ether)s (SPAEs) are one of the high-performing thermoplastic engineering materials.[65] These materials are famous for their excellent thermal and mechanical stabilities, high solubility, physical properties, and improved oxidative stabilities.[65,146-148] Generally, PAEs were prepared by the nucleophilic substitution polycondensation reaction of the activated aromatic dihalo or dinitro compounds with the bisphenoxide at high temperatures in polar aprotic solvents.[65,149] The SPAEs were synthesized either by the direct polymerization of the sulfonated comonomers or by post-sulfonation methods. The direct sulfonated polymerization

method has a few advantages, such as the quick variation of the DS values, which is not possible for the post-sulfonation method.[150,151] Though the grafting of sulfonic acid groups in the post-modification method is complex, several PEMs were still designed using this method with well-defined structures.[147,152] A few of the recent SPAEs developed for the PEMFC applications are discussed here.

Four series of pendant disulfonated naphthol-based PAEs with various sulfonic acid contents were prepared via the two-step nucleophilic-substitution reaction by Oroujzadeh *et al.*, as shown in **Scheme 6**.[153] The IEC values of these four sets of SPAEs were between 1.14-2.15 meq/g (**Table 4**). The number-average (M_n) and weight-average (M_w) molecular weights were determined by the gel permeation chromatography (GPC) analysis and obtained between 33000-65000 g/mol and
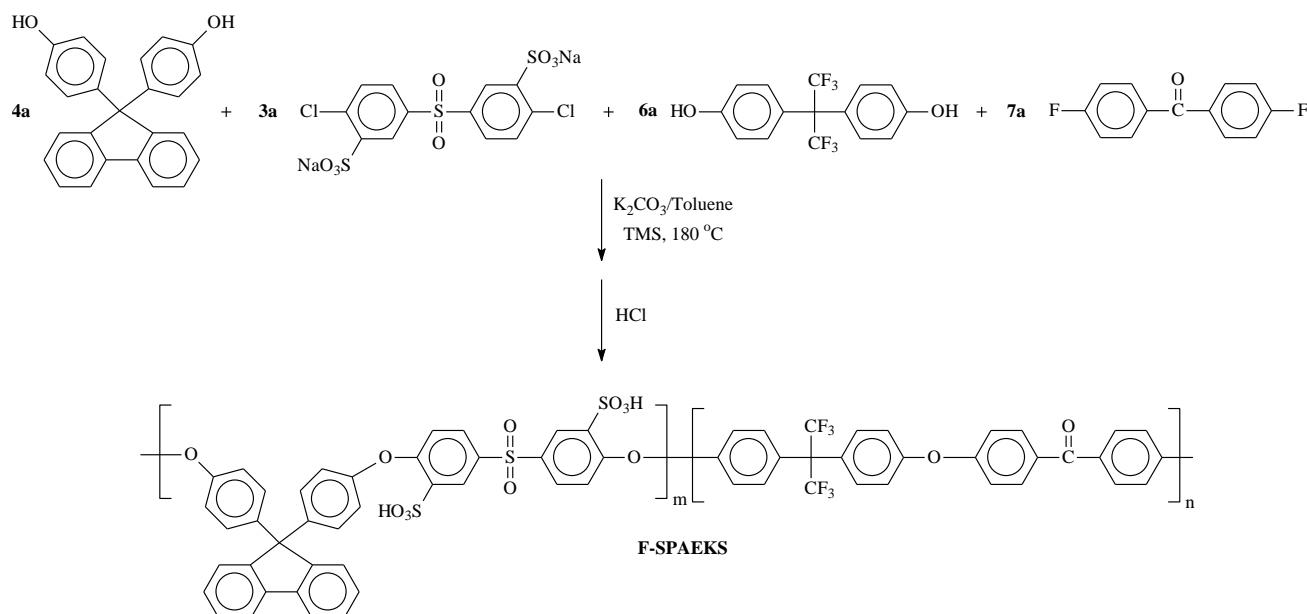
Scheme 7. The synthesis scheme of the semi-fluorinated SPAE copolymers (F-SPAEKS).[154]

97000-163000 g/mol, respectively (**Table 4**). The Dec-AF and Dec-A membranes showed lower water uptake values than the Dec-S and Dec-Res membranes at 80 ℃, as illustrated in **Table 4**.

Among all the membranes, the Dec-AF series membranes exhibited the lowest SR values at 80 ℃, indicating high dimensional stability.[153] The σ values of the SPAEs were obtained between 61-182 mS/cm and 96-217 mS/cm at 30 and 80 ℃, respectively (**Table 4**).[153] The Dec-AF series membranes had the highest oxidative stability in the Fenton reagent.[153] Among all the membranes, the Dec-AF-3 membrane demonstrated the best combined PEM properties [oxidative stability: 118 min; PC: 213 mS/cm at 80 ℃; WU: 66.3% at 80 ℃; and SR: 27% at 80 ℃].[153] Based on the overall PEM properties, the single fuel cell performances were analyzed for the Dec-A-1, Dec-A-3, and Dec-AF-3.[153] Among these three membranes, the Dec-AF-3-based MEA demonstrated the best overall single fuel cell performance with the open circuit voltage (OCV) value 1030 mV, the current density of 1130 mA/cm², and peak power density (PPD) value 336 mW/cm² at 80 ℃ and 100% RH.[153]

4 exhibited a high OCV value of 0.994 V and a maximum PPD value of 466 mW/cm² at 80℃ and 100% RH.[154] Thus, the acid-base bifunctionalized MOFs-based hybrid membrane (FSMNC-4) possessed promising properties as PEM materials. Xu *et al.* synthesized a set of PAEKS copolymers (C-PAEKS-DBS, CPD-x) by the nucleophilic polycondensation reaction, as shown in **Scheme 8**.[155] Finally, a series of pendant sulfonated SPAEKSs (CPDA-x) were synthesized by a simple double bond cross-linking reaction of hydrophilic long alkyl side chains (AMPS) with CPD-x, as depicted in **Scheme 8**.[155] The IEC values of the CPDA-x copolymers were found between 0.67-0.77 mmol/g (**Table 4**).

The CPDA-3 membrane demonstrated higher mechanical properties (TS: 52.2 MPa and YM: 1.72 GPa) than the Nafion-117 membrane.[155] Among all the membranes, the CPDA-3 membrane displayed the lowest water contact angle (40.4º), which confirmed the hydrophilic nature of this membrane.[155] The CPDA-3 membrane showed a high PC value of 77.8 mS/cm at 80 ℃ (**Table 4**) and possessed better oxidative stability [RW: 93.3%] in Fenton's reagent at 80 ℃.[155]

C-PAEKS-DBS-x (CPD-x)
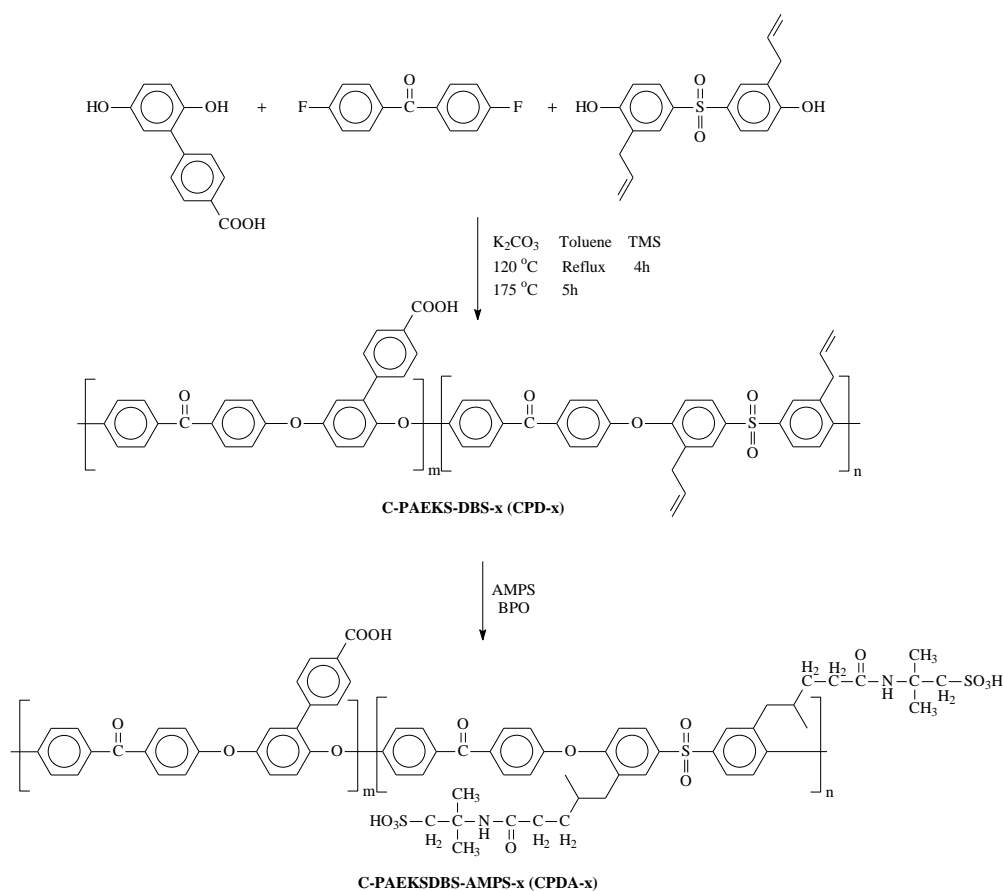
C-PAEKSDBS-AMPS-x (CPDA-x)
Scheme 8. The synthesis scheme of the C-PAEKSDBS-AMPS-x (CPDA-x) copolymer.[155]

A fluorenyl group containing sulfonated poly(arylene ether ketone sulfone)s (SPAEKSs), F-SPAEKS (IEC: 1.05 meq/g) was synthesized by Wang *et al.*[154] Two series of hybrid matrix membranes (FSMN-x and FSMNC-x) were fabricated by mixing two different functionalized metal organic frameworks (MOFs) (MIL-101-NH₂ and MIL-101-NH₂-COOH) with F-SPAEKS.[154] Among all the hybrid membranes, the FSMNC-4 membrane exhibited the highest WU (21.6%) and SR (9.3%) values at 80 ℃ due to its highest IEC value (1.29 meq/g, **Table 4**). The FSMNC-4 hybrid membrane showed the highest σ value (159.9 mS/cm at 80 ℃) and oxidative stability (residual weight, RW: 95.3%).[154] Also, the FSMNC-4 hybrid membrane exhibited high long-term stability, retaining more than 73% of its initial proton conductivity value even after 96 h.[154] The proton conduction-related activation energy (Eₐ) of the FSMNC-4 hybrid membrane was 7.62 kJ/mol.[154] The FSMNC-

A series of densely sulfonated poly(arylene ether sulfone ketone)s (SPAESK-x) copolymers were synthesized by the post-sulfonation of PAESK-x by Pang *et al.*, as depicted in **Scheme 9**.[156] The calculated and experimental IEC values of the SPAESK-x copolymers were found between 0.99-2.26 meq/g and 0.80-1.82 meq/g, respectively (**Table 4**). The M_w and PDI values of the SPAEKS-x copolymers were between 110-174 kg/mol and 1.56-1.62, as provided in **Table 4**. The SPAEKS-x copolymers showed high thermal stabilities (4 wt% decomposition temperature below 300 ℃) and mechanical properties (TS: 43-62 MPa and EB: 28-44%).[156] The morphological analysis of SPAESK-x membranes showed the formation of a well-separated and inter-connected phase morphology by the small-angle X-ray scattering (SAXS) and transmission electron microscopy (TEM) investigation.[156] The
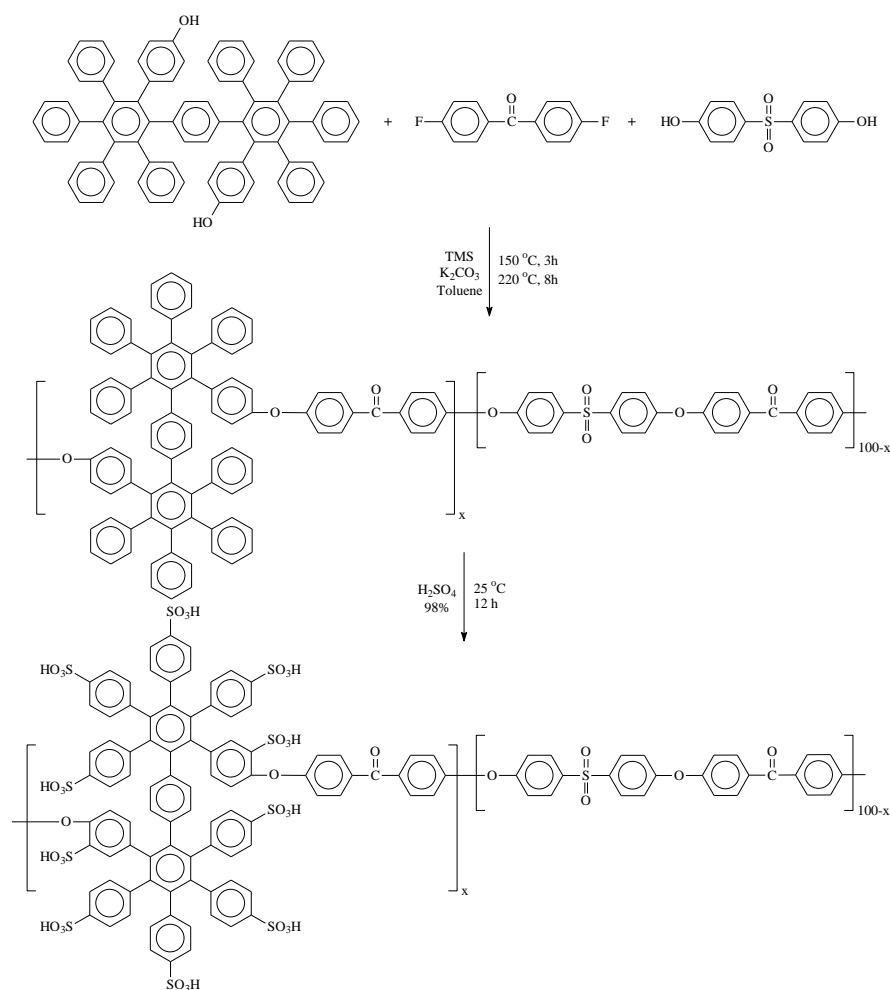
Scheme 9. The synthesis scheme of the PAESK-x and SPAESK-x copolymer.[156]

Table 4. *The IEC, M_w, thermal decomposition temperature (T_d), tensile strength (TS), Young's modulus (YM), elongation at break (EB), WU, τ, and σ values of the SPAEs*

Polymer	IEC (meq/g)[a]	M_w (kDa)[b]	T_d (°C)[c]	TS (MPa)	YM (GPa)	EB (%)	WU (%)[d]	τ (h)[e,f]	σ (mS/cm)[g]	Ref.
Dec-AF-1	1.14	-	320	-	-	4.8[i]	25[h]	2.06[f]	125	153
Dec-AF-2	1.31	163	235	-	-	6.2[i]	42[h]	1.93[f]	148	153
Dec-AF-3	1.65	-	118	45.2[i]	-	8.4[i]	66[h]	1.97[f]	213	153
Dec-S-1	1.6	-	344	-	-	-	43[h]	0.75[f]	213	153
Dec-S-2	1.73	105	345	-	-	-	85[h]	0.53[f]	225	153
Dec-S-3	1.81	-	118	-	-	-	113[h]	0.63[f]	194	153
Dec-A-1	1.28	-	238	-	-	3.0[i]	25[h]	1.80[f]	136	153
Dec-A-2	1.46	128	233	-	-	5.4[i]	47[h]	1.73[f]	189	153
Dec-A-3	1.79	-	91	44.2[i]	-	6.6[i]	70[h]	1.63[f]	217	153
Dec-Res-1	1.70	-	312	-	-	-	37[h]	0.35[f]	96	153
Dec-Res-2	1.81	97	306	-	-	-	58[h]	0.42[f]	160	153
Dec-Res-3	2.15	-	286	-	-	-	227[h]	0.32[f]	-	153
F-SPAEKS	1.05	-	-	32.3	1.84	12.7	15.0	-	89.3	154
FSMN-2	0.97	-	-	27.1	1.59	10.1	15.5	-	119.4	154
FSMN-4	0.95	-	-	34.7	1.98	8.5	16.8	-	127.6	154
FSMN-6	0.98	-	-	21.7	1.43	5.2	15.9	-	93.9	154
FSMNC-2	1.25	-	-	27.7	1.35	9.2	15.8	-	131.7	154
FSMNC-4	1.29	-	-	47.7	2.04	8.5	21.6	-	159.9	154
FSMNC-6	1.03	-	-	22.2	1.60	5.5	18.1	-	82.7	154
CPDA-1	0.67	-	-	29.0	1.20	3.1	27.9	-	52.6	155
CPDA-2	0.72	-	-	33.3	1.39	3.7	32.4	-	70.0	155
CPDA-3	0.77	-	-	52.2	1.72	4.5	33.3	-	77.8	155
SPAESK-5	0.99	174	-	63.2	-	28.6	16[j]	6.5[e]	50[j]	156
SPAESK-10	1.71	110	-	45.8	-	32.5	91[j]	4.5[e]	152[j]	156
SPAESK-15	2.26	165	-	43.7	-	43.4	147[j]	4.0[e]	182[j]	156
Am-SPAEKS	1.04	-	-	31.5	1.5	7.5	38.3	-	67.8	157
SPAEKS-CL-QP5-3%	0.88	-	-	37.5	1.4	10.5	18.4	-	70.0	157
SPAEKS-CL-QP5-5%	0.74	-	-	50.4	1.8	14.9	15.6	-	86.5	157
SPAEKS-CL-QP5-7%	0.66	-	-	44.1	1.5	11.8	14.3	-	88.1	157
SPAEKS-CL-QP5-10%	0.57	-	-	40.0	1.4	11.0	10.7	-	56.8	157
SPAEKS-CL-QP5-15%	0.49	-	-	36.3	1.1	12.3	9.7	-	38.5	157

[a] Theoretical IEC value, [b] weight-average molecular weight, [c] 10% decomposition temperature obtained from TGA analysis, [d] WU at 80 °C, [e] starting fractured time in Fenton's reagent at 80 °C, [f] complete dissolution time in Fenton's reagent at 80 °C, [g] σ values under fully hydrated state at 80 °C, [h] WU at ambient temperature, [i] mechanical properties in the dry state, [j] σ values at 100 °C.conductivity in dry conditions.
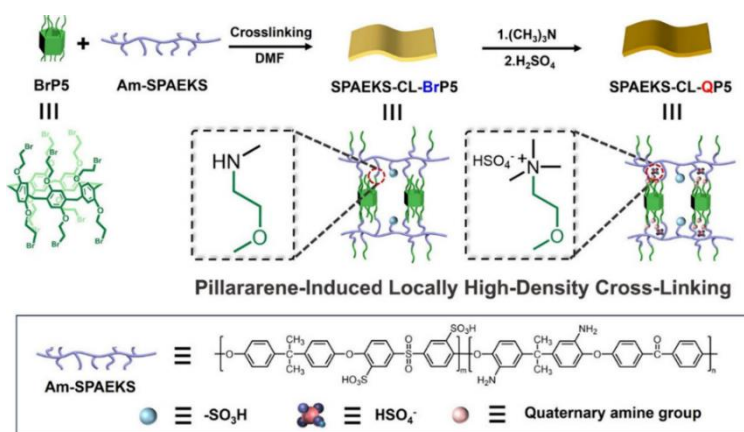
Figure 7. Schematic illustration for the synthesis of Pillararene-Cross-Linked Membranes.[157] (Reprinted with permission from (157). Copyright (2024) American Chemical Society.)
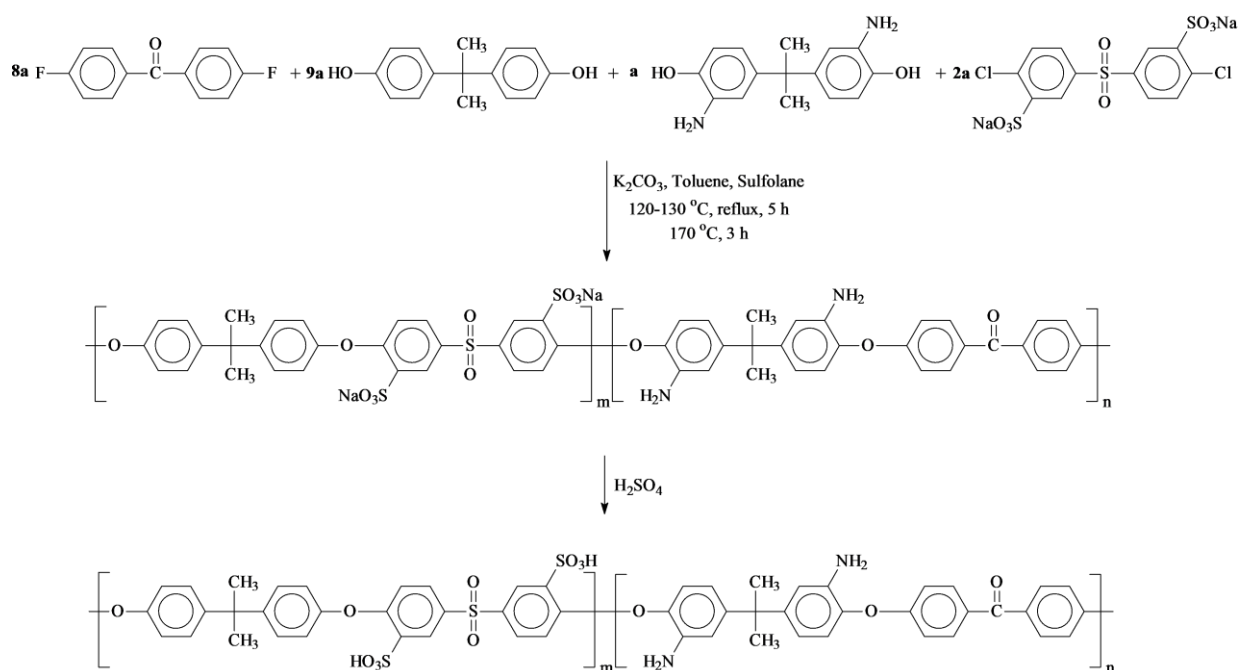
Scheme 10. The synthesis scheme of the Am-SPAEKS copolymers.[157]
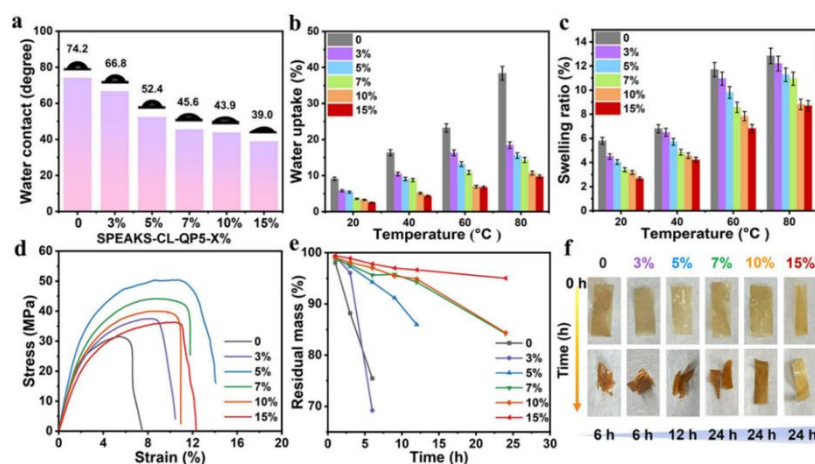
Figure 8. (a-e) Water contact angle, WU, SR, stress-strain, and oxidative stability plots, and (f) oxidative stability-related images of the SPAEKS-CL-QP5-x%.[157] (Reprinted with permission from (157). Copyright (2024) American Chemical Society.)

Banerjee and Ghanti

Innov. Chem. Mater. Sustain. **2025**, *2*(1), 032-073

SPAESK-15 membrane showed higher PC (181.5 mS/cm) and WU (146.5%) values than Nafion-117 at 100 ℃.[156] Also, the SPAESK-15 showed higher PPD value (370.4 mW/cm²) than the Nafion-117 (255.8 mW/cm²) in H_2/air single fuel cell performance at 80 ℃ and 90% RH.[156]

Yang *et al.* synthesized a pendant amino group functionalized SPAEKS (Am-SPAEKS), as shown in **Scheme 10**.[157] Then, a series of macrocycle-cross-linked SPAEKSs (SPAEKS-CL-BrP5) were designed and synthesized by reacting the amino groups of Am-SPAEKS with bromo-functionalized pillar[5]arene (BrP5) and finally, quaternized into the SPAEKS-CL-QP5-x%, as portrayed in **Figure 7**.[157] The gel content of the SPAEKS-CL-QP5-x% (x = 0, 3, 5, 7, 10, and 15) cross-linked copolymers gradually increases with the rise in the degree of the cross-linking.[157] The surface and cross-sectional scanning electron microscopy (SEM) investigation of the cross-linked membranes revealed a dense microstructure without voids, defects, and cracks.[157] The WU values of the cross-linked membranes at 80 ℃ reduced with the increase in the degree of cross-linking, as provided in **Table 4**. The SPAEKS-CL-QP5-x% membranes displayed higher mechanical properties (TS: 36.3-50.4 MPa) than those of the Am-SPAEKS membrane (TS: 31.5 MPa).[157] The cross-linked membranes showed higher oxidative stability than the pristine membrane, as the cross-linked membranes had a higher density, preventing peroxide radical attacks and enhancing oxidative stability.[157] The physical, mechanical, and oxidative properties of the pristine and cross-linked membranes are displayed in **Figure 8**.[157] Among all the cross-linked membranes, the SPAEKS-CL-QP5-7% showed the highest PC value (88.1 mS/cm at 80 ℃), illustrated in **Table 4** and exhibited high long-term stability by retaining more than 98% of its initial PC value after 144 h.[157] The SPAEKS-CL-QP5-7% displayed better single fuel cell performance (4.7 times higher PPD value) than the Am-SPAEKS at 80 ℃ and 100% RH.[157] This study reveals that the cross-linking improved the overall PEM properties and PEMFC results.

4.2.4   Poly(arylene thioether)s, PATEs

Hydrocarbon-based sulfonated poly(arylene thioether)s (SPATEs) are another essential high-performing polymer.[158] These sulfonated copolymers can serve as PEM materials similar to the SPAEs.[158-162] Like SPAEs, SPATEs also show high thermal, mechanical, and proton conductivity values.[158-163] Additionally, the inclusion of the thioether (-S-) groups in place of the ether (-O-) groups in the polymer backbone further improved the dimensional stability, oxidative stability, flame-retardancy properties, and refractive index in the thioester-based polymers compared to the ether-based analogues polymers.[161,162,164-168] Generally, the PATEs are prepared by the nucleophilic substitution polycondensation reaction between the activated aryl dihalo compounds with various types of aryl diphenthiol in polar aprotic solvents.[158-163] Whereas the SPATEs were prepared either by using sulfonated comonomers in polycondensation reactions or by the post-sulfonation process.[161,163] Herein, a few recently developed SPATEs for the PEMFC applications are discussed below.

Bai *et al.* synthesized a trifluoromethyl (-CF₃) groups-containing sulfonated poly(arylene thioether sulfone) [SPATES, 6F-SPTES-50] having 50 mol% of sulfonic acid content by the nucleophilic polycondensation reaction of 4,4-(hexafluoroisopropylidene)-diphenylthiol with two different difluorosulfones (3,3′-disulfonate-4,4′-difluorodiphenylsulfone and 4,4′-difluorodiphenylsulfone), which is shown in **Scheme 11**.[169] The η_{inh} and number-average molecular weight (M_n) of the 6F-SPTES-50 copolymers were 0.92 dL/g and 25800 g/mol.[169] The experimental NMR-based sulfonic acid content (46 mol%) was in close agreement with the theoretical value (50 mol%) of the 6F-SPTES-50 copolymer.[169] The 6F-SPTES-50 copolymer demonstrated high thermal stability (onset decomposition temperature was 450 ℃) in TGA analysis under synthetic air conditions (**Table 5**). The 6F-SPTES-50 copolymer exhibited lower WU values (20-30%) than the non-fluorinated analogues copolymer (SPTES-50).[169] The 6F-SPTES-50 copolymer showed a PC value of 120 mS/cm at 85 ℃ under 85% RH conditions.[169] The H_2/O_2 single fuel cell performance of the 6F-SPTES-50 membrane displayed a current density value of 750 mA/cm² at 80 ℃ with an OCV value of 0.988 V.[169]

Yan *et al.* synthesized a series of hexafluoroisopropylidene moiety-based sulfonated poly(arylene thioether phosphine oxide)s with various DS (sPTPOF-x) by the nucleophilic polycondensation reaction of 4,4'-(hexafluoroisopropylidene) diphenthiol with sulfonated

Table 5. *The IEC, M_w, T_d, TS, YM, EB, WU, τ, and σ values of the SPATs.*

Polymer	IEC (meq/g)[a]	M_w (kDa)[b]	T_d (℃)[c]	TS (MPa)	YM (GPa)	EB (%)	WU (%)[d]	τ (h)[e,f]	σ (mS/cm)[g]	Ref.
6F-SPTES-50	1.51	-	~450[h]	-	-	-	30	-	120[i]	169
PTPOF	-	157	509	57.8	1.28	4.8	-	-	-	170
sPTPOF-60	0.87	119	407	54.6	1.07	5.5	~9	17.5[e]	~5	170
sPTPOF-70	1.00	110	396	53.4	0.99	6.3	~12	15.5[e]	~17	170
sPTPOF-80	1.13	119	391	52.6	0.86	7.9	~16	5.2[e]	~40	170
sPTPOF-90	1.26	210	388	51.3	0.75	9.4	~22	2.2[e]	~55	170
sPTPOF-100	1.38	430	385	38.4	0.69	13	24.8	2.0[e]	90	170
tsPTPO-80	1.36	50.5	388	24.2	0.92	3.3	~32	80[f]	~34	158
tsPTPO-85	1.43	60.2	379	26.0	1.05	5.2	~34	55[f]	~45	158
tsPTPO-90	1.51	113	375	29.2	1.07	5.5	~36	21[f]	~54	158
tsPTPO-95	1.58	91.2	365	40.7	1.13	15	~38	18[f]	~60	158
tsPTPO-100	1.65	70.2	352	42.2	1.17	17	52	13[f]	87	158
msPTPO-100	1.65	134	376	28.9	0.82	18	180	3.0[f]	-	158
SPTES	1.647	-	446[j]	-	-	-	~98	2.4[f]	138	171
SPTES/Si-imP2.5	1.652	-	-	-	-	-	~11	2.7[f]	~150	171
SPTES/Si-imP5.0	1.579	-	456[j]	-	-	-	~115	3.1[f]	173	171
SPTES/Si-imP7.5	1.564	-	-	-	-	-	~95	3.3[f]	~140	171
SPTES/Si-imP10	1.543	-	-	-	-	-	~88	3.8[f]	~136	171
sPATPO-80	1.36	136[163]	412[163]	39.9	0.66	20	30[163]	35	~55[163]	172
sPATPO80/sPBI2	1.36	-	-	42.2	0.82	11	-	205	25	172
sPATPO-90	1.51	156[163]	408[163]	29.3	0.54	19	116[163]	20.5	95.4[163]	172
sPATPO90/sPBI2.5	1.50	-	-	31.4	0.57	31	52	110	~75	172
sPATPO90/sPBI3.0	1.50	-	-	32.9	0.73	30	-	200	67	172
sPATPO90/sPBI3.5	1.50	-	-	34.7	0.75	21	-	210	-	172
sPATPO-100	1.65	199[163]	405[163]	22.9	0.47	7.7	319[163]	6.5	120[163]	172
sPATPO100/sPBI5.5	1.63	-	-	34.0	0.51	28	-	120	84	172
sPATPO100/sPBI6.0	1.63	-	-	35.9	0.58	20	-	276	74	172
sPATPO100/sPBI6.5	1.62	-	-	36.6	0.62	12	34	>288	-	172

[a] Theoretical IEC value, [b] weight-average molecular weight, [c] 5% decomposition temperature obtained from TGA analysis, [d] WU values at 80 ℃, [e] starting fractured time in Fenton's reagent at 80 ℃, [f] complete dissolution time in Fenton's reagent at 80 ℃, [g] σ values under fully hydrated state at 80 ℃, [h] onset decomposition temperature, [i] σ values at 85 ℃ in 85% RH, [j] initial degradation temperature in TGA analysis.
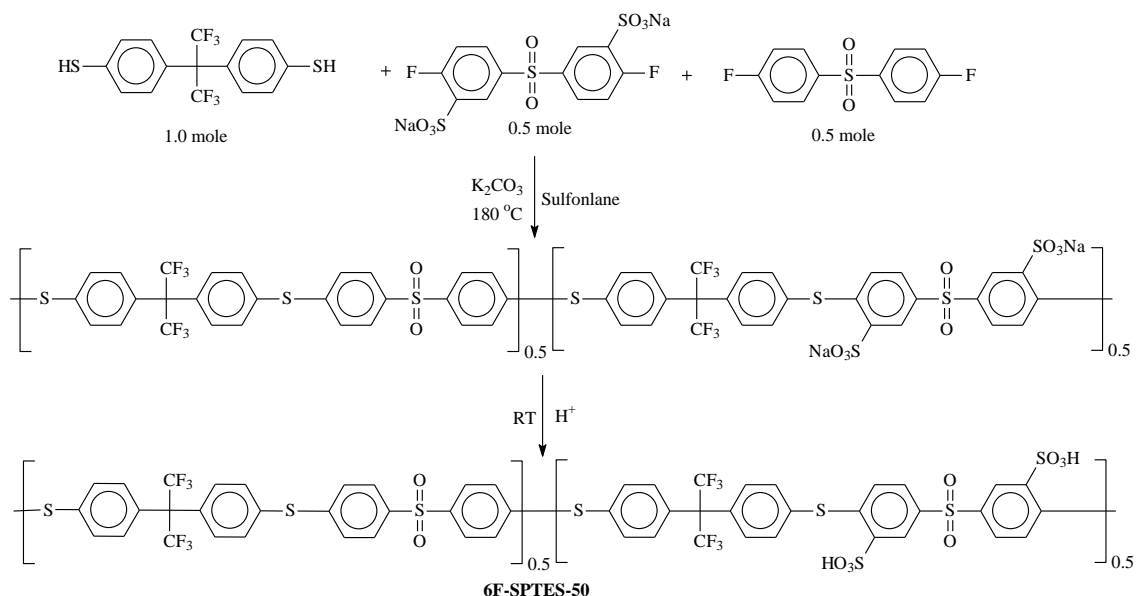
Scheme 11. The synthesis scheme of the fluoro-sulfonated poly(arylene thioether sulfone) copolymer (6F-SPTES-50).[169]

bis(4-fluorophenyl)phenyl phosphine oxide and bis(4-fluorophenyl)phenyl phosphine oxide, as depicted in **Scheme 12**.[170]

The non-sulfonated homopolymer (PTPOF) and sPTPOF-x copolymers showed high M_w (110-430 kg/mol) and PDI (1.57-2.00) values in GPC analysis.[170] The IEC values of the sPTPOF-x copolymers were calculated between 0.87-1.38 meq/g, as illustrated in **Table 5**. The sPTPOF-x copolymers exhibited high thermal ($T_{d5\%} \leq 385$ ℃) and mechanical stabilities (TS: 48-55 MPa and YM: 695-1068 MPa), as tabulated in **Table 5**. Due to the presence of the hydrophobic hexafluoroisopropylidene unit, the sPTPOF-x copolymers demonstrated high dimensional stability (the SR value of the sPTPOF-100 membrane was 5.3% at 80 ℃).[170] The morphological AFM phase images of the sPTPOF-x membranes exemplified a unique nano-scale phase-segregated morphology that favors the agile proton conduction and restricts the excessive swelling.[170] Out of all the membranes, the sPTPOF-100 membrane illustrated the highest σ value (90 mS/cm) at 80 ℃ (**Table 5**). As compiled in **Table 5**, the sPTPOF-x membranes showed oxidative stability (τ) values between 2.0 and 17.5 h.

Yao *et al*. synthesized a series of trisulfonated and monosulfonated poly(arylene thioether phosphine oxide)s [tsPTPO-x and msPTPO-100] with different sulfonic acid contents by the nucleophilic polycondensation reaction as depicted in **Scheme 13**.[158] The IEC values of the copolymers were calculated in the range of 1.36-1.65 meq/g (**Table 5**). The GPC results (M_w: 50-134 kg/mol and PDI: 1.52-1.71) of the copolymers confirmed the formation of the high molecular weight copolymers.[158] All the trisulfonated and monosulfonated copolymers exhibited high thermal and mechanical stability, as tabulated in **Table 5**. The tsPTPO-100 copolymer membrane showed moderate WU (52%) and SR (21%) values at 80 ℃.[158] The tsPTPO-x membranes displayed excellent oxidative stability in Fenton's reagent at 80 ℃, as provided in **Table 5**. The trisulfonated tsPTPO-100 membrane showed the highest proton conductivity value of 87 mS/cm at 80 ℃, which is close to the Nafion-117.[158]

Ding *et al*. synthesized a series of phosphorylated nanocomposite membranes (SPTES/Si-imPx) for PEM applications.[171] The schematic illustration of the synthesis of imino-functionalized phosphorylated silica nanoparticles (Si-imP) is depicted in **Figure 9**. They prepared a series of nanocomposite membranes of sulfonated poly(arylene thioether sulfone), SPTES, of various wt% of nanoparticles loading (2.5, 5.0, 7.5, and 10 wt%).[171] The reaction scheme for synthesizing SPTES is provided in **Scheme 14**. The homogeneous and uniform distribution of the Si-imP nanoparticles in the SPTES/Si-imPx membranes was
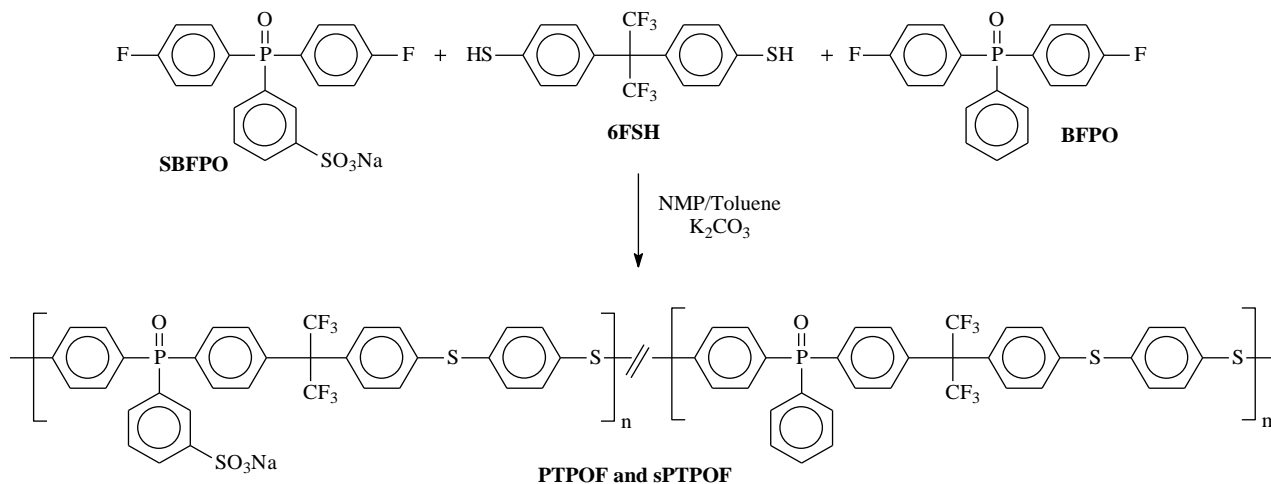
Scheme 12. The synthesis scheme of hexafluoroisopropylidene- and phosphine oxide-based PTPOF and sPTPOF copolymers.[170]

Banerjee and Ghanti

Innov. Chem. Mater. Sustain. **2025,** 2(1), 032-073
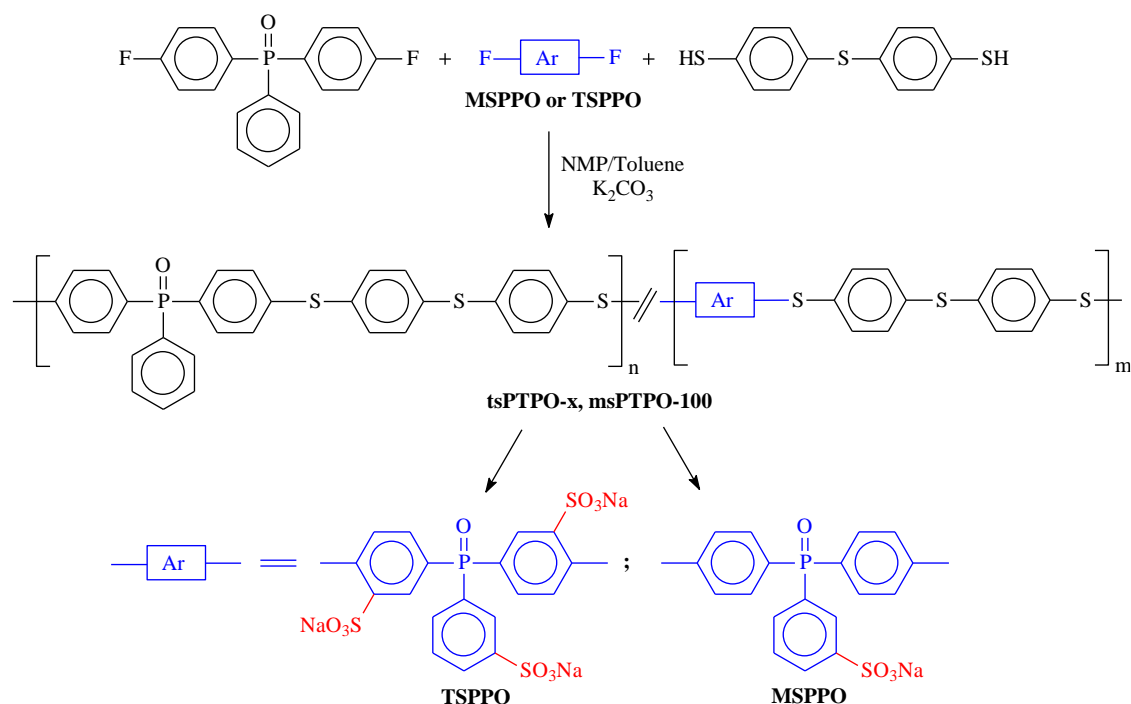
Scheme 13. Synthesis scheme of the phosphine oxide-based TSPPO and MSPPO copolymers [158]
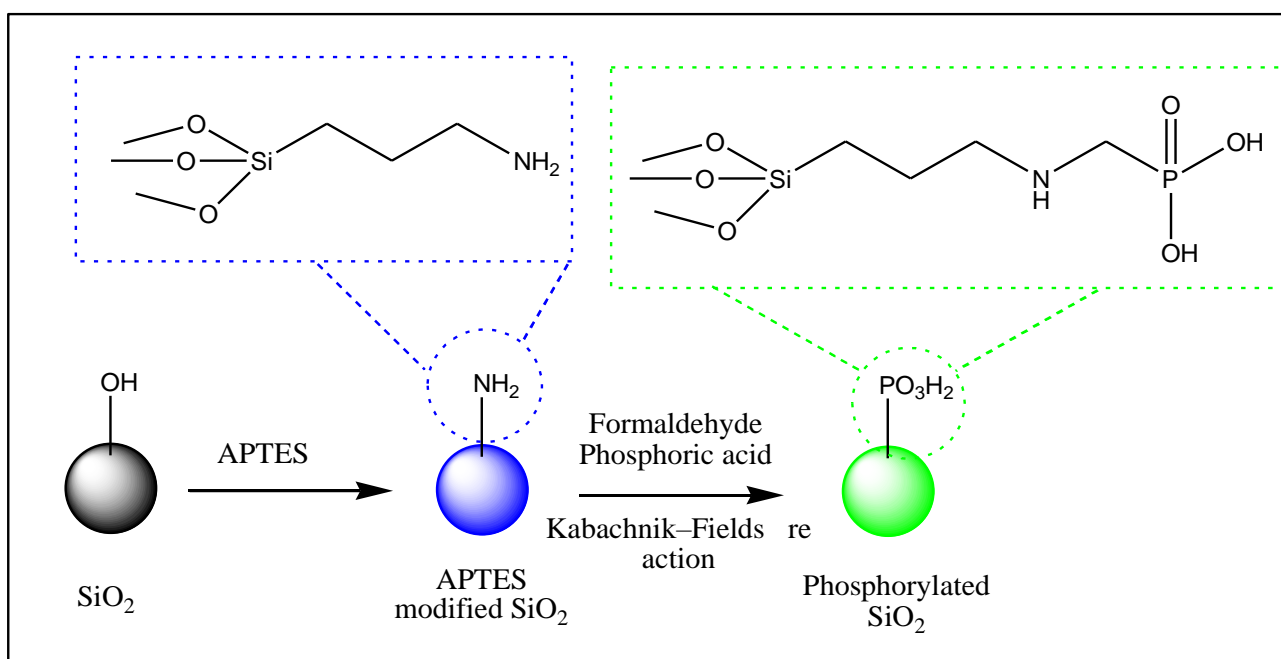

Figure 9. The schematic illustration of the synthesis of imino-containing phosphorylated silica particles (Si-imP).[171]

confirmed by FTIR, SEM, and EDX analysis.[171] The composite membranes demonstrated higher thermal stability than the SPTES membrane, which confirmed that the Si-imP fillers enhanced the thermos-oxidative stability of the composite membranes (**Table 5**). The SPTES/Si-imP5.0 showed the highest WU (~115%) and SR (~55) values among all the membranes.[171] The SPTES/Si-imP10 composite membrane 3.8 h in Fenton's reagent at 80 ℃ (**Table 5**). The SPTES/Si-imP5 composite membrane showed 26% higher proton conductivity (173 mS/cm) than the pristine SPTES membrane (138 mS/cm) at 80 ℃, as provided in **Table 5**. The predicted proton transportation mechanism in the composite membranes shows that the addition of Si-imP nanoparticles into the polymer matrix boosted the proton conduction process through

the additional electrostatic and intermolecular hydrogen bonding interactions.[171]

Yan *et al.* prepared a series of sulfonated blend membranes of sulfonated poly(arylene thioether phosphine oxide)s (sPATPOs) and sulfonated polybenzimidiazoles (sPBIs) to improve the dimensional stability.[172] The synthesis schemes of the sPATPOs and sPBIs are shown in **Schemes 15** and **16**. The theoretical and experimental IEC values of the blend membranes (sPATPOxx/sPBIy, where xx represents the DS value of sPATPO and y represents wt% of sPBI) were obtained between 1.36-1.63 meq/g and 1.28-1.61 meq/g, respectively.[172] The blend copolymers demonstrated higher thermal stability than the pristine sPATPO copolymers due to
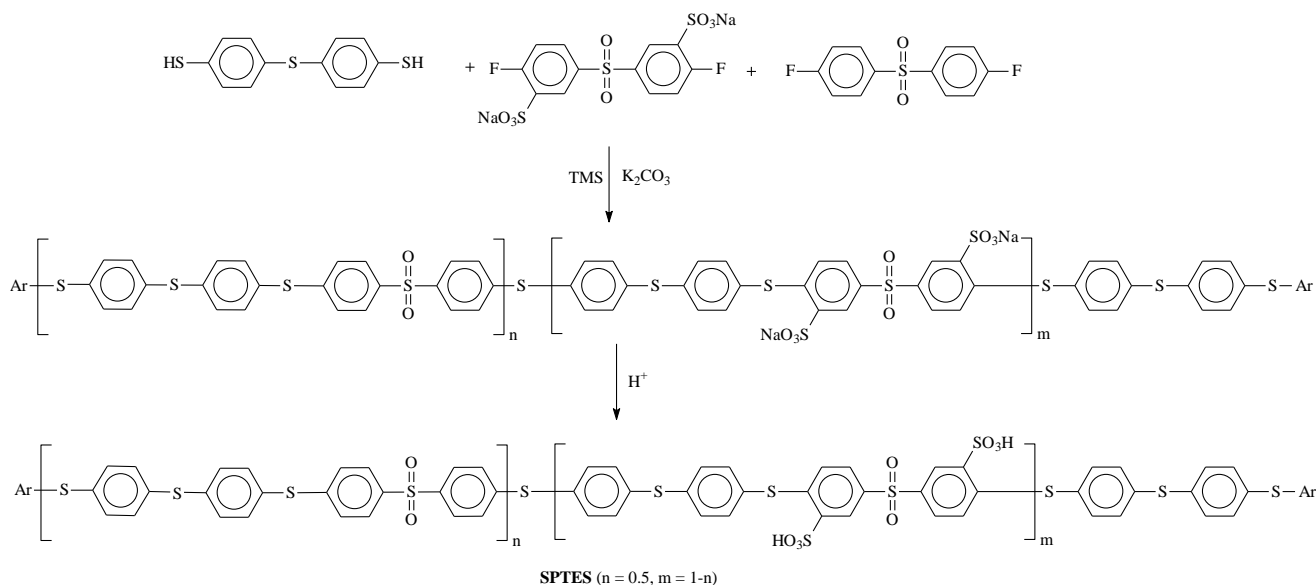
Scheme 14. The synthesis scheme of the sulfonated poly(arylene thioether sulfone), SPTES.[171]

the stronger acid-base interactions between sPATPO and sPBI.[172] The blend membranes (WU: 34-52% and SR: 7-18% at 80 ℃) showed higher dimensional stability than the pristine sPATPO membranes (WU: 30-319% and SR: 9-10% at 80 ℃).[163,172] The blend membranes exhibited higher mechanical stability than the pristine membranes due to the stronger intermolecular interactions, as compiled in **Table 5**. The AFM morphological investigation of the blend membranes revealed that the hydrophilic domains become more interconnected with the increase in wt% of the sPBI.[172] Among all the blend membranes, the sPATPO100/sPBI5.5 membrane showed the highest σ value of 84 mS/cm at 80 ℃, as illustrated in **Table 5**. The blend membranes exhibited outstanding oxidative stability in Fenton's reagent at 80 ℃, mainly due to the lower absorption properties of the blend membranes and the radical resistance property of the sPBIs backbone.[172]

4.2.5 Polybenzimidazoles, PBIs

Hydrocarbon-based aromatic polymers composed of heterocyclic moieties, especially the nitrogen-containing heterocyclic units such as PBIs, polybenzothiazoles (PBTs),

mechanical, dimensional, and oxidative stabilities, and high ion conduction abilities.[61,173-175] Among these, PBIs have gained much consideration in this century owing to their promising properties in the PEMFC applications.[173,176-180] The phosphoric acid (PA)-doped PBIs usually showed extremely high proton conductivity even at anhydrous conditions and a moderate to high-temperature range (up to 200 ℃).[173] The PC values of the PA-doped PBIs mainly depend on the PA-doping levels. However, recent studies revealed that the PA-doped sulfonated polybenzimidazoles (SPBIs) have gained particular interest due to their higher proton conductivity values than those of the non-sulfonated PA-doped PBIs.[179,181-184] Generally, the PBIs are synthesized by the polycondensation reaction between tetramine compounds with diacids or dianhydride in polyphosphoric acid (PPA) or phosphorus pentoxide-methanesulfonic acid (PPMA). As described earlier, the SPBIs are also synthesized by the direct sulfonation and post-sulfonation processes.[173,183,184] Herein, a few recently developed SPBIs for moderate or high-temperature PEMFC applications are described below.

Yan *et al.* synthesized a series of sPBIs with varying DS
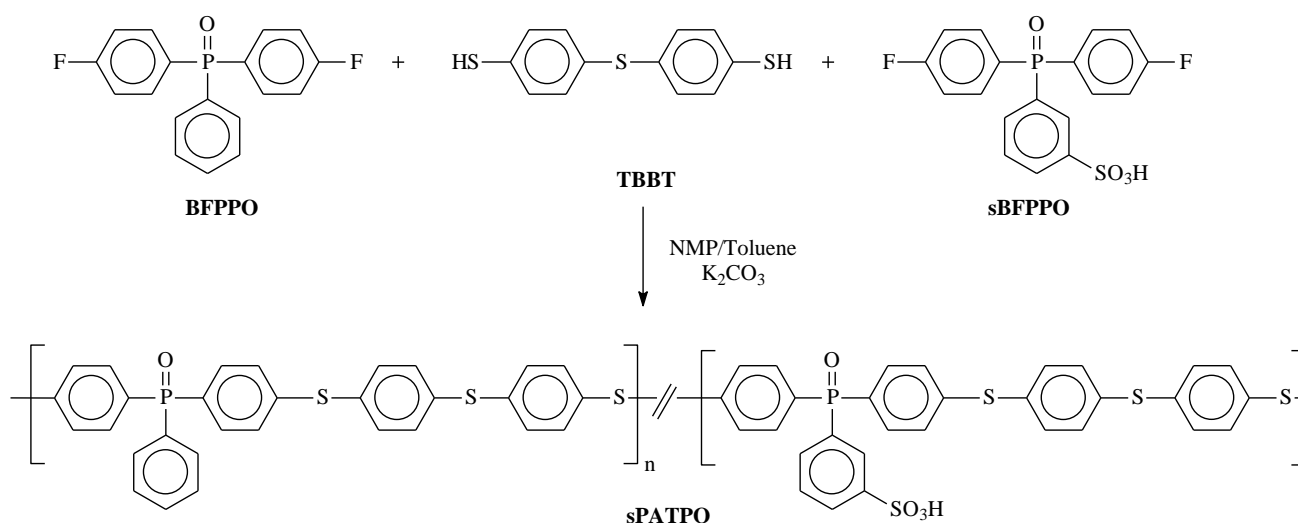
Scheme 15. The synthesis scheme of the sulfonated poly(arylene thioether phosphine oxide)s, sPATPOs.[172]

polybenzoxazoles (PBOs), polytriazoles (PTs), etc., have attracted remarkable attention due to their high thermal,

values by the direct polycondensation reaction of 3,3′-diaminobenzidine (DAB) with 3,3′-Disulfonate-4,4′-

Banerjee and Ghanti

Innov. Chem. Mater. Sustain. **2025**, 2(1), 032-073

dicarboxylbiphenyl (SCBP) and other non-sulfonated diacids, as depicted in **Scheme 17**.[185] The IEC values of sPBI-xx (xx: 30, 40, 50, 60, and 70) copolymers were between 1.12-2.59 meq/g, as compiled in **Table 6**. The GPC results (M$_w$: 147-248 kg/mol and PDI: 2.19-2.86) of the sPBI-xx copolymers confirmed the formation of high molecular weight polymers.[185] The sPBI-xx copolymers showed high thermal and viscoelastic properties.[185] All the sPBI-xx demonstrated anomalous water absorption properties, where both the WU and SR values initially increased up to 50 °C, then decreased between 50-70 °C, and again slightly increased between 70-90 °C.[185] The elapsed time (τ) of all the sPBI-xx membranes was more than 72 h (Table 3), which indicates the superior oxidative stability of those copolymers. Out of all the membranes, the sPBI-70 membrane demonstrated the highest PC value of 2.79 mS/cm at 80 °C.[185]

Chen *et al*. synthesized a series of phosphine oxide-based SPBIs (sPBI-PO) by the random co-polycondensation reaction of sulfonated bis(4-methylbenzoate)phenylphosphine oxide (sBMPO), bis(4-methylbenzoate)phenylphosphine oxide (BMPO), and 3,3′-diaminobenzidine (DAB) in PPA, as shown in **Scheme 18**.[186] The η$_{inh}$ values of the sPBI-POxx copolymers were found between 1.51-2.41dL/g, which confirms the formation of the high molecular weight copolymers by the random co-polycondensation reaction.[186] The sPBI-POxx copolymers exhibited high thermal and mechanical stabilities, as compiled in **Table 6**. All the copolymer membranes displayed higher oxidative stability (τ > 48 h and RW ≥ 95%).[186] The sPBI-POxx membranes showed WU values between 21.3-25.2% at 80 °C, as provided in **Table 6**. The AFM morphological investigation of the sPBI-POxx revealed that the ionic cluster becomes much closer and more prominent with the rise in the DS value of the copolymers.[186] The sPBI-PO90 membrane showed the highest PA uptake of 187.3%, with the lowest volume swelling (170.6%).[186] The undoped sPBI-POxx membranes showed a PC value of 4.6-7.1 mS/cm at 80 °C under a fully hydrated state (**Table 6**). Whereas the PA-doped sPBI-PO90 membranes showed 3.9 times higher PC value (27.6 mS/cm) compared to the undoped sample at 80 °C under 100% RH.[186]

Yan *et al*. synthesized a series of SPBIs (sPBI-x) with a controlled proportion of pendant sulfophenylsulfonyl groups by the direct polycondensation reaction of 3,3′-diaminobenzidine (DAB) with 4′-Sulfonate-2,5-dicarboxyphenyl sulfone (SCPS) and 2,5-dicarboxyphenyl sulfone (CPS) in PPA as shown in **Scheme 19**.[187] The high molecular weight (M$_w$: 111-143 kg/mol and PDI: 170-1.93) sPBI-x copolymers showed excellent solubility in commonly available polar aprotic solvents (DMF, DMSO, DMAc, and NMP).[187] The sPBI-x (x: 60, 70, 80, 90, 100) demonstrated high thermal (T$_{d5\%}$: 387-407 °C), mechanical (TS: 114-123 MPa; YM: 1.65-1.72 GPa; EB: 20-27%), hydrolytic (1% weight loss after 24 h of the hydrolytic stability in deionized water at 140 °C), and oxidative stabilities (τ > 168 h), as illustrated in **Table 6**.[187] The sPBI-100 membrane exhibited the highest water absorption properties (WU: 20.2% and SR: 8.2%) at 80 °C among the sPBI-x membranes.[187] The microstructural analysis of the sPBI-x membranes confirmed the formation of more interconnected ionic aggregation with increased sulfonic acid contents in the copolymer architecture.[187] The sPBI-100
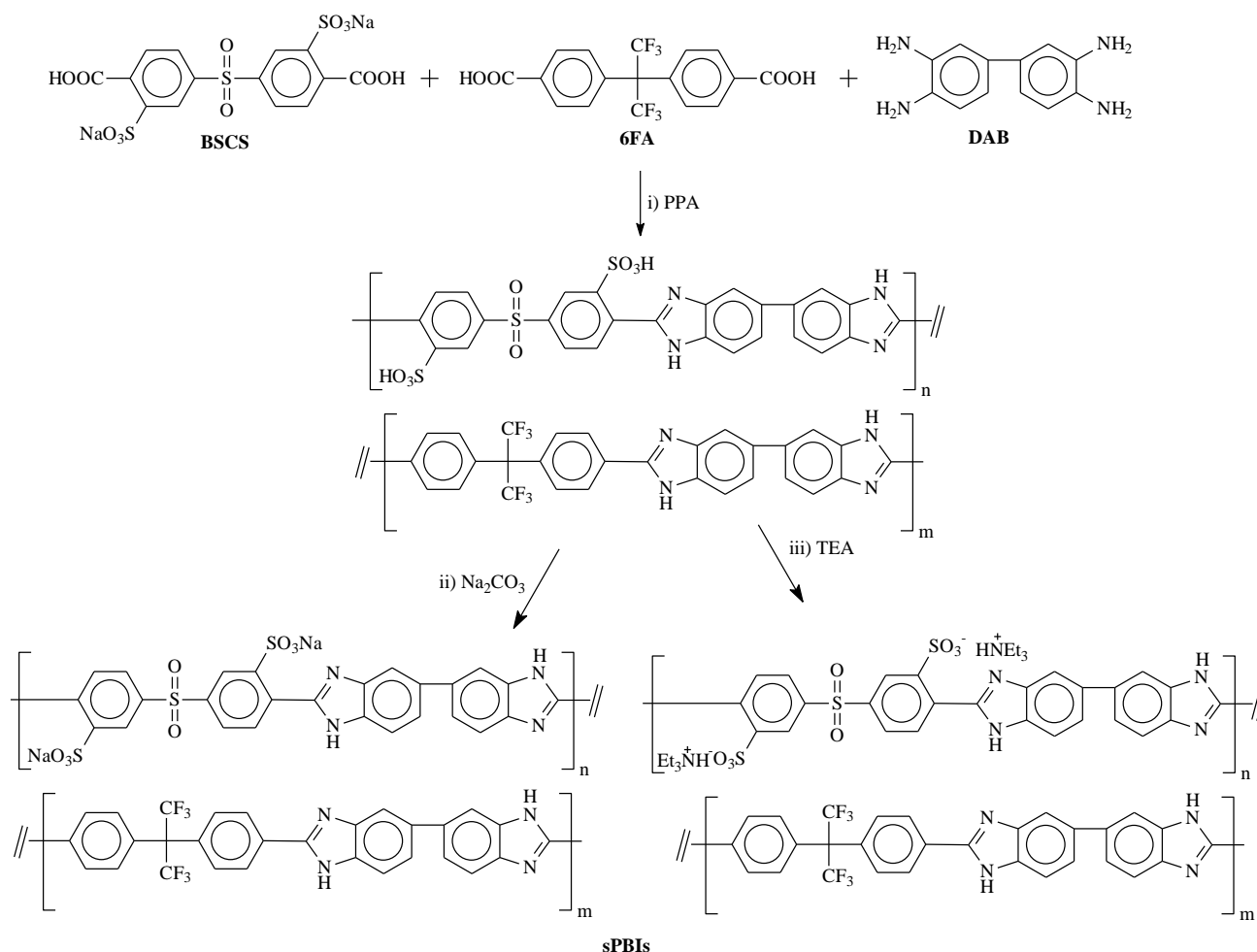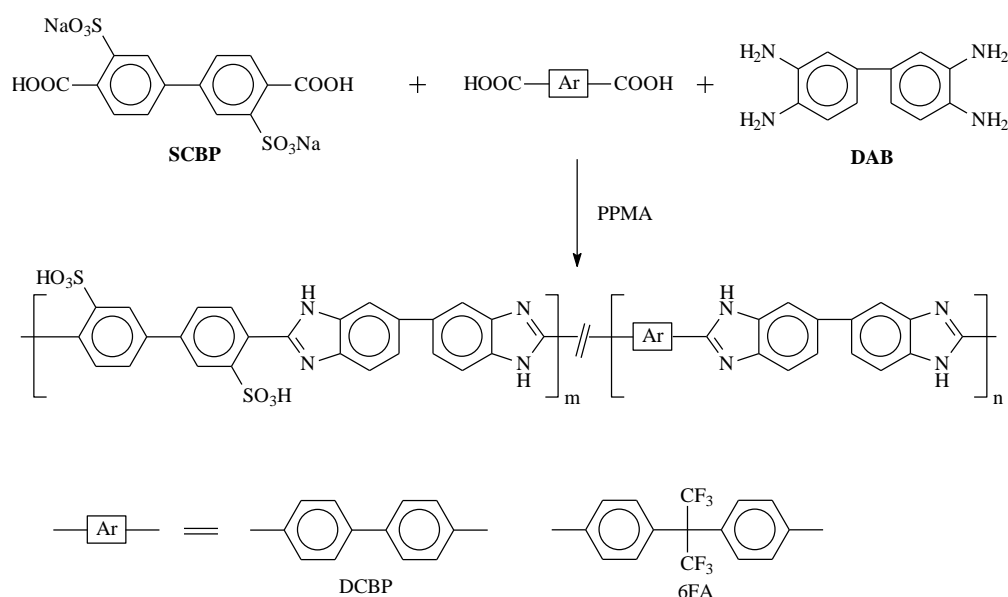

Scheme 16. The synthesis scheme of the sulfonated polybenzimidazoles, sPBIs.[172]

Table 6. *The IEC, M_w, T_d, TS, YM, EB, WU, τ, and σ values of the SPATs.*

Polymer	IEC (meq/g)[a]	M_w (kDa)[b]	T_d (℃)[c]	TS (MPa)	YM (GPa)	EB (%)	WU (%)[d]	τ (h)[e,f]	σ (mS/cm)[g]	Ref.
sPBI-30	1.12	239	480	-	-	-	~15	>72[e]	-	185
sPBI-40	1.49	179	475	-	-	-	~17	>72[e]	-	185
sPBI-50	1.85	248	463	-	-	-	~19	>72[e]	-	185
sPBI-60	2.22	196	461	-	-	-	~20	>72[e]	-	185
sPBI-70	2.59	167	459	-	-	-	~21	>72[e]	2.79	185
sPBI-PO60	1.10	-	491	60	1.56	16.2	21.3	>48[e]	4.6	186
sPBI-PO70	1.27	-	490	45	1.87	6.7	-	>48[e]	4.9	186
sPBI-PO80	1.43	-	488	43	1.81	4.9	-	>48[e]	6.5	186
sPBI-PO90	1.57	-	485	53	1.39	15.2	25.2	>48[e]	7.1	186
sPBI-PO100	-	-	480	-	-	-	-	-	-	186
sPBI-60	1.21	143	407	-	-	-	16.5	>168[f]	~0.9	187
sPBI-70	1.39	133	403	114	1.65	27	17.3	>168[f]	~1.0	187
sPBI-80	1.56	111	396	120	1.71	25	18.0	>168[f]	~1.4	187
sPBI-90	1.73	128	395	123	1.72	20	19.5	>168[f]	~1.7	187
sPBI-100	1.89	139	387	-	-	-	20.2	>168[f]	2.8	187
OPBI	-	-	-	0.50	-	81	11.7	-	67[h]	188
PSM 1-3%	-	-	-	0.76	-	134	13.3	-	202[h]	188
PSM 1-5%	-	-	-	1.55	-	176	16.1	-	233[h]	188
PSM 1-7%	-	-	-	1.51	-	285	18.9	-	266[h]	188
PSM 1-10%	-	-	-	1.31	-	360	19.8	-	290[h]	188
PSM 2-7%	-	-	-	1.45	-	274	18.9	-	277[h]	188
PSM 2-10%	-	-	-	1.18	-	350	20.9	-	308[h]	188
SHBPBI	-	-	259	-	-	-	-	-	-	189
oPBI-TAIC(5%)-SHBPBI(40%)	-	-	326	39.5	-	11.4	-	-	122[i]	189
oPBI-TAIC(10%)-SHBPBI(40%)				54.4	-	9.8	-	-	110[i]	189
oPBI-TAIC(5%)-SHBPBI(50%)	-	-	324	35.8	-	12.9	-	-	147[i]	189
oPBI-TAIC(10%)-SHBPBI(50%)	-	-	302	42.9	-	10.6	-	-	136[i]	189

[a] Theoretical IEC value, [b] weight-average molecular weight, [c] 5% decomposition temperature obtained from TGA analysis, [d] WU values at 80 ℃, [e] starting fractured time in Fenton's reagent at 80 ℃, [f] starting dissolution time in Fenton's reagent (30 ppm $FeSO_4$ in 30% H_2O_2) at 80 ℃, [g] σ values under fully hydrated state at 80 ℃, [h] σ values in anhydrous conditions at 160 ℃, [i] σ values in 100% RH at 180 ℃.
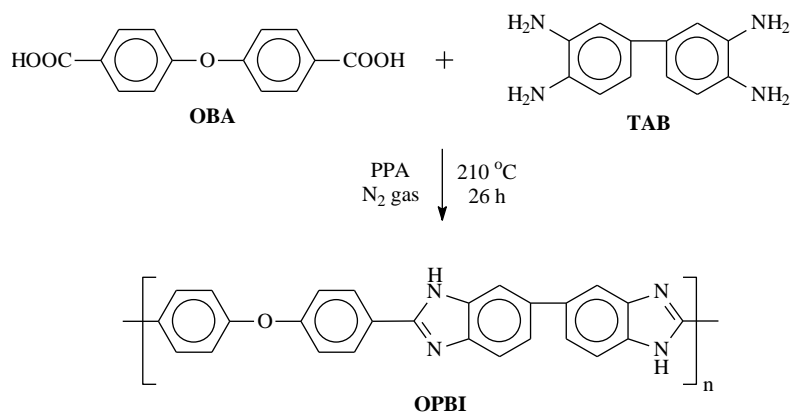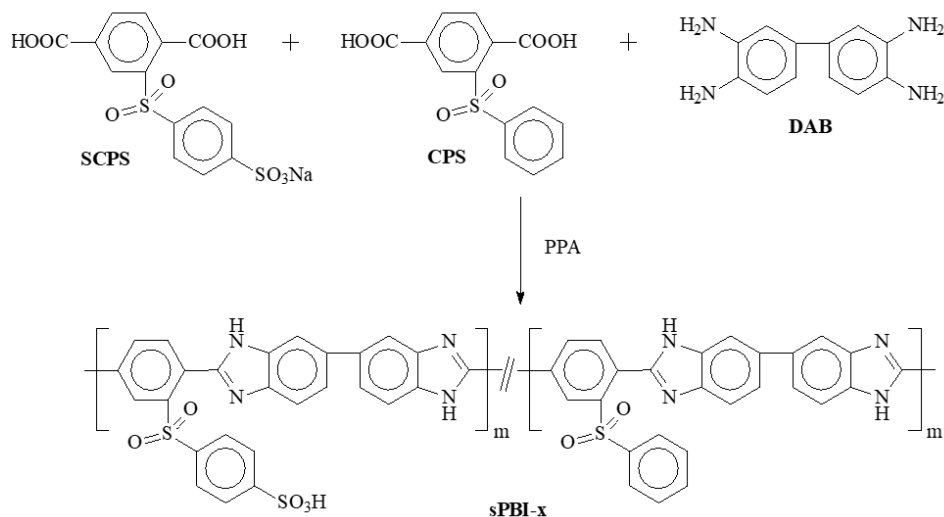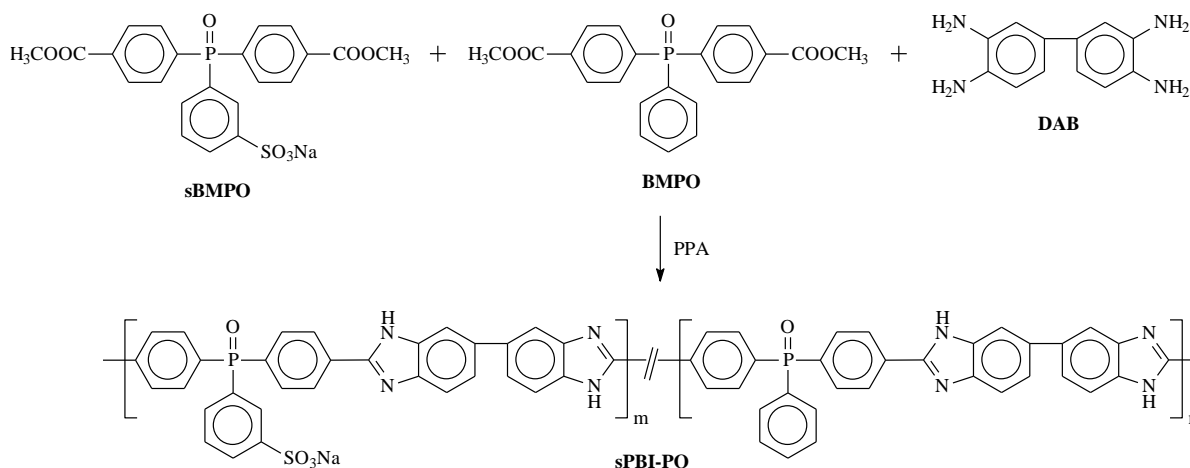

Scheme 17. The synthesis scheme of the SPBI copolymers (sPBI-XX).[185]

membrane demonstrated the highest σ value of 2.8 mS/cm at 80 ℃ in deionized water, as compiled in **Table 6**. The σ values of the sPBI-x membranes were lower than those in the studies performed without the PA-doping.

Das *et al.* synthesized a series of sulfonated MOF-based PBI composite membranes with different wt% of MOF (PSM 1 or PSM 2) loading.[188] The pristine PBI polymer was synthesized by the polycondensation reaction of 3,3',4,4'-tetraaminobiphenyl (TAB) and 4,4'-oxybis(benzoic acid) (OBA), as shown in **Scheme 20**.[188] The PSM 1 and PSM 2 MOFs were synthesized by the post-modification of the UiO-66-NH2 MOF with 1,3-propane sultone and 1,4-butane sultone, respectively.[188] A series of composite PBI membranes were fabricated by the solution blending method with various wt% of MOF loading; the fabrication of PBI composite

membranes is shown in **Figure 10**.[188] The nanocomposite membranes were doped with PA and utilized for the PEM properties evolution. The PA-doped nanocomposite membranes demonstrated higher thermal, mechanical, and oxidative stabilities than the pristine OPBI membrane.[188] The matrix membranes with higher wt% of MOF loading (7 and 10%) showed more fibrous-like networks and porous structures in cross-sectional FESEM analysis.[188] Among the nanocomposite membranes, the PSM 2-10% membranes showed the maximum σ value of 308 mS/cm at 160 ℃ under anhydrous conditions (**Table 6**). The PSM 2 loaded composite membrane showed enhanced proton conductivity due to the extensive interfacial H-bonding in the composite polymer.

Li *et al.* synthesized a series of highly sulfonated covalently cross-linked PBI membranes for high-temperature proton

Scheme 18. Synthesis scheme of the sPBI-PO.[186]

Scheme 19. The synthesis scheme of the pendant sulfophenylsulfonyl groups-containing SPBI copolymers (sPBI-x).[187]

Scheme 20. The synthesis scheme of the pristine OPBI polymer.[188]

exchange membrane (HTPEM) applications[189] The hyperbranched polybenzimidazole (HBPBI) was synthesized by the polycondensation reaction of give 4,4',4''-((2,4,6-trioxo-1,3,5-triazinane-1,3,5-triyl)tris(oxy))tribenzoic acid (TTA) and 3,3'-diaminobenzidine (DAB) in presence of P_2O_5 and methane sulfonic acid (MSA), as shown in **Scheme 21**.[189] Then, the sulfonated hyperbranched polybenzimidazole (SHBPBI) was prepared by the reaction of HBPBI with 1,3-propane sultone in

DMAc, which is depicted in **Scheme 21**.[189] Finally, a series of highly sulfonated covalently cross-linked oPBI-TAIC-SHBPBI membranes were fabricated from the mixing the ether-containing polybenzimidazole (oPBI), triallyl isocyanurate (TAIC), and SHBPBI in DMAc at 160 °C, as shown in **Scheme 22**.[189] The schematic illustration of the fabrication of the oPBI-TAIC-SHBPBI membranes are provided in **Figure 11**.[189] The

Banerjee and Ghanti

Innov. Chem. Mater. Sustain. **2025**, 2(1), 032-073
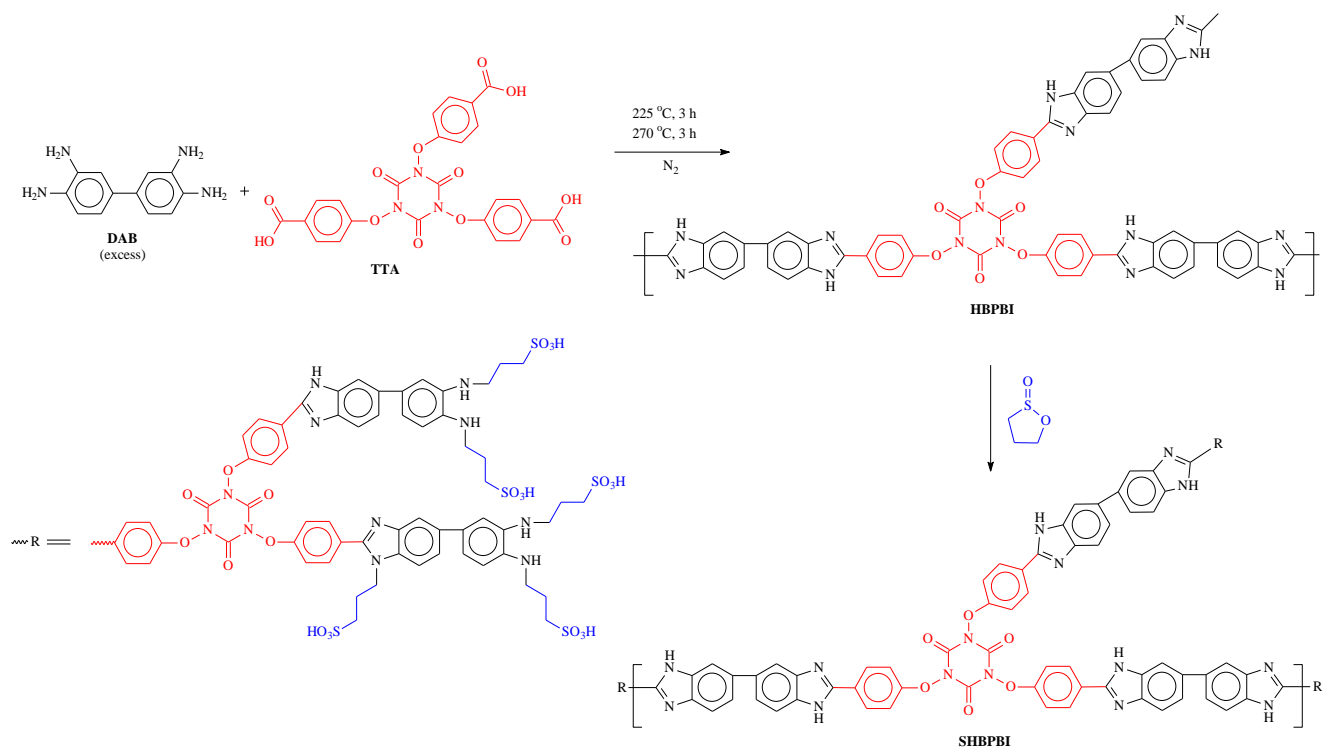
Scheme 21. The synthesis scheme of the sulfonated hyperbranched polybenzimidazole (SHBPBI).[189]
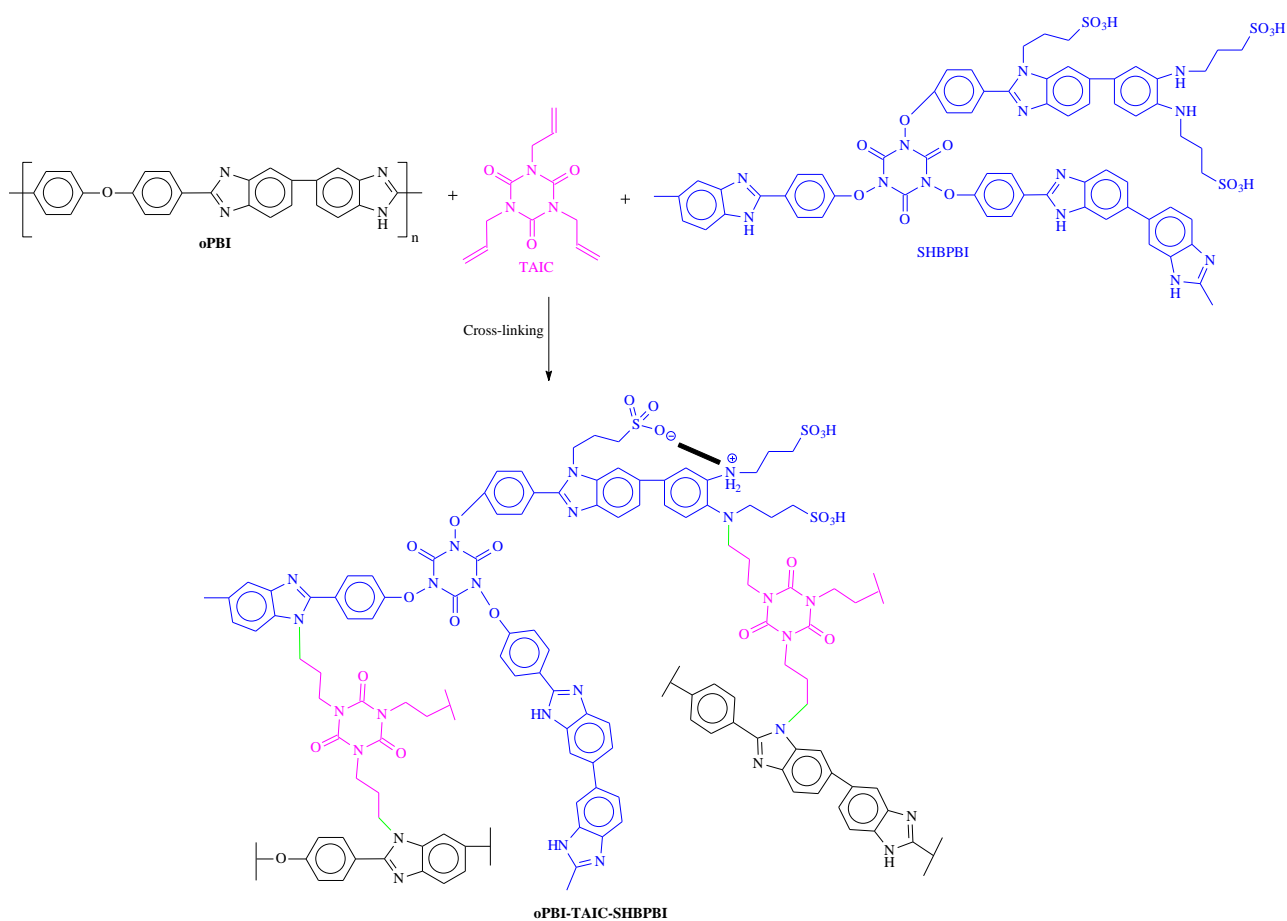
Scheme 22. The synthesis scheme of the highly sulfonated covalently cross-linked oPBI-TAIC-SHBPBI.[189]

covalently cross-linked oPBI-TAIC-SHBPBI showed higher thermal stability than the SHBPBI, as compiled in **Table 6**. The oPBI-TAIC-SHBPBI membranes' SEM analysis showed that the cross-section was homogeneous, dense, and defect-

free.[189] The stress-strain analysis of the oPBI-TAIC-SHBPBI membranes confirmed that the mechanical properties of the cross-linked membranes were increased with the increase in the cross-linking degree (CLD).[189] The membrane with the
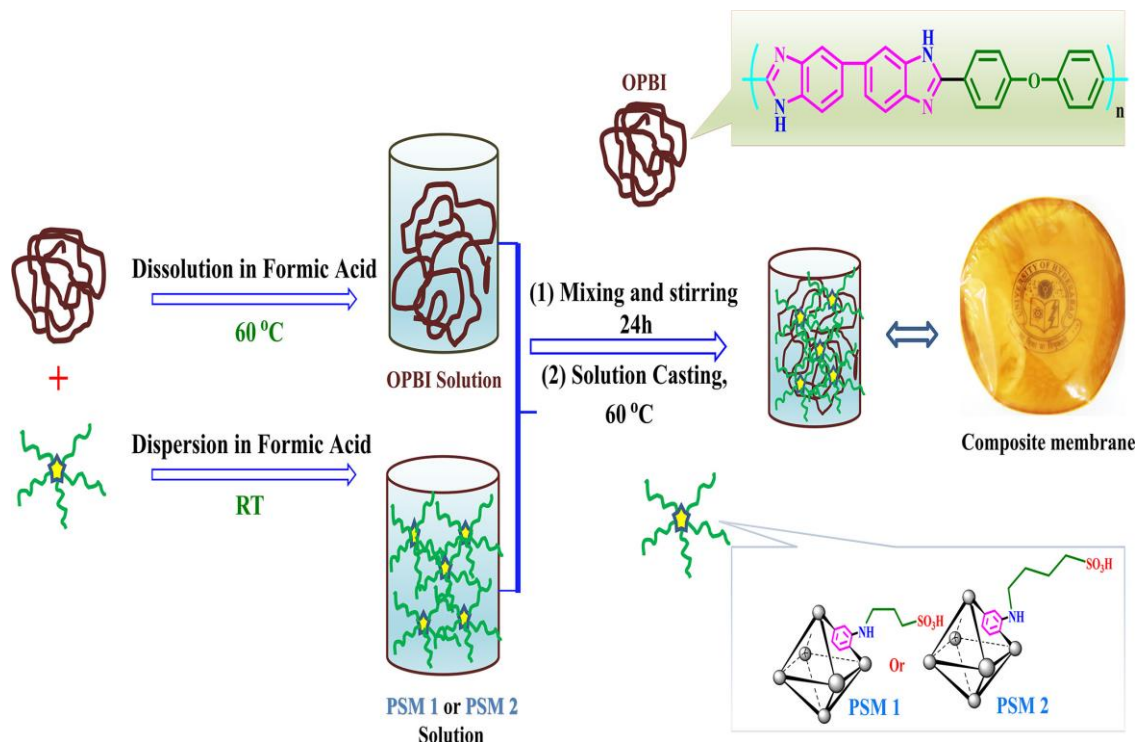
Figure 10. Schematic illustration of PSM 1 and PSM 2 loaded PBI composite membranes.[188] (Reprinted with permission from (188). Copyright (2020) American Chemical Society.)
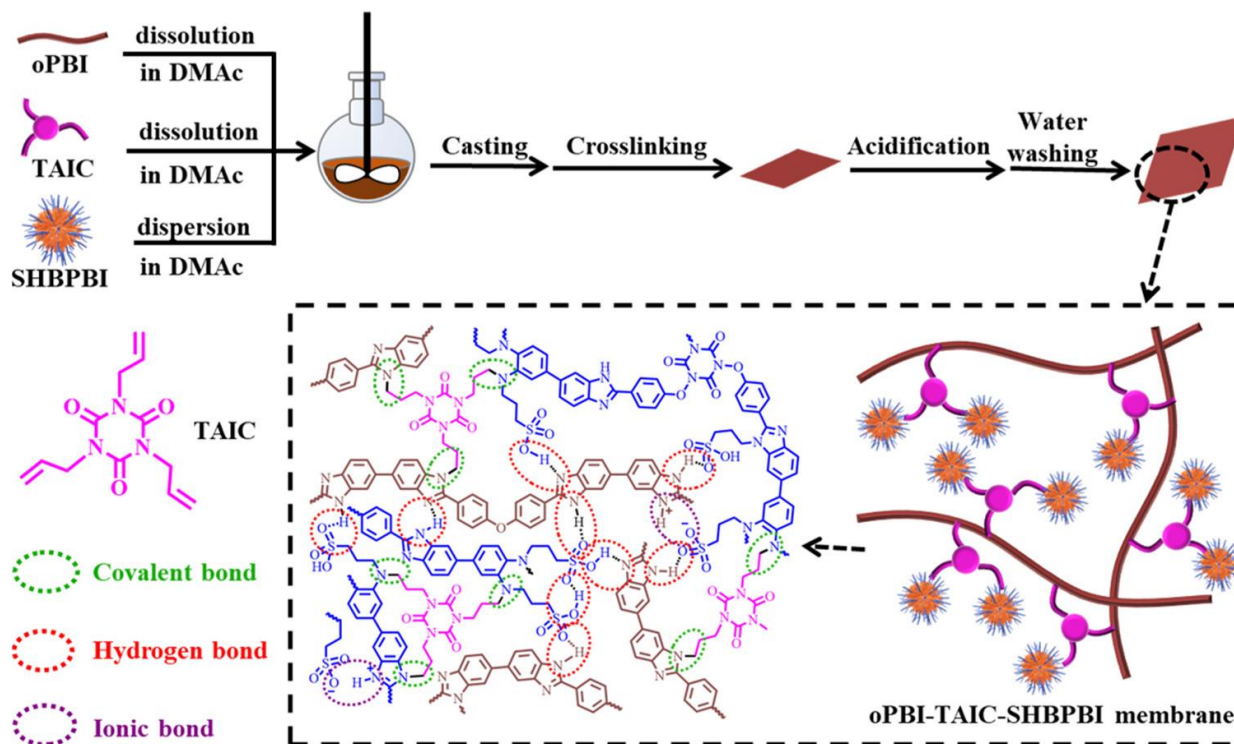
Figure 11. The schematic illustration of the fabrication of oPBI-TAIC-SHBPBI membranes.[189] (Reprinted with permission from (189). Copyright (2022) American Chemical Society.)

higher CLD demonstrated better dimensional stability (lower SR) than the membrane with lower CLD due to the increase in the covalent network with the increase in the CLD in the oPBI-TAIC-SHBPBI membrane.[189] Among all the covalently cross-

inked membranes, the oPBI-TAIC(10%)-SHBPBI(40%) membrane exhibited the highest oxidative stability (retaining 96.4% of weight after the Fenton's test) owing to its higher CLD

and lower proportion of sulfonated units.[189] The oPBI-TAIC(5%)-SHBPBI(50%) membrane demonstrated the maximum σ value of 147 mS/cm at 180 ℃ under 100% RH conditions (**Table 6**). The oPBI-TAIC(5%)-SHBPBI(50%) membrane retained 97.1% of its proton conductivity after washing with DI water for 96 h, which confirmed its durability

and low leaching ability of the cross-linked membrane that is superior for HTPEM applications.[189]

4.2.6 Polyimides, PIs

Hydrocarbon-based aromatic polyimides (PIs) are another special class of high-performing polymers known for their excellent thermal, mechanical, and electrochemical properties.[115,190-194] PIs are prepared by the polycondensation reaction of aromatic diamines with aromatic dianhydrides.[115,190-194] Generally, the polyimidization reaction proceeds through t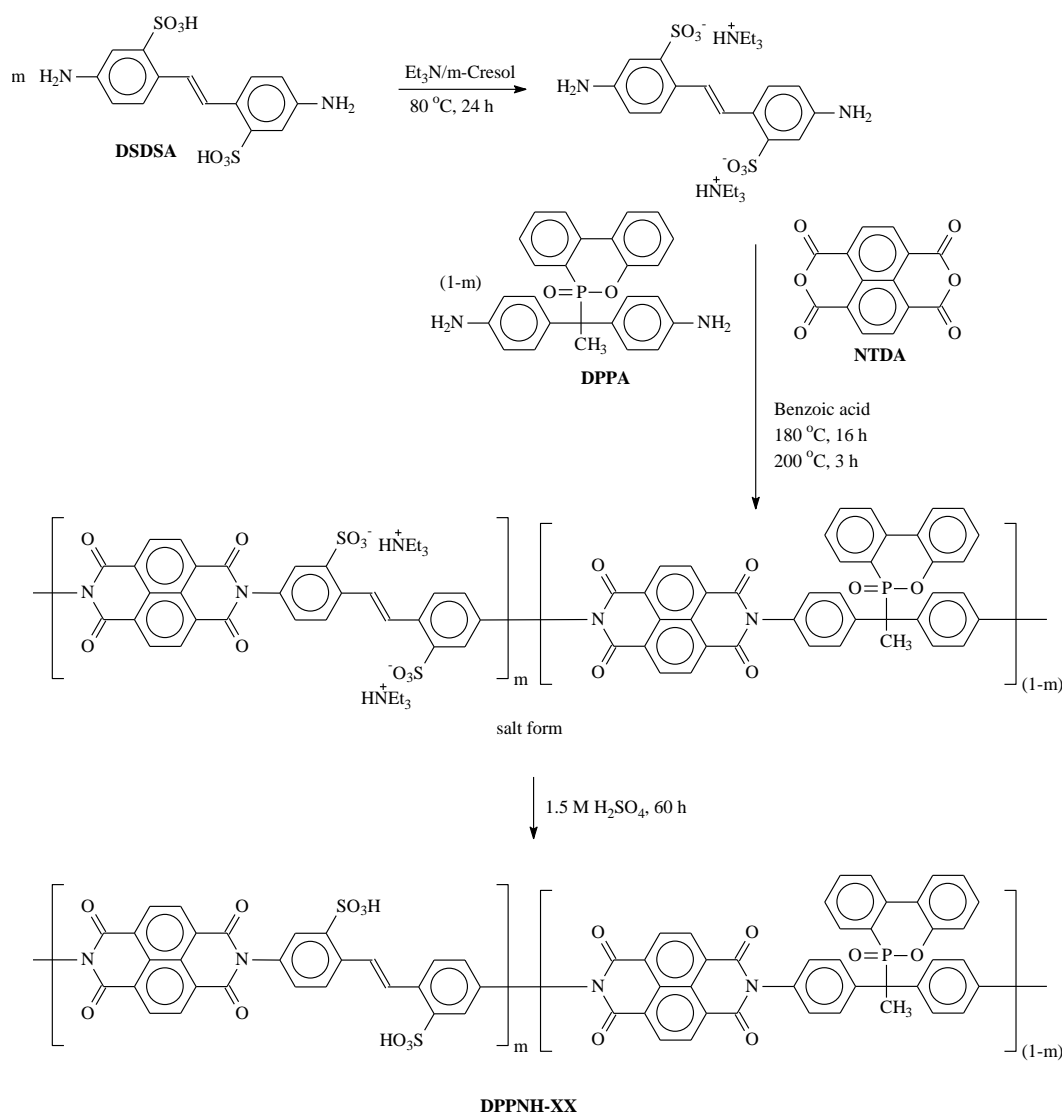wo steps; the first step is the formation of the polyamic acid (PAA) precursor, and the second step is the thermal or chemical cyclodehydration.[115,190-195] The chemical cyclodehydration of PAAs is mainly performed using acetic anhydride in the presence of a sodium acetate base.[115,190-195] Despite their excellent properties, they possessed limited applicability due to their high melting point, low processability, low solubility, and formation of various intermolecular charge transfer complexes (CTCs).[115,196,197] Thus, in recent years, several efforts have been employed to develop soluble, processable, and tractable PIs without compromising their high-performing properties. The sulfonated polyimides (SPIs) have gained remarkable attention as an alternative PFSA-based material due to the imide rings in the polymer backbone, which provide tremendous thermal stability, high mechanical characteristics, superior oxidative stability, and excellent proton conductivity.[96,198-200] Herein, a few recently developed SPI-based PEMs are discussed.

Banerjee *et al.* synthesized a series of 9,10-dihydro-9-oxa-10-phosphaphenanthrene 10-oxide (DOPO)-based SPIs (DPPNH-XX) having various DS values by the polycondensation reaction between 1,4,5,8-naphthalenetetracarboxylic dianhydride (NTDA) with 4,4′-diaminostilbene-2,2′-disulfonic acid (DSDSA) and 1,1-bis (4-aminophenyl)-1-(6-oxido-6H-dibenz <c, e> <1,2> oxaphosphorin-6-yl) ethane (DPPA), as shown in **Scheme 23**.[96] The DPPNH-XX copolyimides demonstrated high solubility in polar aprotic solvents.[96] The η_{inh} values of the DPPNH-XX copolymers were obtained between 1.01-1.22 dL/g.[96] The experimental IEC (IEC_{NMR}) values of the DPPNH-XX copolymers were calculated from the ^{1}H NMR spectra and obtained in close agreement with the theoretical IEC values.[96] The DPPNH-XX membranes showed high thermal and mechanical stabilities, as illustrated in **Table 7**. The DPPNH-XX membranes showed lowered SR values (in-plane SR: 6-10% at 80 ℃) than the other literature-reported sulfonated PEMs, which indicates the higher dimensional stability of the DOPO-based DPPNH-XX copolymers.[96] The DPPNH-XX membranes showed τ values between 7.0-24 h in Fenton's reagent at 80 ℃ (**Table 7**). The microstructural analysis of the DPPNH-XX membranes revealed an interconnected and well-segregated phase morphology.[96] Among all the copolyimides, the DPPNH-90 membrane demonstrated the highest σ value of 235 mS/cm at 80 ℃, as illustrated in **Table 7**. The proton conductivity-related E_a values of the DPPNH-XX copolymers were found between 10.8-13.3 kJ/mol.[96]
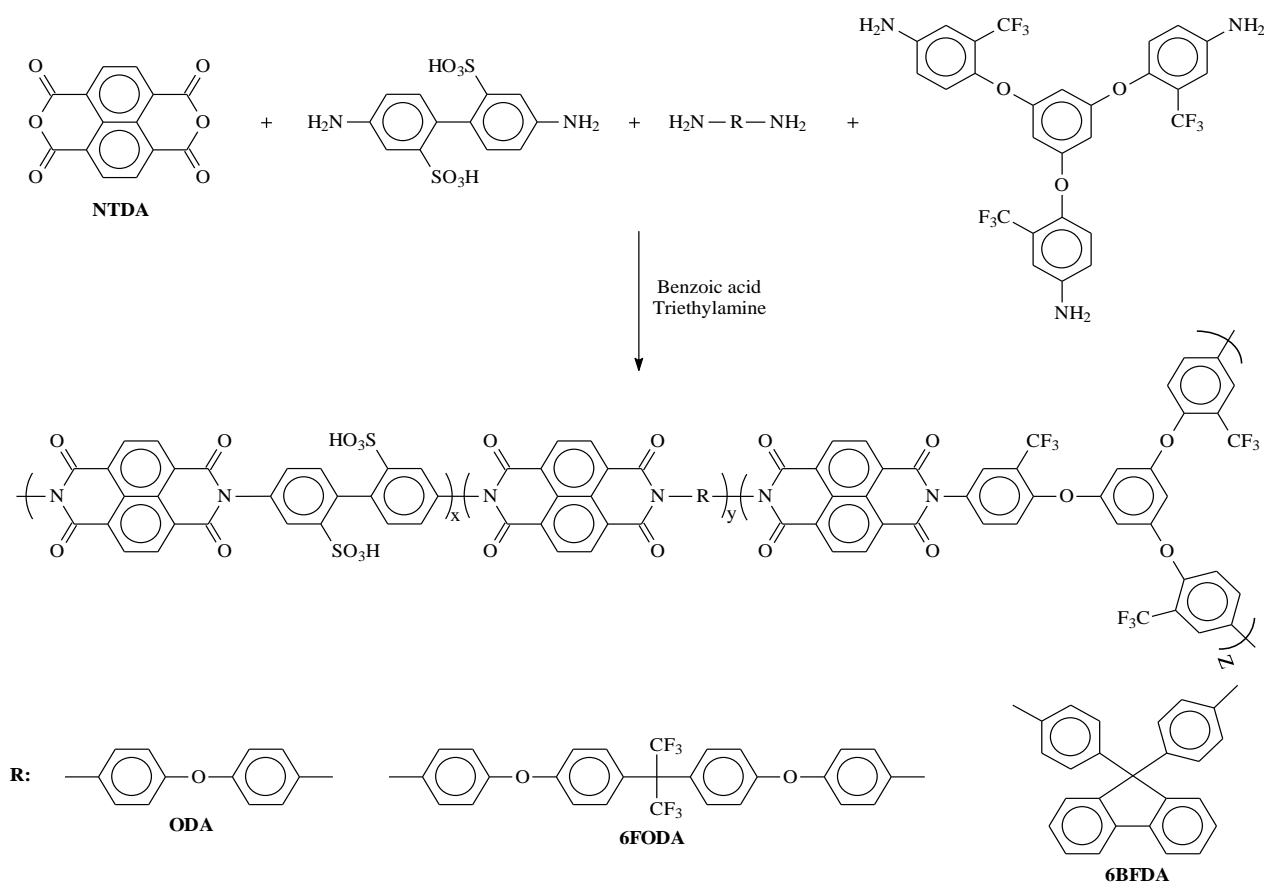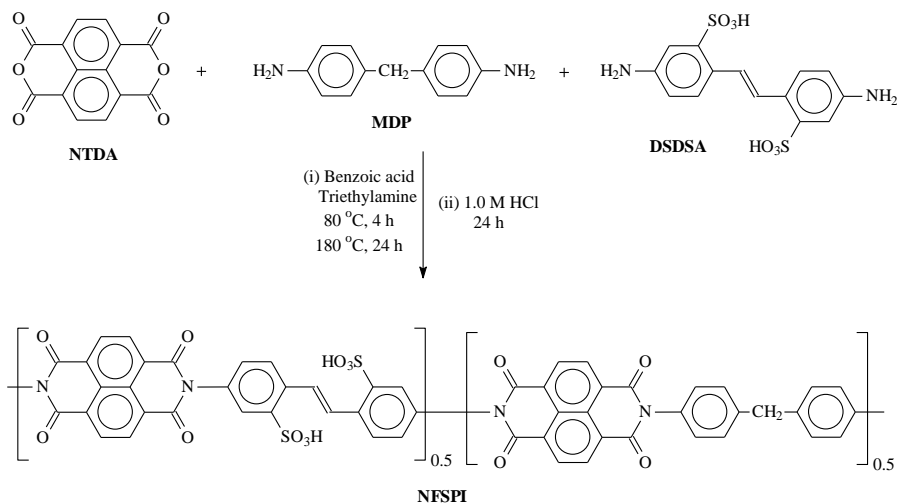

Scheme 23. The synthesis scheme of the sulfonated polyimides (DPPNH-XX).[96]

Banerjee and Ghanti

Innov. Chem. Mater. Sustain. **2025**, 2(1), 032-073

Table 7. *The IEC, Mw, η$_{inh}$, T$_d$, TS, YM, EB, WU, τ, and σ values of the SPIs*

Polymer	IEC (meq/g)[a]	η$_{inh}$ (dL/g)[b]	T$_d$ (°C)[c]	TS (MPa)	YM (GPa)	EB (%)	WU (%)[d]	τ (h)[e,f]	σ (mS/cm)[g]	Ref.
DPPNH-60	1.88	1.01	321	69	1.44	15	31	>24[f]	87	96
DPPNH-70	2.23	1.16	315	60	1.32	13[h]	36	>17[f]	104	96
DPPNH-80	2.58	1.17	301	52	1.22	10	46	>15[f]	202	96
DPPNH-90	2.95	1.22	295	45	1.02	7.0	64	>7[f]	235	96
SPI-ODA-0	-	-	-	62.1	-	-	-	2.3[e]	-	201
SPI-ODA-1	-	-	-	62.0	-	-	-	2.2[e]	-	201
SPI-ODA-2	-	-	-	50.7	-	-	-	2.5[e]	-	201
SPI-6FODA-0	2.01	0.83	-	71.7	1.72	-	-	>120[e]	-	201
SPI-6FODA-3	2.01	0.69	-	47.4	1.33	-	-	>120[e]	-	201
SPI-6FODA-5	1.99	0.72	-	41.7	1.22	-	-	>120[e]	-	201
SPI-6FODA-7	1.97	0.61	-	32.1	1.15	-	-	>120[e]	-	201
SPI-BFDA-0	2.38	0.54	-	62.3	-	-	-	3.5[e]	-	201
SPI-BFDA-1	2.36	-	-	66.4	-	-	-	4.8[e]	-	201
SPI-BFDA-3	2.33	0.46	-	46.2	-	-	-	4.5[e]	-	201
SPI-BFDA-5	2.31	0.49	-	41.2	-	-	-	4.0[e]	-	201
SPI-BFDA-7	2.29	0.31	-	38.2	-	-	-	4.3[e]	-	201
NFSPI	1.54	-	-	-	-	-	21.9[i]	42[f]	280	202
SPI-B20	1.77	-	-	88	-	18.7	47.2[i]	-	~100	203
SPI-B40	1.76	-	-	102	-	12.3	48.3[i]	24[j]	146	203
SPI-B60	1.77	-	-	92	-	16.2	47.8[i]	-	~130	203
SPI-1	1.24	2.46	-	-	-	-	28.4[i]	-	10.3[h]	204
SPI-1-1	1.40	-	-	-	-	-	23.7[i]	-	12.4[h]	204
SPI-1-1.5	1.55	-	-	-	-	-	34.2[i]	-	11.2[h]	204
SPI-2	1.77	1.82	-	74.9	-	-	47.9[i]	-	18.8[h]	204
SPI-2-0.8	1.79	-	-	-	-	-	64.5[i]	-	33.5[h]	204
SPI-2-1	1.81	-	-	67.9	-	-	96.9[i]	-	39.3[h]	204
SPI-2-1.2	1.72	-	-	-	-	-	64.4[i]	-	30.5[h]	204
SPI-2-1.5	1.87	-	-	-	-	-	73.5[i]	-	27.5[h]	204
SPI-3	1.95	1.39	-	73.3	-	-	63.1[i]	-	28.6[h]	204
SPI-3-0.5	1.80	-	-	-	-	-	54.5[i]	-	40.2[h]	204
SPI-3-0.8	1.80	-	-	56.2	-	-	62.3[i]	-	62.2[h]	204
SPI-3-1	1.87	-	-	-	-	-	69.3[i]	-	57.5[h]	204
SPI-3-1.2	1.72	-	-	-	-	-	54.1[i]	-	44.5[h]	204

[a] Theoretical IEC value, [b] inherent viscosity, [c] 10% decomposition temperature obtained from TGA analysis, [d] WU values at 80 °C, [e] starting fractured time in Fenton's reagent (30 ppm FeSO$_4$ in 30% H$_2$O$_2$) at 30 °C, [f] starting dissolution time in Fenton's reagent (30 ppm FeSO$_4$ in 30% H$_2$O$_2$) at 30 °C, [g] σ values under fully hydrated state at 80 °C, [h] through-plane σ value at 80 °C, [i] WU values after 24 h immersion in DI water [j] τ value in 3 ppm FeSO$_4$ in 10% H$_2$O$_2$ at 80 °C.

Scheme 24. Synthesis scheme of the sulfonated polynaphthylimides.[201]

Banerjee and Ghanti

Innov. Chem. Mater. Sustain. **2025**, 2(1), 032-073

NFSPI
Scheme 25. Synthesis scheme of the non-fluorinated SPI (NFSPI).[202]
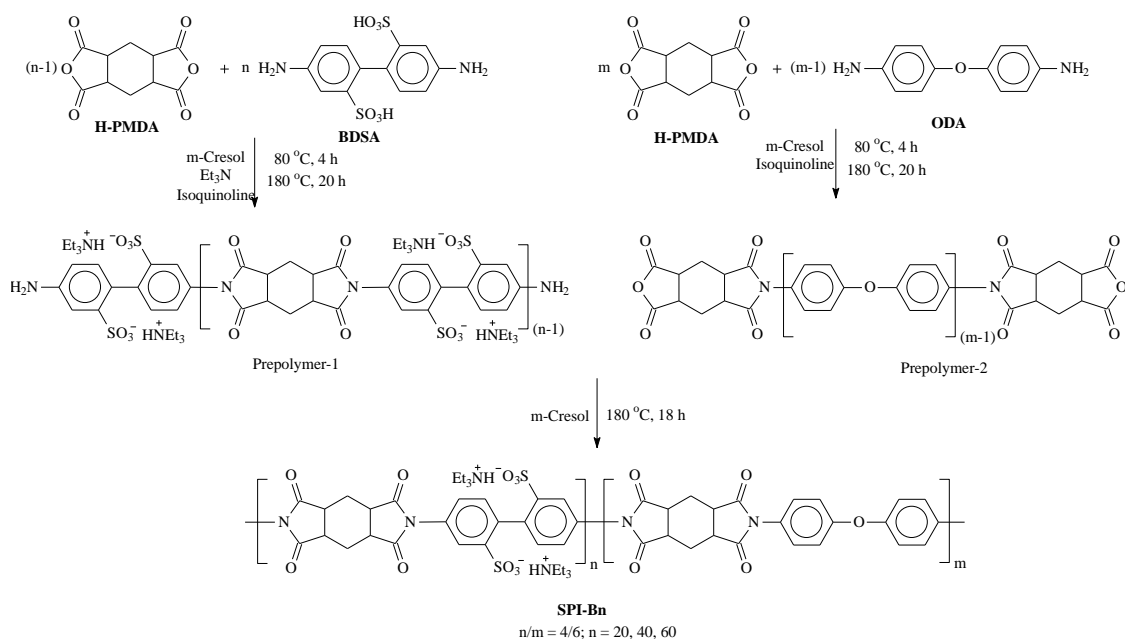
SPI-Bn
n/m = 4/6; n = 20, 40, 60
Scheme 26. The synthesis scheme of the sulfonated block copolyimides (SPI-Bn).[203]

SPI-x (Triethylamine salt form)
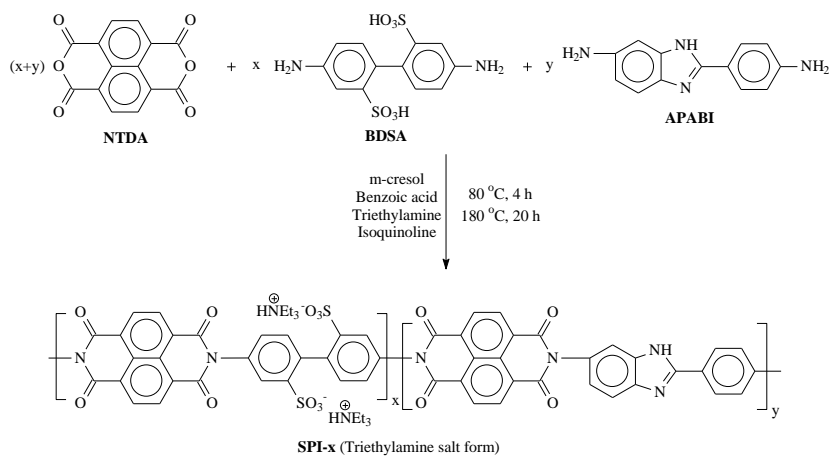
Scheme 27. Synthesis scheme of benzimidazole-containing SPI (SPI-x).[204]

Wang *et al.* synthesized a series of branched SPIs using NTDA as the dianhydride monomer, 4,4′-diamino-2,2′-biphenyldisulfonic acid (DAPS) as the sulfonated diamine monomer, 1,3,5-tris (2-trifluoromethyl-4-aminophenoxy)

benzene as the trifunctional branching monomer, and three other non-sulfonated diamine monomers [4,4′-oxydianiline (ODA), 2,2-bis[4-(4-aminophenoxy)phenyl]hexafluoropropane (6FODA), and 4,4′-(9-fluorenylidene)dianiline (BFDA)], as shown in **Scheme 24**.[201] The theoretical IEC values of the SPI-

Banerjee and Ghanti

Innov. Chem. Mater. Sustain. **2025**, 2(1), 032-073
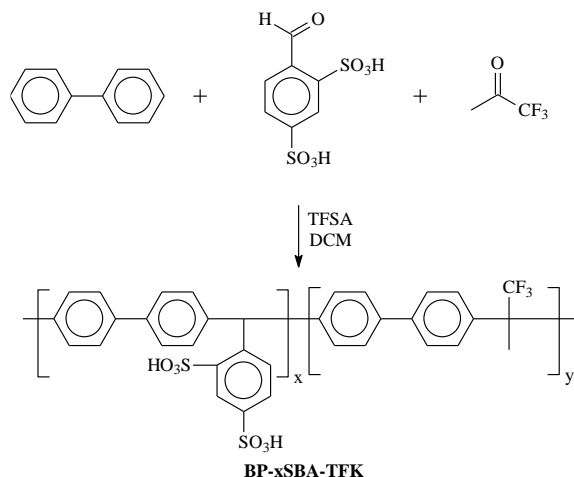
6FODA-x and SPI-6BFDA were obtained between 1.97-2.01 mmol/g and 2.29-2.38 mmol/g, respectively (**Table 7**). The branched SPIs showed appropriate thermal stability and mechanical properties for PEMFC applications.[201] Among all the branched series SPI membranes, the SPI-6BFDA series membranes exhibited the highest WU values due to the more considerable steric hindrance of the side chain in the branched polyimide structures.[201] The SPI-6FODA series membranes demonstrated the highest oxidative stability in Fenton's reagent (20 ppm $FeSO_4$ in 30% H_2O_2) at 30 ℃, as tabulated in **Table 7**. The oxidative stability also increased with the increase in the degree of branching (DB) in the branched SPI membranes.[201] The SPI-6FDA series membranes showed the highest proton conductivity values in coordination with WU values.[201]

Mahajan *et al.* synthesized a non-fluorinated sulfonated polyimide (NFSI) by the polycondensation reaction of the dianhydride NTDA with sulfonated [4,4′-diamino stilbene-2,2-sulfonic acid (DSDSA)] and non-sulfonated [4,4′-diamino diphenyl methane (MDP)] diamines monomers in the presence of benzoic acid and triethylamine (TEA) in m-cresol, as provided in **Scheme 25**.[202] The theoretical IEC value of the NFSPI copolymer was 1.54 meq/g (**Table 7**). The NFSPI membrane showed appropriate water absorption properties (WU: 21.9% and hydration number value: 8).[202] The NFSPI membrane exhibited a σ value of 280 mS/cm at 80 ℃, as illustrated in **Table 7**. The non-fluorinated SPI membrane demonstrated high hydrolytic stability (51 h) and oxidative stability (42 h; 30 ppm $FeSO_4$ in 30% H_2O_2 at 30 ℃).[202] The open circuit potential (OCP) value of the NFSPI membrane in a single fuel cell test was 0.80 V at 80 ℃, whereas that of the Nafion was 0.85 V, which indicates that the NFSPI membrane demonstrated comparable PEMFC performance.[202]

Wang *et al.* synthesized a series of multiblock sulfonated polyimides (SPI-Bn) by the polycondensation reaction of a flexible aliphatic six-membered cyclic dianhydride monomer [1,2,4,5-cyclohexanetetracarboxylic Dianhydride (H-PMDA)] with sulfonated diamine [4,4'-diaminobiphenyl-2,2′-disulfonic acid hydrate (BDSA)] and non-sulfonated diamine [4,4'-oxydianiline (ODA)] monomers, as shown in **Scheme 26**.[203] The theoretical IEC value of the SPI-Bn block copolymers ranged between 1.76-1.77 meq/g (**Table 7**). The sulfonated block copolyimides displayed high thermal and mechanical stability (TS: 88-102 MPa and EB: 12.3-18.7%).[203] The SPI-Bn membranes exhibited WU values between 47.2-48.3%, as compiled in **Table 7**. The SPI-B40 membranes demonstrated the τ value of 24 h in Fenton's reagent (3 ppm $FeSO_4$ in 10% H_2O_2) at 80 ℃.[203] Among all the membranes, the SPI-B40 membrane displayed the highest σ value of 146 mS/cm at 80 ℃ (**Table 7**). In the hydrogen-oxygen (H_2-O_2) fuel

cell performance, the maximum peak power density order was SPI-B20 (641 mW/cm²) < SPI-B60 (727 mW/cm²) < SPI-B40 (869 mW/cm²) at 80 ℃ under 100% RH conditions.[203]

Ding et al. designed and fabricated a series of composite SPI membranes (SPI-x-y) by mixing the SPI and nano carbon sulfonic acid (NCSA) using the solution blending method.[204]
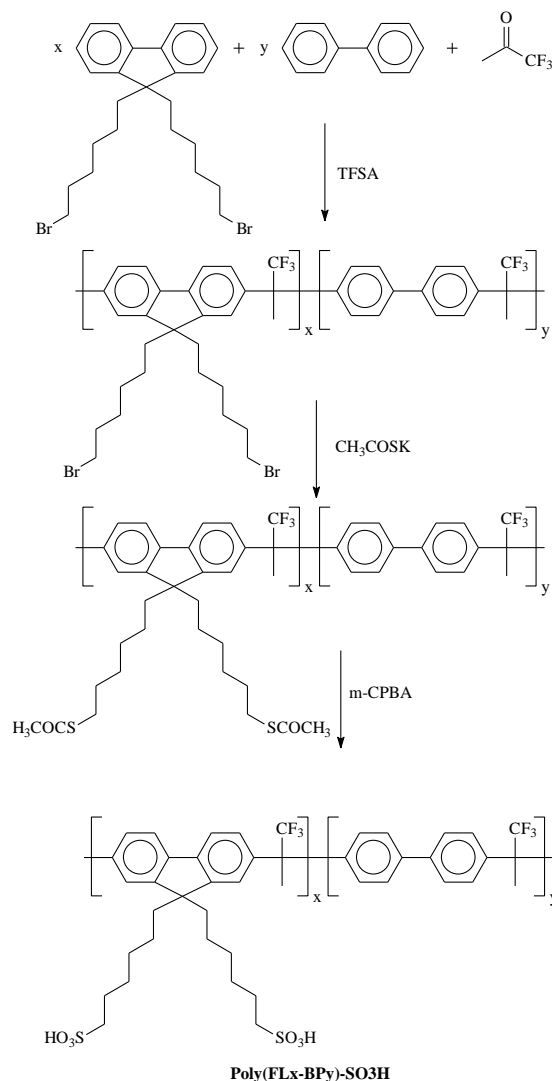
Poly(FLx-BPy)-SO3H
Scheme 29. The synthesis scheme of the poly(FLx-BPy)-SO₃H copolymers.[219]

The pristine SPI copolymer with various DS values is prepared

by the polycondensation reaction of NTDA with sulfonated diamine monomer [2,2′-benzidinedisulfonic acid (BDSA)] and benzimidazole-containing non-sulfonated diamine monomer [2-(4-aminophenyl)-5-aminobenzimidazole (APABI)], as depicted in **Scheme 27**.[204] The NCSA nanoparticle is prepared by the chemical reaction of nano carbon particles (NCPs) with benzenesulfonic acid.[204] The η_{inh} values of the pristine SPI-x copolymers were between 1.39-2.46 dL/g (**Table 7**). Among all the composite membranes, the SPI-2-1 composite membrane displayed the highest water absorption properties (WU: 96.9% and SR: 117.2%) after 24 h of immersion in DI water.[204] The SPI-3-0.8 composite membrane reached the maximum through-plane σ value of 136.8 mS/cm at 90 ℃, which is twice that of the pristine SPI-3 membrane and 50% higher than that of the Nafion-117 membrane.[204] In the PEMFC test, the SPI-3-0.8 composite membrane-based MEA reached the maximum PPD value of 1.584 W/cm² at 80 ℃ without any backpressure, which is 20% higher than that of the pristine SPI-3 membrane-based MEA (1.312 W/cm²).[204] The OCV value of the SPI-3-0.8 composite membrane-based MEA was 0.97 V, whereas that value after one week was close to 0.90 V, which indicates the long-term stability of the SPI-3-0.8 composite membrane.[204]

4.2.7 Poly(phenylene alkane)s, PPAs

Poly(phenylene alkane)s, PPAs are an essential class of high-performing liner polymers, synthesized by the efficient superacid-catalyzed Friedel–Crafts (SACFC) polyhydroxyalkylations reaction of super electrophilic carbonyl compounds and electron-rich aromatic compounds (biphenyl, p-terphenyl, fluorene, carbazole, etc.) in the presence of the superacid, such as trifluoromethanesulfonic acid (TFSA), methanesulfonic acid (MSA), etc.[205-208] PPAs are known for their high thermal stability, good mechanical properties, excellent proton conductivity, and superior oxidative stability owing to the lack of radical attack-prone ether

linkages on the polymer backbone.[205,209-211] Sulfonated poly(phenylene alkane)s, SPPAs are usually prepared either by direct polyhydroxyalkylations reaction of sulfonated monomers or by the post-sulfonation grafting method of the polymers.[212-215] Generally, the SPPAs possessed high molecular weight, good solubility, excellent thermal and mechanical stability, high proton conductivity, and, more specifically, outstanding chemical or oxidative stability.[212-217] In this section, a few recently developed SPPAs for PEMFC applications are discussed below.

Zhang *et al.* synthesized a series of all-carbon backbone and dense SPPAs, designated as P(BP-xSBA-TFK) with various sulfonic acid contents by the SACFC polyhydroxyalkylations reaction of biphenyl (BP) with 1,3-disulfonic acid benzaldehyde (DFD) and 1,1,1-trifluoroacetone (TFK), as shown in **Scheme 28**.[218] The theoretical IEC values of the P(BP-xSBA-TFK) copolymer were between 1.3-4.1 meq/g, as provided in **Table 8**. The P(BP-xSBA-TFK) copolymer displayed η_{inh} values between 1.45-1.65 dL/g (**Table 8**), which confirms the formation of a high molecular weight copolymer by the SACFC polyhydroxyalkylations reaction. The P(BP-xSBA-TFK) copolymer demonstrated high thermal (decomposition

temperature up to 400 ℃) and mechanical stability.[218] The P(BP-0.8SBA-TFK) membrane showed the highest water absorption (WU: 37.9% and SR: 16.9%) at 80 ℃, as tabulated in **Table 8**. The morphological analysis of the P(BP-xSBA-TFK) copolymer displayed an interconnected phase morphology, which benefits the agile ion transportation process.[218] Out of all the SPPA membranes, the P(BP-0.8SBA-TFK) membrane reached the maximum σ value of 404.3 mS/cm at 80 ℃, as illustrated in **Table 8**. The P(BP-0.6SBA-TFK) membrane retained more than 99.2% of its weight after an hour of the Fenton's test at 80 ℃ and reached the maximum
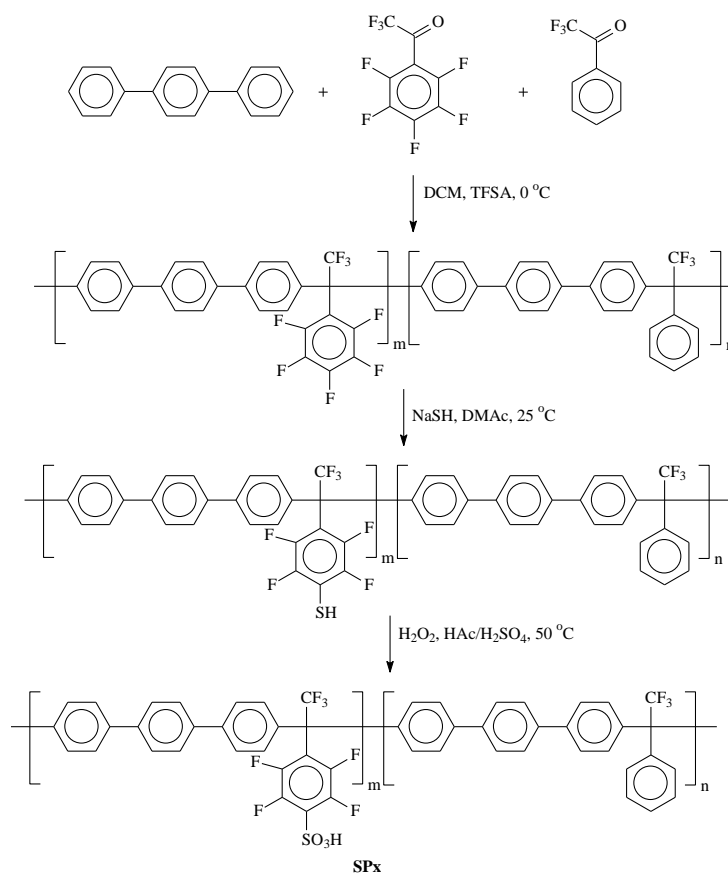
Scheme 30. The synthesis scheme of SPPA copolymers (SPx).[220]

Table 8. *The IEC, η_{inh}, T_d, TS, YM, EB, WU, τ, and σ values of the SPPAs*

Polymer	IEC (meq/g)[a]	η_{inh} (dL/g)[b]	T_d (°C)[c]	TS (MPa)	YM (GPa)	EB (%)	WU (%)[d]	τ (h)[e]	σ (mS/cm)[f]	Ref.
P(BP-0.8SBA-TFK)	4.1	1.45	-	28.2	-	15	37.9	-	404	218
P(BP-0.6SBA-TFK)	3.3	1.56	-	29.4	-	25	30.6	-	352	218
P(BP-0.4SBA-TFK)	2.4	1.61	-	54.0	-	19	15.0	-	231	218
P(BP-0.2SBA-TFK)	1.3	1.65	-	69.3	-	11	7.5	-	85	218
Poly(FL30-BP70)-SO3H	1.71	-	-	37.9	0.89	6.5	47	-	134	219
Poly(FL40-BP60)-SO3H	2.08	-	-	39.5	1.17	4.8	-	-	160	219
Poly(FL50-BP50)-SO3H	2.39	-	-	49.1	1.18	4.5	-	-	191	219
Poly(FL60-BP40)-SO3H	2.65	-	-	51.6	1.19	4.1	91	-	202	219
SP55	1.17	-	285	-	-	-	9.8	-	42	220
SP72	1.45	-	283	-	-	-	21	-	104	220
SP83	1.62	-	284	-	-	-	30	-	136	220
SP100	1.85	-	277	-	-	-	39	-	203	220
TSPHFTP-35	2.23	-	-	28.5	-	39.6	49.2	-	138	221
TSPHFTP-42	2.43	-	-	23.7	-	47.1	86.8	-	227	221
TSPHFTP-50	2.63	-	-	19.7	-	49.1	105	-	303	221
SP1	2.13	-	<300[g]	10.3	0.58	2.5	31.7	6.0	75	222
SP2	1.50	-	<300[g]	24.7	0.81	20.6	16	8.5	25	222
SP3	1.78	-	<300[g]	31.4	0.69	6.2	43.8	10	107	222

[a] Theoretical IEC value, [b] inherent viscosity, [c] onset decomposition temperature obtained from TGA analysis in N_2, [d] WU values at 80 °C, [e] starting fractured time in Fenton's reagent at 80 °C, [f] σ values at 80 °C and 100% RH, [g] 5% decomposition temperature obtained from TGA.

PPD value of 560 mW/cm^2 at 80 °C under 100% RH conditions.[218]

Yang *et al.* designed and synthesized a comb-like structure of SPPAs [Poly(FLx-BPy)-SO3H] having an ether-free all-carbon backbone and flexible double sulfohexyl side chain, as depicted in **Scheme 29**.[219] The theoretical IEC values of the Poly(FLx-BPy)-SO3H copolymers were between 1.71-2.65 meq/g, whereas the experimental IEC values were obtained between 1.64-2.54 meq/g.[219] The Poly(FLx-BPy)-SO3H membranes showed appropriate mechanical stability (TS: 37-52 MPa, YM: 0.89-1.19 GPa, and EB: 6.5-4.1%) and superior oxidative stability (RW ≥ 99.4% after 4 h of the Fenton's test at 80 °C).[219] Among the Poly(FLx-BPy)-SO3H membranes, the Poly(FL60-BP40)-SO3H membranes reached the highest WU value of 91% at 80 °C in DI water, as tabulated in **Table 8**. The morphological investigation of the Poly(FLx-BPy)-SO3H membranes demonstrated a phase-segregated microstructure.[219] The Poly(FLx-BPy)-SO3H membranes exhibited the σ value between 134-202 mS/cm at 80 °C, as illustrated in **Table 8**. The Poly(FL50-BP50)-SO3H-based MEA reached the maximum PPD value of 2.46 W/cm^2 in H$_2$/O$_2$ single fuel cell test at 80 °C under 100% RH conditions.[219]

Jannasch *et al.* synthesized a series of poly(p-terphenyl perfluorophenylsulfonic acid)s [SPx] by the metal-free SACFC polyhydroxyalkylations reaction of p-terphenyl with perfluoroacetophenone and acetophenone, followed by the selective post-sulfonation of the non-sulfonated copolymers by the thiol-oxidation method, as shown in **Scheme 30**.[220] The M_w and PDI values of the non-sulfonated copolymers (Px, x: 55, 72, 83, 100) were between 50-162 kg/mol and 1.5-1.8, respectively.[220] The SPx copolymers showed high thermal stability (T$_{d,onset}$: 277-285 °C), as illustrated in **Table 8**. The SPx membranes exhibited WU values between 9.8-39% at 80 °C
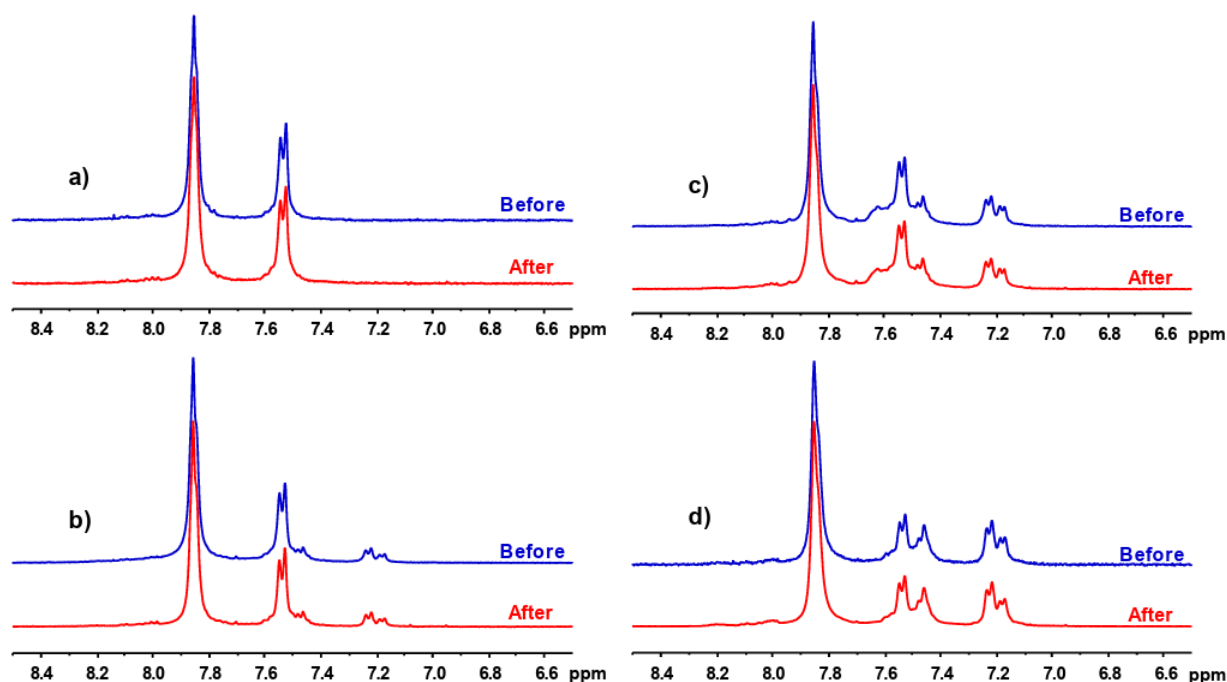

Figure 12. ^{1}H NMR spectra before and 1 h after the Fenton's test in DMSO-d$_6$ of (a) SP100, (b) SP83, (c) SP72, and (d) SP55 copolymers.[220] (Reprinted with permission from (220). Copyright (2019) American Chemical Society.)

Banerjee and Ghanti

Innov. Chem. Mater. Sustain. **2025**, *2*(1), 032-073

(**Table 8**). The through-plane SR and hydration number (λ) values of the SPx membranes at 80 ℃ were 5.9-21% and 4.8-12.[220] Among the SPx membranes, the SP100 membrane reached the highest σ value of 203 mS/cm at 80 ℃ in fully hydrated conditions (**Table 8**). The SPx membranes displayed superior oxidative stability after an hour of the Fenton's test at 80 ℃, as no change in copolymer structures was observed in the ^{1}H NMR spectra (**Figure 12**).[220]

Zhu *et al.* designed and synthesized a series of graft-type pendant dual 1,2,3-triazole and disulfonated moieties-based ether-free all-carbon backbone SPPAs (TSPHFTP-x) copolymers for the PEMFC applications, as shown in **Scheme 31**.[221] The M_w and PDI values of the BPHFTP-x copolymers were between 144-176 kg/mol and 2.15-2.63, which confirms the formation of the high molecular weight copolymer by the SACFC polyhydroxyalkylations reaction.[221] The theoretical IEC values of the TSPHFTP-x copolymers ranged from 2.23-2.63 meq/g (**Table 8**). The TSPHFTP-x copolymers exhibited high thermal stability (5% weight loss temperature up to 300 ℃) and mechanical stability (TS: 19.7-28.5 MPa and EB: 39.6-49.1%).[221] The TSPHFTP-x membranes demonstrated high oxidative stability (RW ≥ 94%) after an hour of the Fenton test at 80 ℃.[221] The TSPHFTP-x membranes exhibited a high σ value (138-303 mS/cm) at 80 ℃ under 100% RH conditions (**Table 8**). In the H_2/O_2 single fuel cell test, the OCV, PPD, and current density values of the TSPHFTP-50 PEMs were 0.98 V, 1.013 W/cm^2, and 2.54 A/cm^2 at 60 ℃ and 100% RH.[221] The OCV value of the TSPHFTP-50 MEA dropped from 0.75 V to 0.67 V after 55 h of the durability test, which confirms the long-term durability of the TSPHFTP-50 PEMs.[221]

Liu *et al.* synthesized three all-carbone backbone PPAs (P1, P2, P3) by the SACFC polyhydroxyalkylations reaction of 2,3,4,5,6-pentafluorobenzaldehyde (PFBA) with three different commercially available aromatic compounds (1,4-dimethoxybenzene, 6,6′-dimethoxy-3,3,3′,3′-tetramethyl-1,1′-spirobisindane, and p-Terphenyl) in presence of the methanesulfonic acid (MSA) in DCM, as shown in **Scheme 32**.[222] The M_w and PDI values of the PPAs (Px) polymers were 115-888 kDa and 1.83-7.24, respectively.[222] Then, the SPPAs (SP1, SP2, and SP3) were prepared by the aromatic nucleophilic substitution reaction between para-aryl-F and sodium 4-oxybenzenesulfonate at 120 ℃ (**Scheme 32**). The theoretical and experimental NMR-based IEC values of the SPx copolymers were obtained between 1.78-2.13 and 1.25-1.78 meq/g, respectively.[222] The SPx copolymers exhibited high thermal and mechanical stability, as illustrated in **Table 8**. The SPx membranes displayed high dimensional stability (WU: 16-44% and SR: 4.9-12.9%) at 80 ℃.[222] Among the SPx membranes, the SP3 membranes showed the highest σ value of 107 mS/cm at 80 ℃ and 100% RH conditions, as compiled in **Table 8**. The all-carbon backbone SPx membranes demonstrated high oxidative stability (after 1 h of test, RW ≥ 96% and τ ≥ 6.0 h) in Fenton's reagent at 80 ℃.[222] In the H_2/Air single fuel cell test, the OCV, PPD, and current density values of the SP3 PEMs were 0.93 V, 532 mW/cm^2, and 1.2 A/cm^2 at 80 ℃ and 100% RH.[221] During the long-term durability test of SP3 MEA, the OCV value slowly decreased from 0.95 to 0.81 V after 108 h.[222]

4.2.8 Polytriazoles, PTs

PTs are another special type of high-performing polymer, well known for their diverse functionalities in various fields, such as heat resistivity, metal coordinator, and antimicrobial activities.[223-225] PTs are mainly synthesized by the metal-catalyzed (Cu, Ir, Ru, Ni) azide-alkyne cycloaddition (MCAAC) "click" polymerization reactions.[226-228] The Cu(I)-catalyzed azide-alkyne cycloaddition (CuAAC) reaction is the most employed due to its excellent yield, high selectivity, high specificity, outstanding efficiency, and simplistic synthesis procedure.[229-232] The CuAAC polymerization reaction mainly produced 1,4-substituted 1,2,3-triazole rings with high selectivity and yield.[89,129,229-232] Sulfonated polytriazoles (SPTs) are also synthesized by the CuAAC "click" polymerization reaction, and they have gained remarkable consideration for their high thermal and mechanical stabilities, good solubility, high dimensional stability, excellent ionic conductivity, and better oxidative stability.[61,89,129,221,232] The presence of the 1,2,3-triazole rings in the SPT backbone improved the thermal
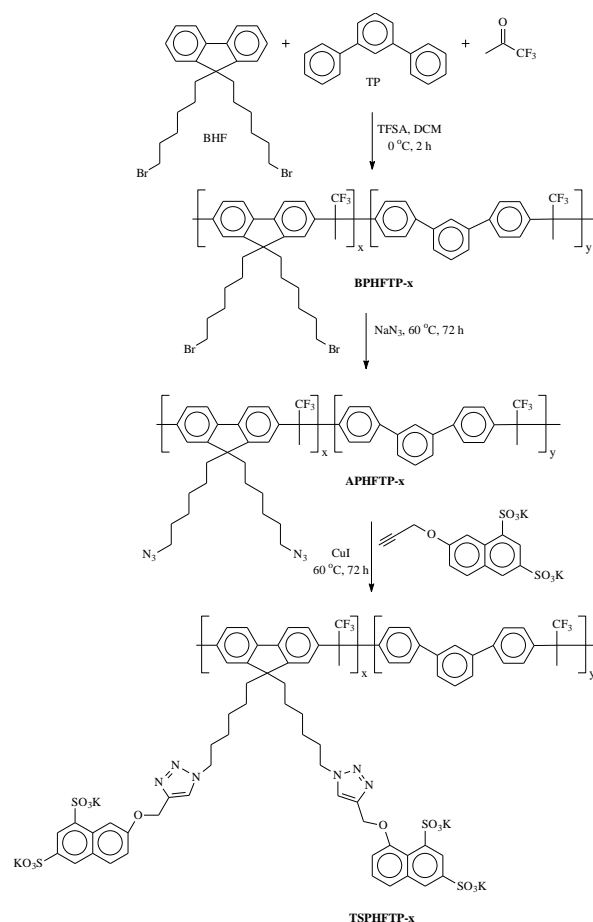
Scheme 31. The synthesis scheme of the pendant 1,2,3-triazole-based dual SPPAs (TSPHFTP-x) copolymers.[221]
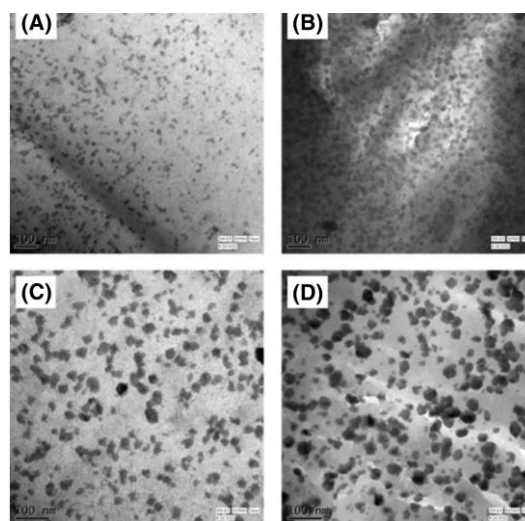

Figure 13. The lead acetate-stained TEM images of the (A) BABPSSH-60, (B) BABPSSH-70, (C) BABPSSH-80, and (D) BABPSSH-90.[80] (Copyright 2023, Adopted with permission from (80) John Wiley & Sons, Inc.)

Table 9. The IEC, M_w, T_d, TS, YM, EB, WU, τ, and σ values of the SPTs.

Polymer	IECw (meq/g)[a]	Mw (kDa)[b]	Td10 (°C)[c]	TS (MPa)	YM (GPa)	EB (%)	WU (%)[d]	τ (h)[e]	σ (mS/cm)[f]	Ref.
BABPSSH-60	1.60	-	271	33	1.47	13	11	>24	25.5	80
BABPSSH-70	1.88	-	269	27	1.45	26	15	>24	29.4	80
BABPSSH-80	2.17	-	265	24	1.28	11	23	13	53.7	80
BABPSSH-90	2.46	-	260	17	0.68	11	32	6	91.5	80
PTPFDSH-70	2.24	63.8	317	68	1.82	89	28	>24	91	233
PTPFDSH-80	2.67	71.4	279	56	1.66	66	33	>24	138	233
PTPFDSH-90	3.13	77.5	266	50	1.47	61	49	14.5	176	233
PYPYSH-70	2.28	451	350	65	2.37	13	26	48	95	100
PYPYSH-80	2.70	283	321	46	1.86	17	35	44	110	100
PYPYSH-90	3.15	222	312	40	1.53	14	53	30	155	100
PYPYSH-100	3.64	265	274	18	0.59	21	65	17	184	100
PYPOSSH-60	1.34	274	304	45	1.82	45	8.4	>48	20	99
PYPOSSH-70	1.61	230	287	41	1.66	42	11	>48	53	99
PYPOSSH-80	1.88	144	283	47	1.8	34	16	38	78	99
PYPOSSH-90	2.17	126	281	33	1.05	17	28	26	114	99
PTSF-FeS-3	-	-	-	31.3	1.2	40	21	27	66	234
PTSF-FeS-5	-	-	-	-	-	30	27	30	69	234
PTSF-FeS-7	-	-	-	-	-	28	31	31	80	234
PTSF-FeS-9	-	-	-	20.8	0.91	20	38	34	78	234

[a] Theoretical IEC value, [b] weight-average molecular weight, [c] 10% decomposition temperature obtained from TGA analysis, [d] WU values at 80 °C, [e] complete dissolution time in Fenton's reagent (2 ppm $FeSO_4$ in 3% H_2O_2) at 80 °C, [f] σ values under fully hydrated state at 80 °C.
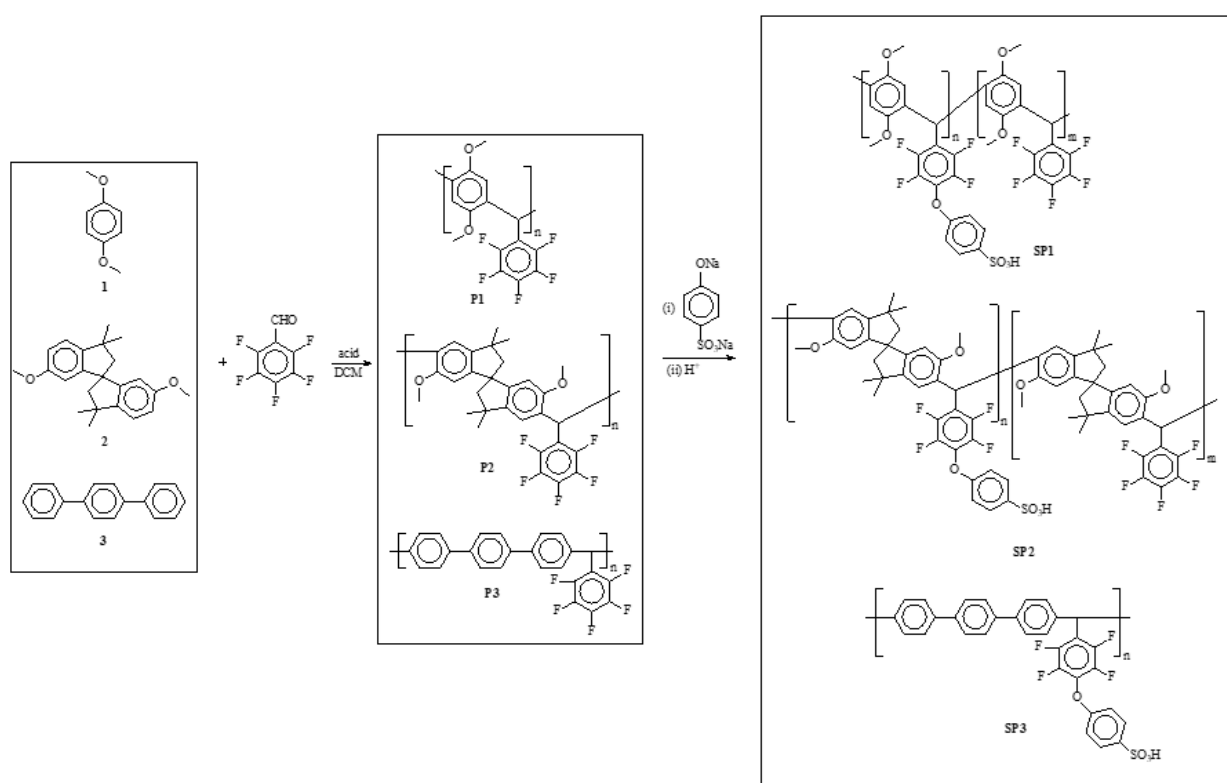
Scheme 32. The synthesis scheme of the PPAs (P1-P3) and SPPAs (SP1-SP3).[222]

and dimensional stability through its aromatic nature. It enhanced the proton conductivity by creating additional hydrogen bonding sites via its basic nitrogen atom of the 1,2,3-triazole rings.[61,89,129,221,232] Herein, a few recently developed SPTs for PEMFC applications are discussed below.

Banerjee *et al*. designed and synthesized a series of semi-fluorinated SPTs (BABPSSH-XX) with various DS values by the CuAAC "click" polymerization reaction of 4,4′-(propane-2,2′-diyl)bis((prop-2-ynyloxy)benzene) [BPAAL] with 1,4-bis(4-azido-2-(trifluoromethyl)phenoxy)benzene [BATFB] and 4,4′-diazido-2,2′-stilbenesulfonic acid disodium salt tetrahydrate [DASSA] in DMSO at 80 °C, as shown in **Scheme 33**.[80] The

η_{inh} values of the BABPSSH-XX copolymers were obtained between 1.15-1.35 dL/g.[80] The experimental NMR-based IEC values (IEC_NMR: 1.62-2.49 meq/g) match the theoretical IEC values (IEC_theo: 160-2.46 meq/g).[80] The BABPSSH-XX copolymers showed high thermal (T_d10: 260-271 °C) and mechanical stabilities (TS: 17-24 MPa, YM: 0.68-1.47 GPa), as provided in **Table 9**. All the copolymer membranes demonstrated high dimensional and oxidative stability owing to the presence of the semi-fluorinated unit in the copolymer architecture.[80] The TEM morphological investigation confirms the formation of the well-segregated and interconnected phase morphology (**Fig. 13**), which is beneficial for the facile proton transportation process. The BABPSSH-90 membrane
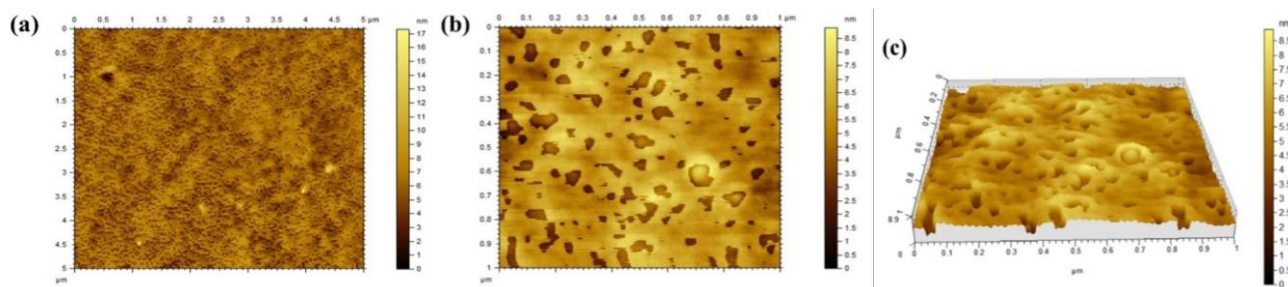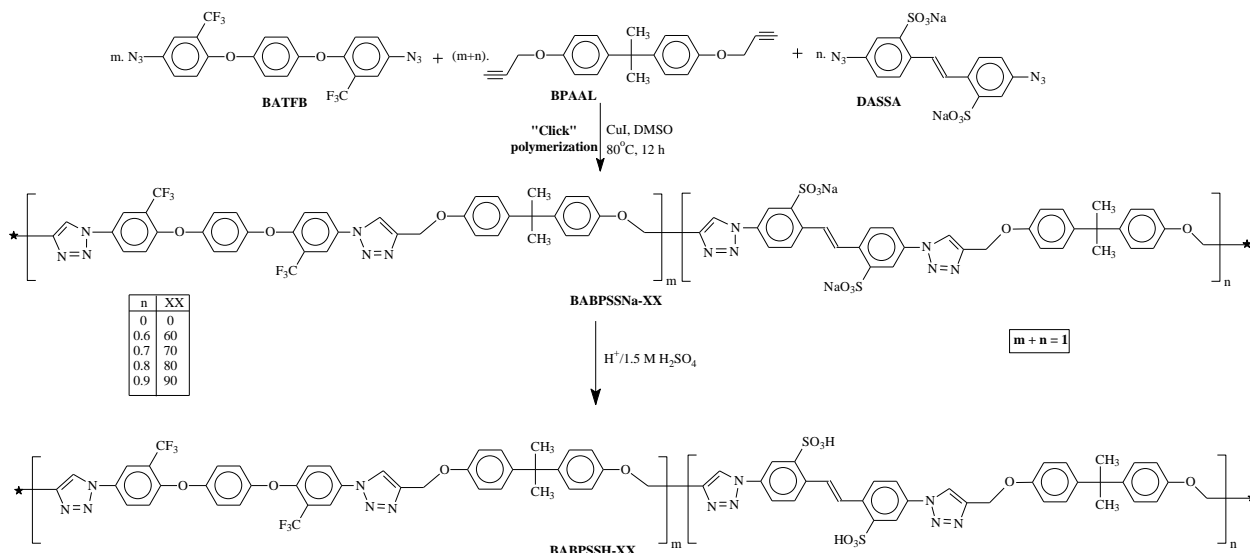
Banerjee and Ghanti

Innov. Chem. Mater. Sustain. **2025**, 2(1), 032-073

Figure 14. The TM surface images of the PYPYSH-80 membrane (a) 2D 5×5 μm², (b) 2D 1×1 μm², and (c) 3D 1×1 μm².[100] (Reprinted with permission from (100). Copyright (2022) American Chemical Society.)
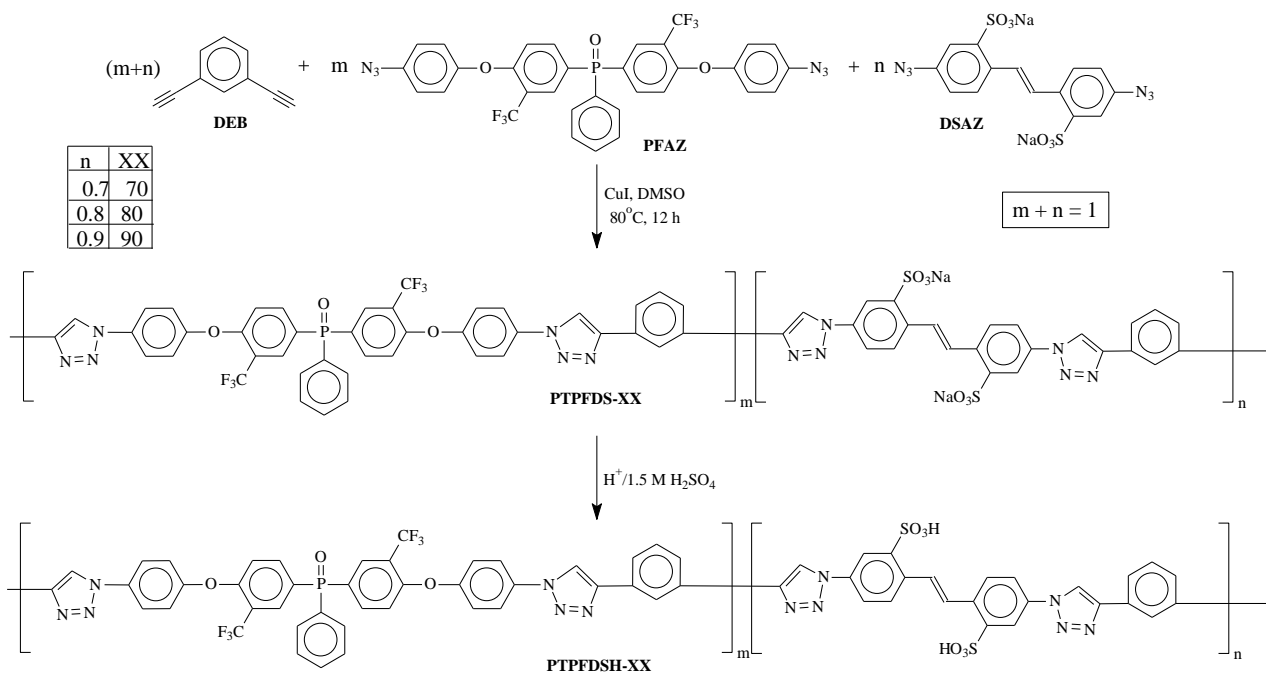

Scheme 33. The synthesis scheme of the semi-fluorinated SPTs (BABPSSH-XX).[80]

demonstrated the highest σ value of 91.5 mS/cm at 80 °C in DI water, as compiled in **Table 9**.

Banerjee *et al*. designed and synthesized a series of phosphine oxide (P=O)-based SPTs (PTPFDSH-XX) with various sulfonic acid content utilizing 1,3-diethynylbenzene (DEB), bis[4-(4′-azidophenoxy)-3-trifluoromethylphenyl] phenylphosphine oxide (PFAZ), and 4,4'-diazido-2,2'-stilbenesulfonic acid disodium salt (DSAZ) by CuAAC "click" polymerization reaction, as depicted in **Scheme 34**.[233] The M$_w$

Scheme 34. The synthesis scheme of the phosphine oxide (P=O)-based semi-fluorinated SPTs (PTPFDSH-XX) copolymers.[233]

Banerjee and Ghanti

Innov. Chem. Mater. Sustain. **2025**, 2(1), 032-073
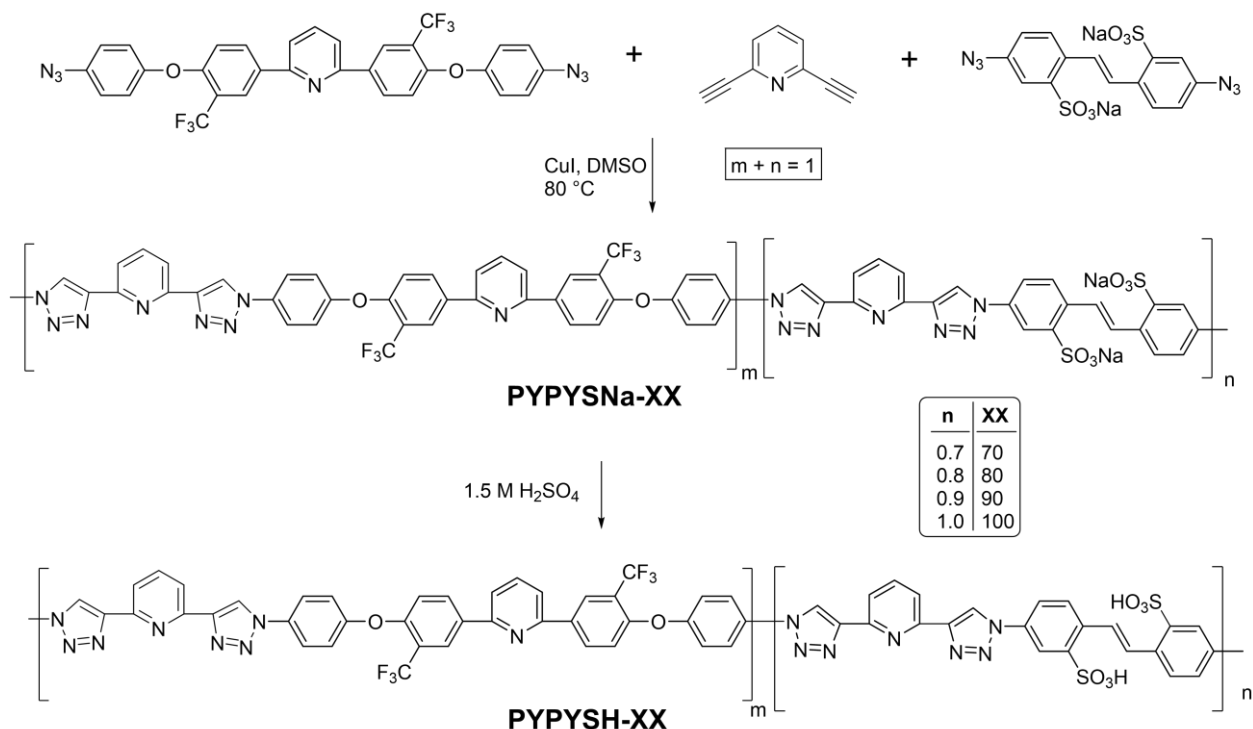
Scheme 35. The synthesis scheme of the 2,6-sterically hindered pyridinyl-based SPTs (PYPYSH-XX).[100]
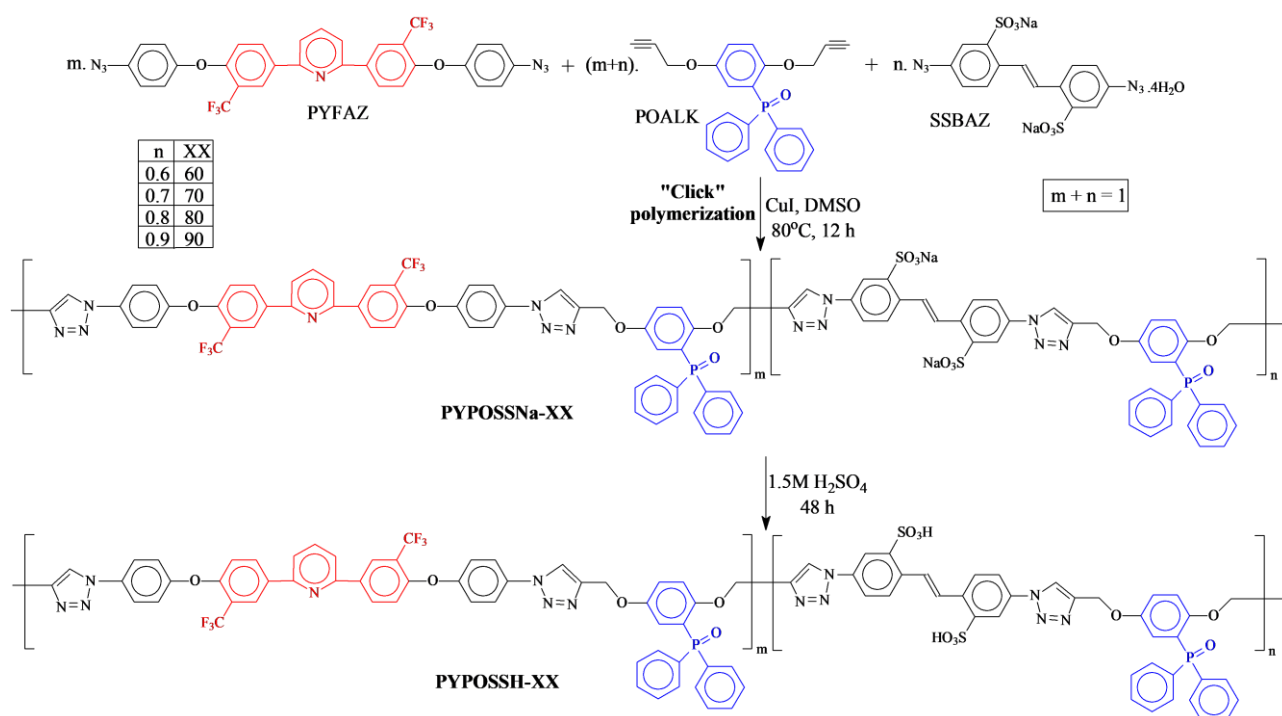
Scheme 36. The synthesis scheme of the pyridinyl- and P=O-based semi-fluorinated SPTs (PYPOSSH-XX).[99]

and PDI values of the PTPFDSH-XX copolymers were obtained between 63800-77500 g/mol and 1.71-2.29.[233] The theoretical IEC values of the SPTs were between 2.24-3.13 meq/g (**Table 9**). The PTPFDSH-70 to -90 copolymers exhibited desired thermal and mechanical stabilities, as illustrated in **Table 9**. The WU and in-plane SR values of the P=O-based semi-fluorinated SPT membranes were between 28-49% and 6.2-7.3% at 80 ℃, which revealed their high dimensional stability.[233] Among all the membranes, the PTPFDSH-90 membranes showed the highest σ value of 176 mS/cm at 80 ℃ (**Table 9**). The PTPFDSH-70 to -90

membranes showed superior oxidative stability in Fenton's reagent at 80 ℃, as tabulated in **Table 9**.

Banerjee *et al.* designed and synthesized a series of 2,6-sterically hindered pyridinyl-based SPTs (PYPYSH-XX) copolymers with DS values between 70-100% by the CuAAC "click" polymerization reaction in DMSO at 80 ℃, as reported in **Scheme 35**.[100] The theoretical IEC and M_w values of the PYPYSH-XX copolymers were obtained between 2.28-3.64 meq/g and 222000-451000 g/mol, respectively (**Table 9**). The pyridinyl-based SPT copolymers showed high thermal (Td10%: 274-350 ℃) and mechanical stabilities (TS: 18-65
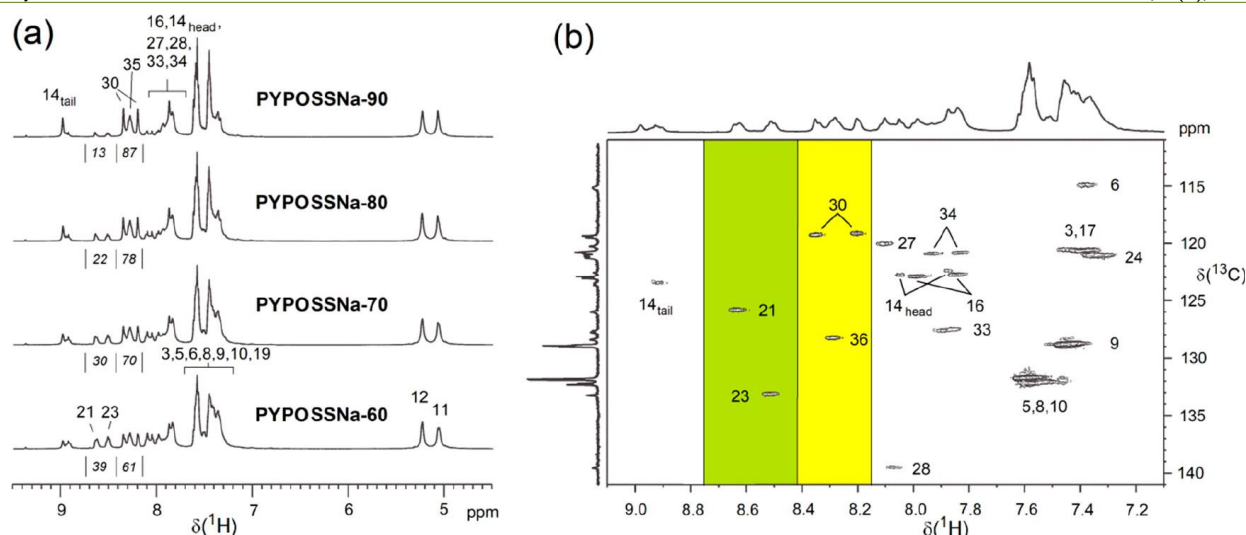
Banerjee and Ghanti

Innov. Chem. Mater. Sustain. **2025**, 2(1), 032-073

Figure 15. The (a) ^{1}H NMR spectra and (b) HSQC spectrum of the aromatic C-H region of the PYPOSSH-XX copolymers in DMSO-d_6.[99] (Reprinted with permission from (99). Copyright (2024) American Chemical Society.)

MPa, YM: 0.59-2.37 GPa, EB: 13-21%), as illustrated in **Table 9**. The PYPYSH-XX membranes showed WU and through-plane SR values between 25-65% and 2.8-6.8% at 80 °C.[100] The AFM microstructural investigation reveals an interconnected and phase-segregated morphology, as depicted in **Figure 14**.[100] The PYPYSH-XX membranes exhibited excellent σ values (95-184 mS/cm) and superior oxidative stability (τ: 17-48 h) in Fenton's reagent at 80 °C, due to the presence of the H-bond propagating and radical scavenging pyridinyl units in both the hydrophobic and hydrophilic segments of the copolymer backbone (**Table 9**). In the H_2-O_2 single-cell experiment, the PYPYSH-100 MEA demonstrated the open circuit potential (OCP) and maximum PPD values of 0.75 V and 966 mW/cm² at 80 °C and 100% RH.[100]

Banerjee *et al*. designed and synthesized a series of pyridinyl- and P=O-moieties containing SPTs (PYPOSSH-XX) with sulfonic acid content values between 60 to 90% by the CuAAC reaction of the bisalkyyne monomer, 2,5-bis(prop-2′-ynyloxy)phenyl](diphenyl)phosphine oxide [POALK] with the semi-fluorinated bisazide monomer, 2,6-bis-[4′-(4″-azidophenoxy)-3′-(trifluoromethyl)phenyl]pyridine [PYFAZ] and sulfonated bisazide monomer, 4,4′-diazido-2,2′-stilbenesulfonic acid disodium salt [SSBAZ], as shown in **Scheme 36**.[99] The theoretical and NMR-based IEC values of the PYPOSSH-XX copolymers were obtained between 1.34-

2.17 and 1.37-2.10 meq/g.[99] The ^{1}H NMR spectra and HSQC correlation spectrum of the aromatic C-H of PYPOSSH-XX copolymers are provided in **Figure 15**. The PYPOSSH-60 to -90 copolymers showed high thermal and mechanical stabilities, as illustrated in **Table 9**. The maximum storage modulus values of the PYPOSSH-60 to -90 membranes ranged between 2027 and 7862 MPa.[99] The PYPOSSH-90 membrane exhibited the highest WU and SR values of 27.6% and 12.8% at 80 °C; this confirms the high dimensional stability of the PYPOSSH-XX copolymers.[99] Among the PYPOSSH-XX membranes, the PYPOSSH-90 membrane exhibited the highest σ value of 114 mS/cm at 80 °C in hydrated conditions (**Table 9**). The PYPOSSH-XX membranes demonstrated outstanding oxidative stability values (τ: ≥ 26 h and RW after 1 h: > 95%) in Fenton's reagent at 80 °C.[99] The extremely high oxidative stability of the PYPOSSH-XX membranes is due to the synergistic effect of pyridinyl and phosphine oxide moieties of the copolymer framework.[99]

Banerjee *et al*. fabricated a series of sulfonated Fe-MOF (Fe-S MOF)-containing SPT hybrid membranes (PTSF-FeS-X) for the PEMFC applications.[234] pristine PTSF-60 copolymer was synthesized by the CuAAC "click" polymerization reaction, as depicted in **Scheme 37**.[234] The Fe-S MOF was synthesized by the post-sulfonation process of the Fe-MIL-53-NH₂ MOF with 1,3-propane sultone, as shown in **Scheme 38**.[234] The microstructure of the FeS-MOF and PTSF-FeS-X composite
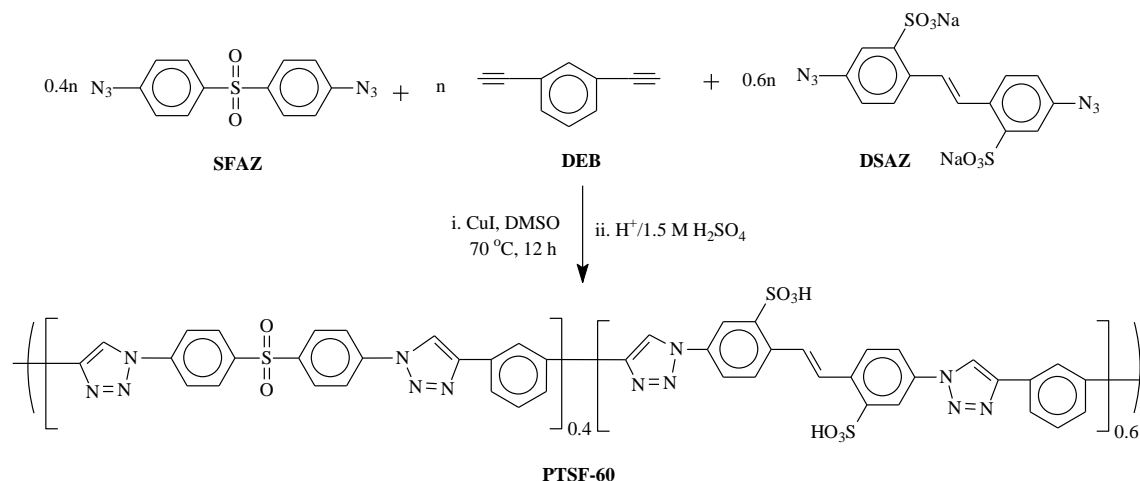
Scheme 37. The synthesis scheme of the pristine PTSF-60 copolymer.[234]

Banerjee and Ghanti

Innov. Chem. Mater. Sustain. **2025,** *2*(1), 032-073
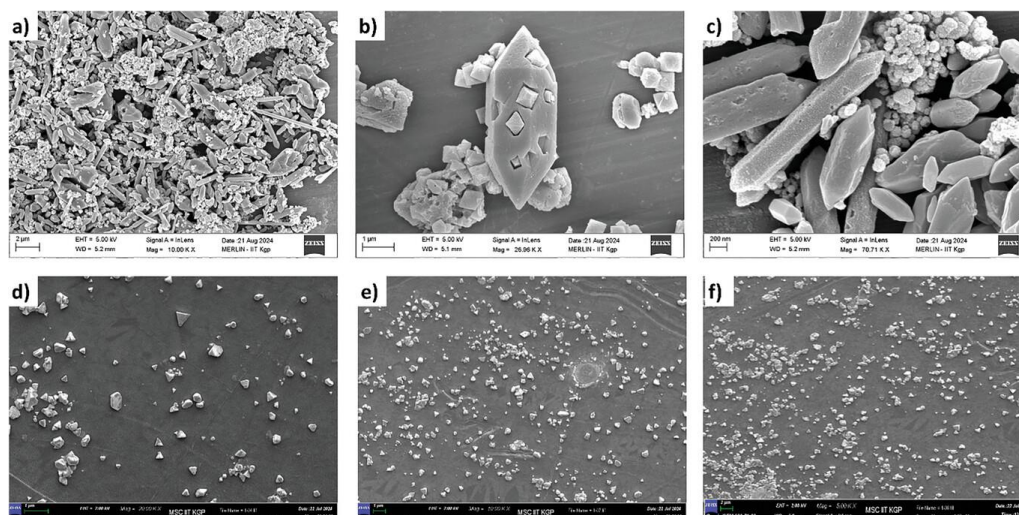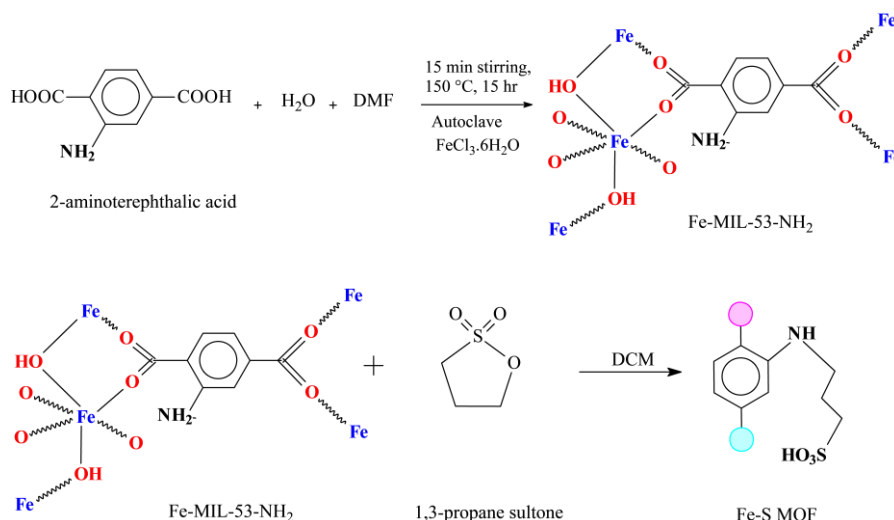

Figure 16. The FESEM surface images of (a-c) Fe-S MOF and (d-f) PTSF-FeS-3, -7, -9.[234] (Copyright 2025, Adopted with permission from (234) John Wiley & Sons, Inc.)

Scheme 38. The synthesis scheme of the sulfonated Fe-MOF (Fe-S MOF).[234]

membranes was investigated by the FESEM surface analysis, and the corresponding outcomes are depicted in **Figure 16**. The composite PTSF-FeS-X membranes demonstrated high thermal and mechanical stability values.[234] The WU values of the PTSF-FeS-X composite membranes were between 21-38% at 80 ℃, as compiled in **Table 9**. The PTSF-FeS-X composite membranes showed better oxidative stability (τ: 27-34 h) than the pristine SPT membrane in Fenton's reagent at 80 ℃, which is primarily due to the incorporation of the Fe-S MOF into the copolymer backbone.[234] Among all the composite membranes, the PTSF-FeS-7 membrane exhibited the highest σ value of 80 mS/cm at 80 ℃, as illustrated in **Table 9**. The proton conduction-related E_a values of the PTSF-FeS-X membranes were obtained between 9-13 kJ/mol.[234]

4.2.9 Others

Besides those mentioned above, sulfonated heteroaromatic polymeric backbones and a few other high-performing sulfonated heteroaromatic polymeric backbones have been employed for PEMFC applications. Those kinds of high-performing sulfonated heteroaromatic polymeric backbones are sulfonated polyoxadiazoles (SPODs), sulfonated polybenzoxazoles (SPBOs), sulfonated poly(phenylene oxide)s (SPPOs), sulfonated polybenzothiazoles (SPBTs), and sulfonated poly(oxindole

biphenylene)s (SPOBPs) etc.[235-239] These types of sulfonated heteroaromatic polymeric backbones also possess high thermal stability, mechanical properties, good solubility, high proton conductivity, and excellent oxidative stability. Still, there are a few studies that have been reported on those types of polymeric architecture.[235-239] Herein, the aforementioned types of sulfonated heteroaromatic PEMs are discussed below.

Abdolmaleki *et al*. synthesized two types of phenol-containing sulfonated polyoxadiazoles (SPPOD and SCDPPOD) by the one-spot high-temperature polycondensation reaction of dicarboxylic acid derivative and hydrazine sulfate in PPA medium, as depicted in **Scheme 39**.[235] The theoretical IEC values of the SPPOD and SCDPPOD were 3.0 and 2.4 meq/g, as illustrated in **Table 10**. The η_{inh} value of the SCDPPOD copolymer was 0.6 dL/g in DMSO, which confirms the formation of a high molecular weight copolymer (**Table 10**). The SCDPPOD copolymer showed high thermal stability ($T_{d5\%}$ value 320 ℃), as compiled in **Table 10**. The SCDPPOD membrane demonstrated a WU value of 38% in DI water at 25 ℃.[235] The SCDPPOD membrane showed the highest σ value of 65 mS/cm at 80 ℃ and 100% RH.[235] Thus, the phenol-containing sulfonated polyoxadiazoles exhibited good proton conductivity value, which is attributed to the presence of the various heteroatomic sites in the polymeric backbone and made them a potential candidate for PEMFC applications.[235]

Banerjee and Ghanti

Innov. Chem. Mater. Sustain. **2025**, 2(1), 032-073

Table 10. The IEC, η_{inh}, T_d, TS, YM, EB, WU, τ, and σ values of the SPODs, SPBOs, SPPOs, SPBTs, and SPOBPs.

Polymer	IEC$_w$ (meq/g)[a]	η_{inh} (dL/g)[b]	T_d (°C)[c]	TS (MPa)	YM (GPa)	EB (%)	WU (%)[d]	τ (h)[e]	σ (mS/cm)[f]	Ref.
SPPOD	3.0	-	265	-	-	-	400	-	-	235
SCDPPOD	2.4	0.6	320	-	-	-	38	-	65	235
PTEBO	0	1.19	-	-	-	-	-	>200	-	236
SPTESBO-20	0.61	0.96	261[g]	-	-	-	~5	18.5	17[h]	236
SPTESBO-40	1.16	0.86	253[g]	-	-	-	~15	21.6	52[h]	236
SPTESBO-60	1.81	0.83	247[g]	-	-	-	~25	10	130[h]	236
PTEBO-HFB	0	1.89	-	-	-	-	-	>200	-	236
SPTESBO-HFB-20	0.65	1.46	263[g]	-	-	-	~7	30	24[h]	236
SPTESBO-HFB-40	1.36	1.47	257[g]	-	-	-	~12	25	78[h]	236
SPTESBO-HFB-60	1.56	1.67	248[g]	-	-	-	~30	18	130[h]	236
SNO40%-BPPO	0.93	-	-	35	-	24	16	-	38[h]	237
SNO65%-BPPO	1.42	-	-	26	-	20	22	-	~4h[i]	237
SNO80%-BPPO	1.55	-	-	21	-	13	25	-	~55[h]	237
SNO100%-BPPO	1.62	-	-	16	-	9	34	-	71[h]	237
sPBT-F70	2.32	-	361	-	-	-	30	6.0	110	238
sPBT-F72.5	2.38	-	350	-	-	-	32	5.6	-	238
sPBT-F75	2.45	-	340	-	-	-	37	5.2	-	238
sPBT-F77.5	2.51	-	317	-	-	-	41	4.8	~120	238
sPBT-F80	2.58	-	316	-	-	-	42	4.5	130	238
sPBT-F82.5	2.64	-	299	-	-	-	46	4.2	143	238
SPOBP100	2.75	-	-	54	1.11	13	366	5.5	203	239
SPOBP$_{50}$-FPOBP$_{50}$	1.50	-	-	82	1.87	24	33	>48	74	239
SPOBP$_{50}$-ClPOBP$_{50}$	1.47	-	-	84	2.12	15	-	>48	-	239
SPOBP$_{50}$-BrPOBP$_{50}$	1.38	-	-	82	1.93	12	-	>48	-	239
SPOBP$_{50}$-IPOBP$_{50}$	1.29	-	-	50	0.91	20	-	4.5	-	239
SPOBP$_{50}$-NO$_2$POBP$_{50}$	1.45	-	-	80	1.91	13	39	>48	76	239
SPOBP$_{50}$-CH$_3$OPOBP$_{50}$	2.64	-	-	47	0.66	22	-	5.0	-	239

[a] Theoretical IEC value, [b] inherent viscosity, [c] 5% decomposition temperature obtained from TGA analysis in N_2 flow, [d] WU values at 80 °C, [e] complete dissolution time in Fenton's reagent, [f] σ values at 80 °C and 100% RH, [g] decomposition temperature of the -SO_3H group obtained from TGA analysis, [h] σ values at room temperature under fully humidified condition.
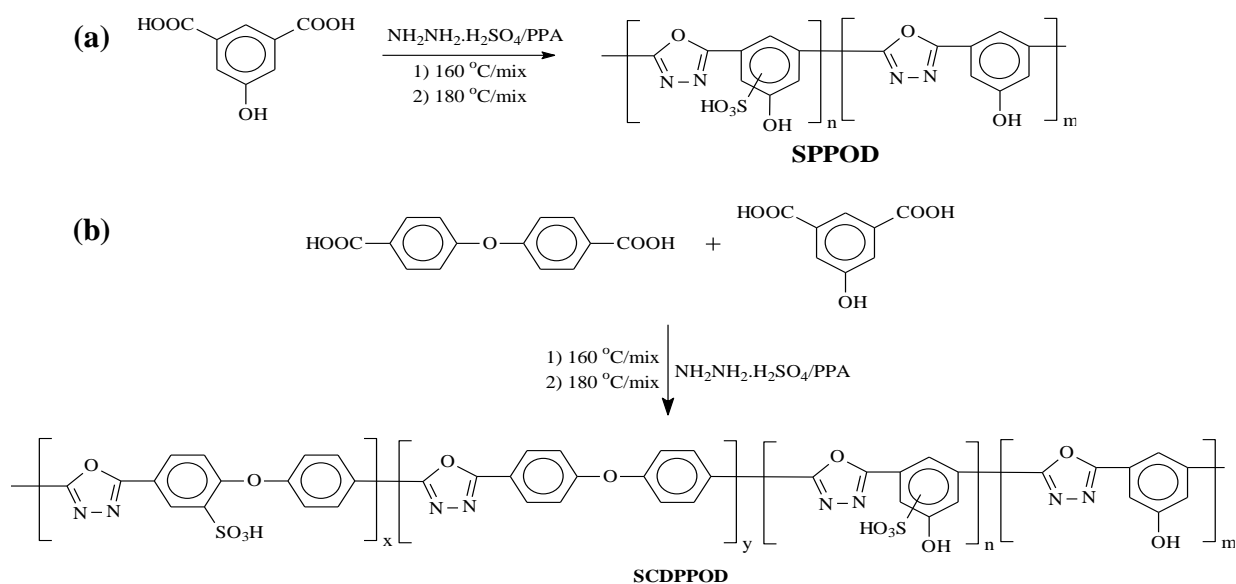
Scheme 39. The synthesis schemes of (a) SPPOD and (b) SCDPPOD copolymers.[235]

Liu *et al.* designed and synthesized a series of thioether-containing sulfonated polybenzoxazoles (SPTESBO-x) with various DS values, as depicted in **Scheme 42**.[236] Additionally, a series of end-capping thioether-containing sulfonated polybenzoxazoles (SPTESBO-HFB-x) were synthesized by the reaction of hexafluorobenzene (HFB) with PTESBO-x in DMAc at 80 °C to further enhance the oxidative stability of the sulfonated copolymers.[236] The theoretical IEC values of the SPTESBO-x and SPTESBO-HFB-x copolymers were obtained between 0.61-1.81 and 0.65-1.56 meq/g, respectively (**Table 10**). The end-capped SPTESBO-HFB-x copolymers showed higher η_{inh} values than the SPTESBO-x copolymers with the same DS values, which evidences the formation of high molecular weight copolymers during the end-capping polymerization reaction (**Table 10**). The end-capped

SPTESBO-HFB-x membranes demonstrated better τ values compared to the SPTESBO-x membranes in the accelerated Fenton test at 80 °C, which is associated with the elimination of the unstable end-groups for the end-capped SPTESBO-HFB-x copolymers.[236] The high DS value-containing sulfonated polybenzoxazole (SPTESBO-60 and SPTESBO-HFB-60) membranes exhibited an identical σ value of 0.13 S/cm at room temperature under fully humidified conditions, as compiled in **Table 10**. In the H_2-O_2 fuel cell test, the SPTESBO-HFB-60 MEA showed the maximum PPD value of 640 mW/cm^2 at 80 °C and 100% RH conditions.[236]

Xu *et al.* designed and synthesized a series of pendant naphthalene sulfonated poly(phenylene oxide)s (SPPOs; SNOx–BPPOs) via the etherification reaction of the bromomethylated PPO (BPPO) with Sodium 6-hydroxy-2-

Banerjee and Ghanti

Innov. Chem. Mater. Sustain. **2025**, *2*(1), 032-073

naphthalenesulfonate, as shown in **Scheme 41**.[237] The theoretical IEC values of the SNOx–BPPO copolymers were calculated between 0.93-1.62 mmol/g, as tabulated in **Table 10**. All the acidified SNOx–BPPO copolymers showed high thermal and mechanical (in the hydrated state, TS: 16-35 MPa and EB: 9-24%) stabilities, which is beneficial for PEMFC applications.[237] The SNOx–BPPO membranes demonstrated WU values between 15-28.2% and 16-34% at 25 and 80 ℃, respectively.[237] The SNOx–BPPO membranes exhibited lower water absorption properties due to incorporating the pendant naphthalene sulfonic acid group that restricts the excessive water intake.[237] The AFM morphological investigation revealed

that the hydrophilic ionic segments have become more significant in size and interconnected with the increase in the sulfonic acid contents of the SNOx–BPPO copolymers.[237] Among all the membranes, the SNO100%–BPPO membrane showed the highest σ value of 71 mS/cm at 25 ℃ and 100% RH conditions, as illustrated in **Table 10**.

Lee *et al.* synthesized a series of sulfonated polybenzothiazoles (sPBT-Fx) by the polycondensation reaction of 2,5-diamino-1,4-benzenedithiol dihydrochloride (DABDT) with the fluoro-sulfonated monomer 3,3′-disulfonate-2,2-bis(4-carboxyphenyl)hexafluoropropane (SCFA) and non-
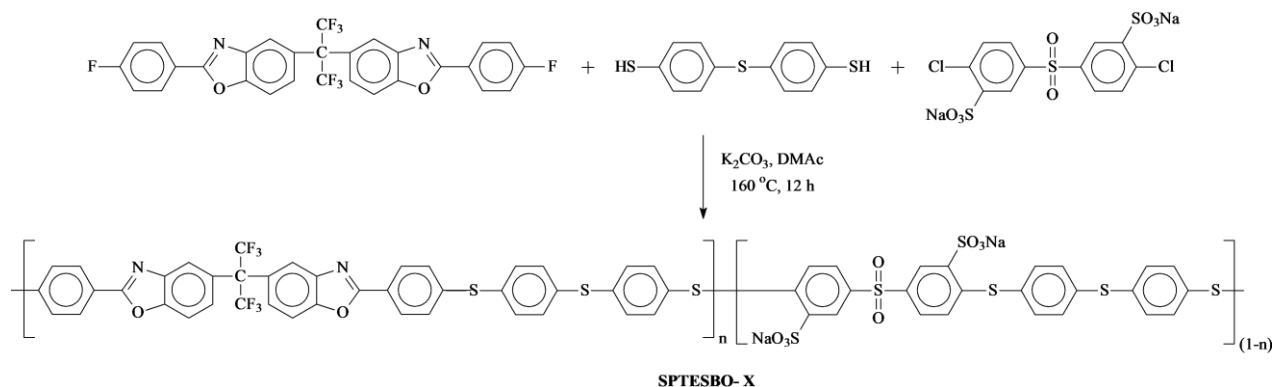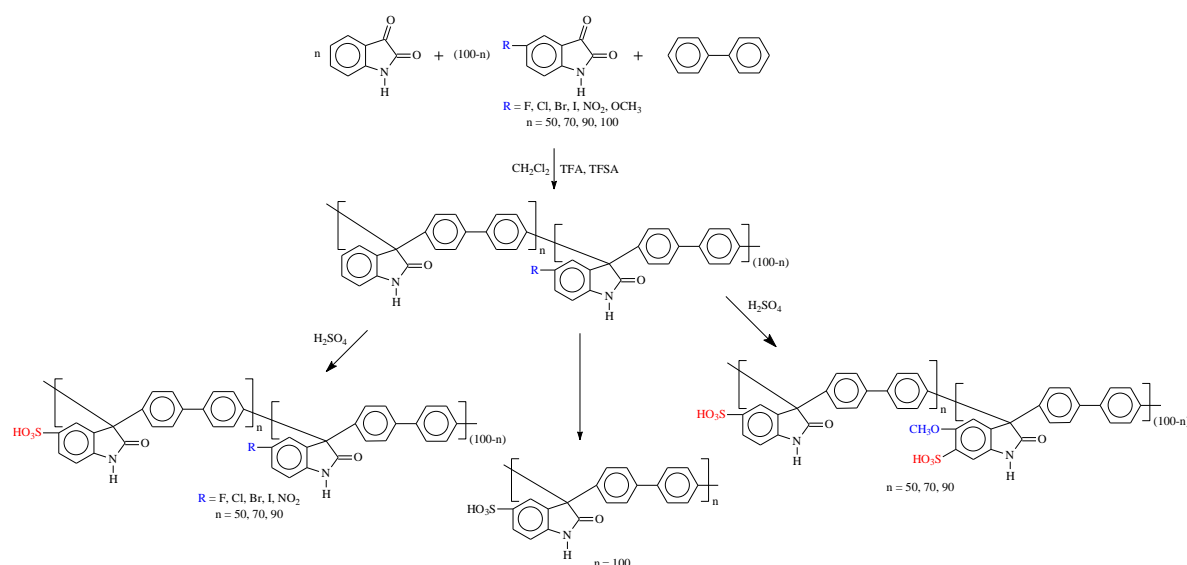

Scheme 40. The synthesis scheme of sulfonated poly(benzoxazole thioether sulfone)s (SPTESBO-x).[236]
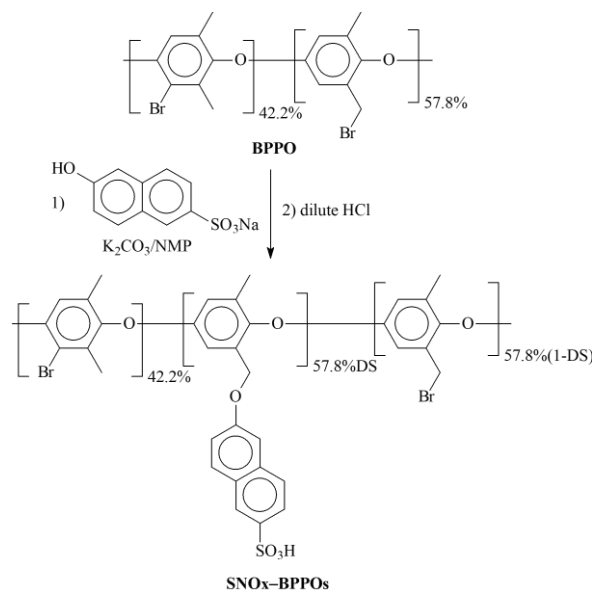
Scheme 41. The synthesis scheme of the pendant sulfonated poly(phenylene oxide) (SNOx–BPPOs) via the etherification reaction.[237]
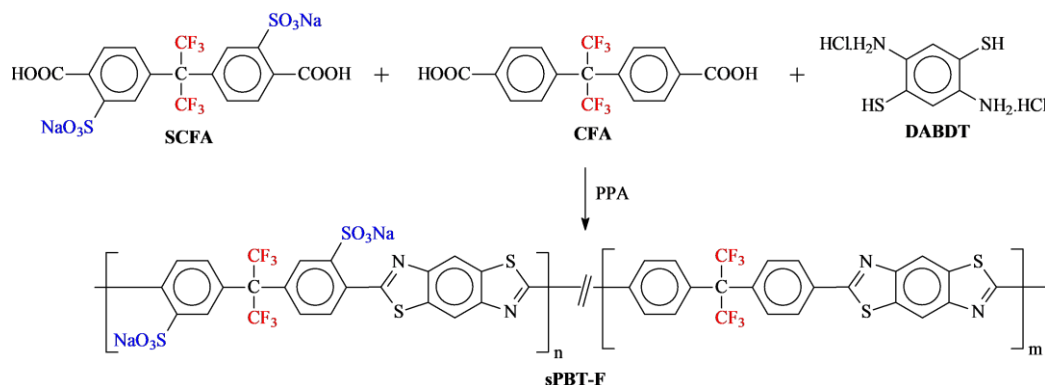
Scheme 42. The synthesis scheme of the semi-fluorinated sulfonated polybenzothiazoles (sPBT-F).[238]

Banerjee and Ghanti

Innov. Chem. Mater. Sustain. **2025**, 2(1), 032-073

Scheme 43. The synthesis scheme of the sulfonated poly(oxindole biphenylene) copolymers [SPOBP$_n$-RPOBP$_{(100-n)}$, R = F, Cl, Br, I, NO$_2$, and OCH$_3$].[239]

sulfonated monomer 2,2-bis(4-carboxyphenyl)hexafluoropropane (CFA) in the presence of PPA, as depicted in **Scheme 42**.[238] The M$_w$ and PDI values of the sPBT-Fx copolymers were obtained between 327.9-337.5 kg/mol and 2.36-2.43.[238] The theoretical and titration-based experimental IEC values of the sPBT-Fx copolymers were found between 2.32-2.64 and 2.34-2.66 meq/g, respectively.[238] The sPBT-Fx copolymers showed excellent thermal stability (T$_{d5\%}$: 299-361 ℃ in TGA analysis under N$_2$ flow) and better oxidative stability (τ: 4.2-6.0 h) in Fenton's experiment at 80 ℃, as illustrated in **Table 10**. The sPBT-Fx membranes exhibited closer or better WU values (30-46%) than those of the Nafion (30%) at 80 ℃ (**Table 10**). Among all the sPBT-Fx membranes, the sPBT-F82.5 membrane showed the highest σ value of 143 mS/cm at 80 ℃ and 100% RH conditions, as compiled in **Table 10**. The proton conduction-related E$_a$ values of the sPBT-Fx membranes were obtained between 4.38-6.62 kJ/mol, which indicates the continuous and accelerated proton transportation in the sPBT-Fx membranes.[238]

Li *et al*. designed and synthesized a series of ether-free sulfonated poly(oxindole biphenylene) copolymers [SPOBP$_n$-RPOBP$_{(100-n)}$, R = F, Cl, Br, I, NO$_2$, and OCH$_3$] by the SACFC polyhydroxyalkylations reaction of isatin, various substituted isatin, and biphenyl, followed by the post-sulfonation method, as shown in **Scheme 43**.[239] The η$_{inh}$ values of the non-sulfonated copolymers [POBP$_n$-RPOBP$_{(100-n)}$] were obtained between 1.21-1.69 dL/g.[239] The theoretical IEC values of the [SPOBP$_{50}$-RPOBP$_{50}$, R = F, Cl, Br, I, NO$_2$, and OCH$_3$] copolymers were found between 1.29-2.64 meq/g, as tabulated in **Table 10**. Among all the substituted copolymers, the -F, -Cl, and -Br group-containing sulfonated copolymers showed improved thermal stability in the TGA analysis under N$_2$ flow.[239] The -F, -Cl, -Br, and -NO$_2$ group-containing sulfonated poly(oxindole biphenyl) [SPOBP$_{50}$-RPOBP$_{50}$] membranes showed higher mechanical characteristics in the dry state than the other substituted membranes, as compiled in **Table 10**. The SPOBP$_{50}$-RPOBP$_{50}$ (R = F, Cl, Br, and NO$_2$) membranes exhibited WU and SR values of 33-39% and 10-13% at 80 ℃.[239] The SPOBP$_{50}$-RPOBP$_{50}$ (R = F, Cl, Br, and NO$_2$) membranes demonstrated extremely higher oxidative stability compared to the SPOBP$_{50}$-RPOBP$_{50}$ (R = I and CH$_3$O) membranes in Fenton's experiment at 80 ℃, as compiled in **Table 10**. The SPOBP$_{50}$-RPOBP$_{50}$ (R = F, Cl, Br, and NO$_2$) membranes showed the σ value of 29-34 and 74-76 mS/cm at 20 and 80 ℃ in 100% RH conditions.[239] In the H$_2$/O$_2$ fuel cell test, the SPOBP$_{50}$-FPOBP$_{50}$ MEA demonstrated the maximum PPD value of 950 mW/cm^2 with an OCV value of 0.90 V at 80 ℃ and 100% RH conditions.[239]

5. Future Perspective

Despite the impressive design and development of alternative hydrocarbon-based PEM materials, there are still some challenges and endeavors in designing and developing new ionic polymer architectures for PEMFC applications:

- Despite the lower molecular weight and η$_{inh}$ values of the partially fluorinated sulfonated PEMs, they demonstrated higher thermal and dimensional (lower WU and SR values) stabilities than the analogous non-fluorinated sulfonated PEMs.[143] Thus, the design and synthesis of new partially fluorinated sulfonated PEMs may benefit PEMFC applications.

- The end-capped sulfonated copolymers showed superior oxidative or chemical stability and enhanced thermal stability compared to the non-end-capped sulfonated copolymers, along with identical proton conductivity values.[236] So, this approach might be fruitful for synthesizing alternative hydrocarbon-based sulfonated PEMs with improved oxidative stability.

- The filler-loaded (MOF, nano-particles, etc.) composite membranes exhibited improved thermal stability, oxidative stability, proton conductivity value, and single-cell performance.[171,204,234] However, there is a requirement for optimization of filler loading percentage in the composite membranes for future PEMFC applications, as some of the high filler-loaded hybrid membranes demonstrated low PEMFC performances.

- Usually, the cross-linkers often compromise the proton conductivity values of the PEMs by enhancing the dimensional and oxidative stabilities.[157] However, few multiterm covalently cross-linked PEMs showed enhanced proton conductivity values with higher mechanical, dimensional, and oxidative stability values.[157,189] Hence, the appropriate multiterm cross-linked PEMs design may benefit the PEMFC applications.

- The blend PEMs showed remarkably higher thermal stability, mechanical properties, oxidative stabilities, and proton conductivity values than the pristine PEMs.[79,119,172] Therefore, the designing and synthesis of blend sulfonated PEMs are also beneficial for future PEMFC applications.

- The hydrocarbon-based N-heterocyclic sulfonated polazoles, such as sulfonated polybenzimidazoles, sulfonated polytriazoles, sulfonated polybenzoxazoles, sulfonated polybenzothiazoles, sulfonated polyoxadiazoles, etc., have appeared as a promising candidate for PEMFC applications.[99,102,173-175,231,238] Among these sulfonated polyazoles, only sulfonated polybenzimidazoles and

Banerjee and Ghanti

Innov. Chem. Mater. Sustain. **2025**, *2*(1), 032-073

sulfonated polytriazoles have been well-studied for PEMFC applications. Thus, the other sulfonated polyazole types must be explored more for PEMFC applications in the future.

- The phosphonic acid-based PEMs are relatively less evaluated than the sulfonic acid-based PEMs for PEMFC applications due to the lower proton conductivity value of the phosphonic acid-based PEMs.[105-107] Recently, a few phosphonated sulfonated PEMs have been investigated for PEMFC applications, and those PEMs exhibited higher proton conductivity values.[240-242] Hence, the designing and synthesis of these types of phosphonated sulfonated PEMs should have been a beneficial route for future PEMFC applications.

- Some of the alternative sulfonated PEMs demonstrated better fuel cell performances than the commercially available PFSA-based PEMs.[156,204,219,221] However, they have faced substantial challenges in their commercial market growth due to their primary challenges in large-scale production, long-term chemical durability, and economic restrictions. Therefore, continuous rational design and innovation of extended chemical durability, efficient power density, and more economical and environmentally friendly alternative sulfonated PEMs will be substantial for replacing PFSA-based PEMs.

6. Conclusion

FC technologies are on the verge of creating a massive evolution in the energy and automobile sectors for their sustainable energy generation capabilities. This review article provides a brief history of the FC and the various advantages, disadvantages, and limitations of FC technologies. The classifications of FCs based on the electrolyte types are summarized in this article, along with their limitations and particular applications. The working principle and essential components of a PEMFC are also described. The PEM of the PEMFCs is a solid polymer electrolyte membrane that allows the passage of protons but not electrons. Various factors that influence the performance of the PEM in PEMFC are also summarized. The PFSA-based membranes have been the most employed PEM materials in the PEMFC application due to their excellent proton conductivity and superior chemical stability. However, PFSA-based PEM materials are expensive, and their PEM characteristics are deuterated at higher temperatures and low RH levels. This review article beheld a variety of novel hydrocarbon-based sulfonated PEMs (such as SPAs, SPAEs, SPATEs, SPBIs, SPIs, SPTs, SPPAs, SPODs, SPBOs, SPBOs, SPPOs, SPBTs, and SPOBPs) that might be utilized as an alternative to the PFSA-based membranes in PEMFC applications. The synthetic methodologies, various PEM properties (thermal stability, mechanical properties, WU, proton conductivity, and oxidative stability values), H_2-O_2 fuel cell performance, and benefits of those novel hydrocarbon-based alternative PEMs are summarized.

Author Contribution Declaration

Bholanath Ghanti: Conceptualization, Data curation, Writing – original draft. **Susanta Banerjee:** Supervision, Conceptualization, Review and Editing of the manuscript, Funding acquisition.

Data Availability Declaration

There are no new data were created, hence data sharing is not applicable.

Declaration of Conflicts of Interest

The authors declare no competing financial interest.

References

1. A. E. Léodé, F. H. Agnimonhan, G. K. n'Gobi, B. Glinma, C. A. Kouchadé, B. Kounouhéwa. Review on the Proton Exchange Membrane Fuel Cell (PEMFC) in Benin Republic (West Africa). *Res. J. Physical Sci.*, **2024**, *12*, 1. ISSN.;2320:4796.
2. A. Ajanovic, R. Haas. Prospects and impediments for hydrogen and fuel cell vehicles in the transport sector. *Int. J. Hydrogen Energy*, **2021**, *46*, 10049. https://doi.org/10.1016/j.ijhydene.2020.03.122
3. A. B. Ali, A. K. Nemah, Y. A. Al Bahadli. Principles and performance and types, advantages and disadvantages of fuel cells: A review. Case Stud. Chem. Environ. Eng., **2024**, *10*, 100920. https://doi.org/10.1016/j.cscee.2024.100920
4. B. P. Statistical Review of World Energy, 69th ed.; BP p.l.c.: London, UK, 2020; Available online: https://www.bp.com/en/global/corporate/energy-economics/statistical-review-of-world-energy.html (accessed on 30 August **2021**)
5. B. Su, Y. Wang, Z. Xu, W. Han, H. Jin, H. Wang. Novel ways for hydrogen production based on methane steam and dry reforming integrated with carbon capture. *Energy Convers. Manag.*, **2022**, *270*, 116199. https://doi.org/10.1016/j.enconman.2022.116199
6. Y. Yang, X. Yu, W. Zhu, C. Xie, B. Zhao, L. Zhang, Y. Shi, L. Huang, R. Zhang. Degradation prediction of proton exchange membrane fuel cells with model uncertainty quantification, *Renew. Energy*, **2023**, *219*, 119525. https://doi.org/10.1016/j.renene.2023.119525
7. Z. Xu, W. Xu, E. Stephens, B. Koeppel. Mechanical reliability and life prediction of coated metallic interconnects within solid oxide fuel cells. Renew. Energy, **2017**, 113, 1472. https://doi.org/10.1016/j.renene.2017.06.103
8. Y. Zhou, R. Li, Z. Lv, J. Liu, H. Zhou, C. Xu. Green hydrogen: A promising way to the carbon-free society. *Chin. J. Chem. Eng.*, **2022**, 43, 2. https://doi.org/10.1016/j.cjche.2022.02.001
9. S. S. Kumar, H. Lim. An overview of water electrolysis technologies for green hydrogen production. *Energy Rep.*, **2022**, *8*, 13793. https://doi.org/10.1016/j.egyr.2022.10.127
10. S. Li, M. Tabatabaei, F. Li, S.-H. Ho. A review of green biohydrogen production using anoxygenic photosynthetic bacteria for hydrogen economy: Challenges and opportunities. *Int. J. Hydrogen Energy*, **2024**, *54*, 218. https://doi.org/10.1016/j.ijhydene.2022.11.014
11. L. A. Omeiza, A. M. Abdalla, B. Wei, A. Dhanasekaran, Y. Subramanian, S. Afroze, M. S. Reza, S. A. Bakar, A. K. Azad. Nanostructured Electrocatalysts for Advanced Applications in Fuel Cells. *Energies* (Basel), **2023**, *16*, 1876. https://doi.org/10.3390/en16041876
12. M. C. Heller, G. A. Keoleian. Greenhouse Gas Emission Estimates of U.S. Dietary Choices and Food Loss. *J. Ind. Ecol.*, **2015**, *19*, 391. https://doi.org/10.1111/jiec.12174
13. S. Li, X. Li, S.-H. Ho. How to enhance carbon capture by evolution of microalgal photosynthesis? *Sep. Purif. Technol.*, **2022**, *291*, 120951. https://doi.org/10.1016/j.seppur.2022.120951
14. R. V. Vardhan, R. Mahalakshmi, R. Anand, A. Mohanty. A Review on Green Hydrogen: Future of Green Hydrogen in India, in: 2022 6th International Conference on Devices, Circuits and Systems (ICDCS), IEEE, **2022**, 303. https://doi.org/10.1109/ICDCS54290.2022.9780805
15. A. Bajoria, J. Kanpariya, A. Bera. Greenhouse gases and global warming. In Advances and Technology Development in Greenhouse Gases: Emission, Capture and Conversion, Elsevier, **2024**, 121. https://doi.org/10.1016/B978-0-443-19066-7.00006-0
16. M. Zavala-Méndez, A. Vargas, J. Carrillo-Reyes. Maximization of bio-hydrogen production from winery vinasses using on-line feedback control. *Int. J. Hydrogen Energy*, **2022**, *47*, 33259. https://doi.org/10.1016/j.ijhydene.2022.07.196
17. P. P. Edwards, V. L. Kuznetsov, W. I. F. David, N. P. Brandon. Hydrogen and fuel cells: Towards a sustainable energy future. *Energy Policy*, **2008**, *36*, 4356. https://doi.org/10.1016/j.enpol.2008.09.036
18. S. J. C. Cleghorn, D. K. Mayfield, D. A. Moore, J. C. Moore, G. Rusch, T. W. Sherman, N. T. Sisofo, U. Beuscher. A polymer electrolyte fuel cell life test: 3 years of continuous operation. *J. Power Sources*, **2006**, *158*, 446. https://doi.org/10.1016/j.jpowsour.2005.09.062
19. T. K. Maiti, J. Singh, P. Dixit, J. Majhi, S. Bhushan, A. Bandyopadhyay, S. Chattopadhyay. Advances in perfluorosulfonic acid-based proton exchange membranes for fuel cell applications: A review. *Chem. Eng. J. Adv.*, **2022**, *12*, 100372. https://doi.org/10.1016/j.ceja.2022.100372
20. J. You, L. Dou, K. Yoshimura, T. Kato, K. Ohya, T. Moriarty, K. Emery, C. C. Chen, J. Gao, G. Li, Y. Yang. A polymer tandem solar cell with 10.6% power conversion efficiency. *Nat. Commun.*, **2013**, *4*, 1446. https://doi.org/10.1038/ncomms2411

Banerjee and Ghanti

Innov. Chem. Mater. Sustain. **2025**, *2*(1), 032-073

21. J. R. Kim, S. W. Choi, S. M. Jo, W.S. Lee, B. C. Kim. Electrospun PVdF-based fibrous polymer electrolytes for lithium-ion polymer batteries. *Electrochim. Acta.*, **2004**, *50*, 69. https://doi.org/10.1016/j.electacta.2004.07.014

22. J. Xi, Z. Wu, X. Qiu, L. Chen. Nafion/SiO₂ hybrid membrane for vanadium redox flow battery. *J. Power Sources*, **2007**, *166*, 531. https://doi.org/10.1016/j.jpowsour.2007.01.069

23. N. S. Rathore, N. L. Panwar. Renewable energy sources for sustainable development. New Delhi, India: New India Publishing Agency, **1996**.

24. A. Hussain, S. M. Arif, M. Aslam. Emerging renewable and sustainable energy technologies: State of the art. Renew. Sustain. Energy Rev., **2017**, *71*, 12. https://doi.org/10.1016/j.rser.2016.12.033

25. N. L. Panwara, S. C. Kaushik, K. Surendra. Role of renewable energy sources in environmental protection: a review. *Renew. Sustain. Energy Rev.*, **2011**, *15*, 1513. https://doi.org/10.1016/j.rser.2010.11.037

26. N. H. Ravindranath, D. O. Hall. Biomass, energy, and environment: a developing country perspective from India. Oxford, United Kingdom, Oxford University Press, **1995**. https://doi.org/10.1093/oso/9780198564362.001.0001

27. H. Zhang, P. K. Shen. Advances in the high performance polymer electrolyte membranes for fuel cells. *Chem. Soc. Rev.*, **2012**, *41*, 2382. https://doi.org/10.1039/c2cs15269j

28. O. M. Babatunde, B. D. Akintayo, M. U. Emezirinwune, O. A. Olanrewaju. Environmental impact assessment of a 1 kW proton-exchange membrane fuel cell: a mid-point and end-point analysis. *Hydrogen*, **2024**, *5*, 352. https://doi.org/10.3390/hydrogen5020020

29. O. Sel, A. Soules, B. Améduri, B. Boutevin, C. Laberty-Robert, G. Gebel, C. Sanchez. Original fuel-cell membranes from crosslinked terpolymers via a "sol–gel" strategy. *Adv. Funct. Mater.*, **2010**, *20*, 1090. https://doi.org/10.1002/adfm.200902210

30. K. Jiao, J. Xuan, Q. Du, Z. Bao, B. Xie, B. Wang, Y. Zhao, L. Fan, H. Wang, Z. Hou, S. Huo, N.P. Brandon, Y. Yin, M. D. Guiver. Designing the next Generation of Proton-Exchange Membrane Fuel Cells. *Nature*, **2021**, *595*, 361. https://doi.org/10.1038/s41586-021-03482-7

31. W. Li, W. Liu, W. Jia, J. Zhang, Q. Zhang, Z. Zhang, J. Zhang, Y. Li, Y. Liu, H. Wang, Y. Xiang, S. Lu. Dual-Proton Conductor for Fuel Cells with Flexible Operational Temperature. *Adv. Mater.*, **2024**, *36*, 2310584. https://doi.org/10.1002/adma.202310584

32. U. Lucia. Overview on fuel cells. *Renew. Sustain. Energy Rev.*, **2014**, *30*, 164. https://doi.org/10.1016/j.rser.2013.09.025

33. W. Vielstich, H. Gasteiger, A. Lamm. Handbook of Fuel cells— fundamentals, technology, applications. New York, Wiley, ISBN: 978-0-471-49926-8, **2003**, 2720.

34. H. Davy. The collected works of Sir Humphry Davy...: Discourses delivered before the Royal society. Elements of agricultural chemistry, pt. I. Smith, Elder and Company, **1840**.

35. R. Meldola, S. C. Friedrich. Ein Blatt zur Geschichte des 19 Jahrhunderts. *Nature*, **1900**, *62*, 97. https://doi.org/10.1038/062097a0

36. W. R. Grove. On a new voltaic combination. London and Edinburgh Philosophical Magazine, **1838**, *13*, 430.

37. W. R. Grove. On a new voltaic combination of gasses by platinum. London and Edinburgh Philosophical Magazine, **1839**, *14*, 127. https://doi.org/10.1080/14786443908649684

38. J. M. Andújar, F. Segura. Fuel cells: history and updating. A walk along two centuries. *Renew. Sustain. Energy Rev.*, **2009**, *13*, 2309. https://doi.org/10.1016/j.rser.2009.03.015

39. P. Grimes. Historical pathways for fuel cells. The new electric century. *Proc. Annu. Batter. Conf. Appl. Adv.*, **2000**, 41. https://doi.org/10.1109/BCAA.2000.838369

40. C. Spiegel. Designing and Building Fuel Cells, McGraw-Hill, New York, **2007**.

41. M. L. Perry, T. F. Fuller. A Historical Perspective of Fuel Cell Technology in the 20th Century. *J. Electrochem. Soc.*, **2002**, *149*, S59. https://doi.org/10.1149/1.1488651

42. S. Shamim, K. Sudhakar, B. Choudhary, J. Anwar. A review on recent advances in proton exchange membrane fuel cells: materials, technology and applications. *Adv. Appl. Sci. Res.*, **2015**, *6*, 89, ISSN: 0976-8610.

43. B. C. H. Steele. Material science and engineering: The enabling technology for the commercialisation of fuel cell systems. *J. Mater. Sci.*, **2001**, *36*, 1053. https://doi.org/10.1023/A:1004853019349

44. L. Mond, C. Langer. A new form of gas battery, communicated by Lord R.S. Rayleigihs. Proceedings of the Royal Society of London XLVI, **1889**, 296–304.

45. A. Kirubakaran, S. Jain, R. K. Nema. A review on fuel cell technologies and power electronic interface. *Renew. Sustain. Energy Rev.*, **2009**, *13*, 2430. https://doi.org/10.1016/j.rser.2009.04.004

46. H. Morikawa, H. Kikuchi, N. Saito. Development and advances of a V-flow FC tack for FCX clarity. SAE Tech. Pap., **2009**, *2*, 955. https://doi.org/10.4271/2009-01-1010

47. N. A. Qasem, G. A. Abdulrahman. A recent comprehensive review of fuel cells: history, types, and applications. *Int. J. Energy Res.*, **2024**, *2024*, 7271748. https://doi.org/10.1155/2024/7271748

48. J. M. Andújar, F. Segura. Fuel cells: history and updating. A walk along two centuries. *Renew. Sustain. Energy Rev.*, **2009**, *13*, 2309. https://doi.org/10.1016/j.rser.2009.03.015

49. L. Carrette, K. A. Friedrich, U. Stimming. Fuel cells: principles, types, fuels, and applications. *ChemPhysChem*, **2000**, *1*, 162. https://doi.org/10.1002/1439-7641(20001215)1:4<162::AIDCPHC162>3.0.CO;2-Z

50. R. E. Rosli, A. B. Sulong, W. R. W. Daud, M. A. Zulkifley, T. Husaini, M. I. Rosli, E. H. Majlan, M. A. Haque. A Review of High-Temperature Proton Exchange Membrane Fuel Cell (HTPEMFC) System. *Int. J. Hydrogen Energy*, **2017**, *42*, 9293. https://doi.org/10.1016/j.ijhydene.2016.06.211

51. S. Mekhilef, R. Saidur, A. Safari. Comparative study of different fuel cell technologies. *Renew. Sustain. Energy Rev.*, **2012**, *16*, 981. https://doi.org/10.1016/j.rser.2011.09.020

52. R. Rath, P. Kumar, S. Mohanty, S. K. Nayak. Recent advances, unsolved deficiencies, and future perspectives of hydrogen fuel cells in transportation and portable sectors *Int. J. Energy Res.*, **2019**, *43*, 8931. https://doi.org/10.1002/er.4795

53. A. Javed, P. P. Gonzalez, V. Thangadurai. A critical review of electrolytes for advanced low-and high-temperature polymer electrolyte membrane fuel cells. *ACS Appl. Mater. Interfaces*, **2023**, *15*, 29674. https://doi.org/10.1021/acsami.3c02635

54. S. Bose, T. Kuila, T. X. Nguyen, N. H. Kim, K. T. Lau, J. H. Lee. Polymer membranes for high temperature proton exchange membrane fuel cell: Recent advances and challenges. *Prog. Polym. Sci.*, **2011**, *36*, 813. https://doi.org/10.1016/j.progpolymsci.2011.01.003

55. J. Wang, B. Wang, C. Tongsh, T. Miao, P. Cheng, Z. Wang, Q. Du, K. Jiao. Combining proton and anion exchange membrane fuel cells for enhancing the overall performance and self-humidification. *Chem. Eng. J.*, **2022**, *428*, 131969. https://doi.org/10.1016/j.cej.2021.131969

56. J. H. Wee. Applications of proton exchange membrane fuel cell systems. *Renew. Sustain. Energy Rev.*, **2007**, *11*, 1720. https://doi.org/10.1016/j.rser.2006.01.005

57. L. Zhang, S. R. Chae, Z. Hendren, J. S. Park, M. R. Wiesner. Recent advances in proton exchange membranes for fuel cell applications. *Chem. Eng. J.*, **2012**, *204*, 87. https://doi.org/10.1016/j.cej.2012.07.103

58. Z. Shang, R. Wycisk, P. Pintauro. Electrospun composite proton-exchange and anion-exchange membranes for fuel cells. *Energies*, **2021**, *14*, 6709. https://doi.org/10.3390/en14206709

59. A. K. Mohanty, E. A. Mistri, A. Ghosh, S. Banerjee. Synthesis and characterization of novel fluorinated poly (arylene ether sulfone)s containing pendant sulfonic acid groups for proton exchange membrane materials. *J. Membr. Sci.*, **2012**, *409*, 145. https://doi.org/10.1016/j.memsci.2012.03.048

60. E. A. Mistri, A. K. Mohanty, S. Banerjee. Synthesis and characterization of new fluorinated poly(ether imide) copolymers with controlled degree of sulfonation for proton exchange membranes. *J. Membr. Sci.*, **2012**, *411*, 117. https://doi.org/10.1016/j.memsci.2012.04.023

61. A. Singh, R. Mukherjee, S. Banerjee, H. Komber, B. Voit. Sulfonated polytriazoles from a new fluorinated diazide monomer and investigation of their proton exchange properties. *J. Membr. Sci.*, **2014**, *469*, 225. https://doi.org/10.1016/j.memsci.2014.06.043

62. D. R. Dekel. Review of Cell Performance in Anion Exchange Membrane Fuel Cells. *J. Power Sources*, **2018**, *375*, 158. https://doi.org/10.1016/j.jpowsour.2017.07.117

63. M. M. Hossain, Z. Yang, L. Wu, X. Liang, T. Xu. Introducing a New Generation of Anion Conducting Membrane Using Swelling Induced Fabrication of Covalent Methanol Barrier Layer. *J. Membr. Sci.*, **2021**, *620*, 118840. https://doi.org/10.1016/j.memsci.2020.118840

64. Y. Zha, M. L. Disabb-Miller, Z. D. Johnson, M. A. Hickner, G. N. Tew. Metal-Cation-Based Anion Exchange Membranes. *J. Am. Chem. Soc.*, **2012**, *134*, 4493. https://doi.org/10.1021/ja211365r

65. R. Mukherjee, S. Banerjee, H. Komber, B. Voit. Carboxylic acid functionalized fluorinated sulfonated poly (arylene ether sulfone) copolymers with enhanced oxidative stability. *J. Membr. Sci.*, **2016**, *510*, 497. https://doi.org/10.1016/j.memsci.2016.03.028

66. Y. Xue, L. Shi, X. Liu, J. Fang, X. Wang, B. P. Setzler, W. Zhu, Y. Yan, Z. Zhuang. A highly active, stable, and low-cost platinum-free anode catalyst based on RuNi for hydroxide exchange membrane fuel cells. *Nat. Commun.*, **2020**, *11*, 5651. https://doi.org/10.1038/s41467-020-19413-5

67. D. Henkensmeier, M. Najibah, C. Harms, J. Žitka, J. Hnát, K. Bouzek. Overview: State-of-the-Art Commercial Membranes for Anion Exchange Membrane Water Electrolysis. *J. Electrochem. Energy Convers. Storage*, **2020**, *18*, 024001. https://doi.org/10.1115/1.4047963

68. J. R. Varcoe, P. Atanassov, D. R. Dekel, A. M. Herring, M. A. Hickner, P. A. Kohl, A. R. Kucernak, W. E. Mustain, K. Nijmeijer, K. Scott, T. Xu. Anion-Exchange Membranes in Electrochemical Energy Systems. *Energy Environ. Sci.*, **2014**, *7*, 3135. https://doi.org/10.1039/C4EE01303D

69. Amel, A.; Smedley, S.B.; Dekel, D.R.; Hickner, M.A.; Ein-Eli, Y. Characterization and Chemical Stability of Anion Exchange Membranes Cross-Linked with Polar Electron-Donating Linkers. *J. Electrochem. Soc.*, **2015**, *162*, F1047. https://doi.org/10.1149/2.0891509jes

70. D. R. Dekel, M. Amar, S. Willdorf, M. Kosa, S. Dhara, C. E. Diesendruck. Effect of Water on the Stability of Quaternary Ammonium Groups for Anion Exchange Membrane Fuel Cell Applications. *Chem. Mater.*, **2017**, *29*, 4425. https://doi.org/10.1021/acs.chemmater.7b00958

71. Z. Tao, C. Wang, X. Zhao, J. Li, M. D. Guiver. Progress in high-performance anion exchange membranes based on the design of stable cations for alkaline fuel cells. *Adv. Mater. Technol.*, **2021**, *6*, 2001220. https://doi.org/10.1002/admt.202001220

Banerjee and Ghanti

Innov. Chem. Mater. Sustain. **2025**, 2(1), 032-073

72. G. Couture, A. Alaaeddine, F. Boschet, B. Ameduri. Polymeric materials as anion-exchange membranes for alkaline fuel cells. *Prog. Polym. Sci.*, **2011**, *36*, 1521. https://doi.org/10.1016/j.progpolymsci.2011.04.004

73. W. E. Mustain, M. Chatenet, M. Page, Y. S. Kim. Durability challenges of anion exchange membrane fuel cells. *Energy Environ. Sci.*, **2020**, *13*, 2805. https://doi.org/10.1039/D0EE01133A

74. Y. Prykhodko, K. Fatyeyeva, L. Hespel, S. Marais. Nafion®-based membranes for proton exchange fuel cell application. *Chem. Eng. J.*, **2021**, *409*, 127329. https://doi.org/10.1016/j.cej.2020.127329

75. M. J. Workman, A. Serov, L. Tsui, P. Atanassov, K. Artyushkova. Fe–N–C Catalyst Graphitic Layer Structure and Fuel Cell Performance. *ACS Energy Lett.*, **2017**, *2*, 1489. https://doi.org/10.1021/acsenergylett.7b00391

76. J. Wang, Y. Zhao, B. P. Setzler, S. Rojas-Carbonell, C. B. Yehuda, A. Amel, M. Page, L. Wang, K. Hu, L. Shi, S. Gottesfeld, B. Xu, Y. Yan. Poly(aryl piperidinium) membranes and ionomers for hydroxide exchange membrane fuel cells. *Nat. Energy*, **2019**, *4*, 392. https://doi.org/10.1038/s41560-019-0372-8

77. X. Wu, S. Xing, J. Luo, H. Wang, F. Huang, C. Zhao. Progress and Challenges on Air-cooled Open-cathode Proton Exchange Membrane Fuel Cells: Materials, Structures, and Systems. *Energy Rev.*, **2025**, *4*, 100130. https://doi.org/10.1016/j.enrev.2025.100130

78. A. Singh, S. Banerjee, H. Komber, B. Voit. Synthesis and characterization of highly fluorinated sulfonated polytriazoles for proton exchange membrane application. *RSC advances*, **2016**, *6*, 13478. https://doi.org/10.1039/C5RA26821D

79. B. Campagne, G. David, B. Améduri, D. J. Jones, J. Rozière, I. Roche. Novel blend membranes of partially fluorinated copolymers bearing azole functions with sulfonated PEEK for PEMFC operating at low relative humidity: influence of the nature of the N-heterocycle. *Macromolecules*, **2013**, *46*, 3046. https://doi.org/10.1021/ma400239f

80. B. Ghanti, R. Kamble, S. Roy, S. Banerjee. Synthesis and characterization of sulfonated polytriazoles utilizing 1, 4-bis (4-azido-2-(trifluoromethyl) phenoxy) benzene for the proton exchange membrane applications. *J. Polym. Sci.*, **2023**, *61*, 1792. https://doi.org/10.1002/pol.20220769

81. H. Pourrahmani, C. M. Bernier, J. Van Herle. The application of fuel-cell and battery technologies in unmanned aerial vehicles (UAVs): a dynamic study. *Batteries*, **2022**, *8*, 73. https://doi.org/10.3390/batteries8070073

82. Y. Liu, H. Ma, Y. Tong, A. Uma, Y. Luo, S. Zhao. Progress of Polyhedral Oligomeric Silsesquioxanes in Proton Exchange Membrane Fuel Cells: A Review. *Process. Saf. Environ. Prot.*, **2024**, *187*, 1322. https://doi.org/10.1016/j.psep.2024.05.057

83. X. Z. Yuan, C. Nayoze-Coynel, N. Shaigan, D. Fisher, N. Zhao, N. Zamel, P. Gazdzicki, M. Ulsh, K. A. Friedrich, F. Girard, U. Groos. A review of functions, attributes, properties and measurements for the quality control of proton exchange membrane fuel cell components. *J. Power Sources*, **2021**, *491*, 229540. https://doi.org/10.1016/j.jpowsour.2021.229540

84. Y. Wang, D. F. Ruiz Diaz, K. S. Chen, Z. Wang, X. C. Adroher. Materials, Technological Status, and Fundamentals of PEM Fuel Cells – A Review. *Mater. Today*, **2020**, *32*, 178. https://doi.org/10.1016/j.mattod.2019.06.005

85. Y. Sun, S. Polani, F. Luo, S. Ott, P. Strasser, F. Dionigi. Advancements in cathode catalyst and cathode layer design for proton exchange membrane fuel cells. *Nat. Commun.*, **2021**, *12*, 5984. https://doi.org/10.1038/s41467-021-25911-x

86. D. Wu, C. Peng, C. Yin, H. Tang. Review of system integration and control of proton exchange membrane fuel cells. *Electrochem. Energy Rev.*, **2020**, *3*, 466. https://doi.org/10.1007/s41918-020-00068-1

87. B. Smitha, S. Sridhar, A. A. Khan. Solid polymer electrolyte membranes for fuel cell applications—a review. *J. Membr. Sci.*, **2005**, *259*, 10. https://doi.org/10.1016/j.memsci.2005.01.035

88. A. G. Kumar, A. Singh, H. Komber, B. Voit, B. R. Tiwari, M. T. Noori, M. M. Ghangrekar, S. Banerjee. Novel sulfonated Co-poly(ether imide)s containing trifluoromethyl, fluorenyl and hydroxyl groups for enhanced proton exchange membrane properties: Application in microbial fuel cell. *ACS Appl. Mater. Interfaces*, **2018**, *10*, 14803. https://doi.org/10.1021/acsami.8b03452

89. A. Ghorai, S. Banerjee. Phosphorus-containing aromatic polymers: Synthesis, structure, properties and membrane-based applications. *Prog. Polym. Sci.*, **2023**, *138*, 101646. https://doi.org/10.1016/j.progpolymsci.2023.101646

90. E. Qu, X. Hao, M. Xiao, D. Han, S. Huang, Z. Huang, S. Wang, Y. Meng. Proton exchange membranes for high temperature proton exchange membrane fuel cells: Challenges and perspectives. *J. Power Sources*, **2022**, *533*, 231386. https://doi.org/10.1016/j.jpowsour.2022.231386

91. H. Pourrahmani, A. Yavarinasab, M. Siavashi, M. Matian. Progress in the proton exchange membrane fuel cells (PEMFCs) water/thermal management: From theory to the current challenges and real-time fault diagnosis methods. *Energy Rev.*, **2022**, *1*, 100002. https://doi.org/10.1016/j.enrev.2022.100002

92. J. Fan, M. Chen, Z. Zhao, Z. Zhang, S. Ye, S. Xu, H. Wang, H. Li. Bridging the gap between highly active oxygen reduction reaction catalysts and effective catalyst layers for proton exchange membrane fuel cells. *Nat. Energy*, **2021**, *6*, 475. https://doi.org/10.1038/s41560-021-00824-7

93. A. Kusoglu, A. Z. Weber. New insights into perfluorinated sulfonic-acid ionomers. *Chem. Rev.*, **2017**, *117*, 987. https://doi.org/10.1021/acs.chemrev.6b00159

94. B. Ghanti, R. Kamble, H. Komber, B. Voit, S. Banerjee. High proton-conducting phosphine oxide-and pyridinyl-based fluoro-sulfonated proton exchange membranes with enhanced chemical stability. *J. Power Sources*, **2025**, *631*, 236201. https://doi.org/10.1016/j.jpowsour.2025.236201

95. Z. Li, Y. Wang, Y. Mu, B. Wu, Y. Jiang, L. Zeng, T. Zhao. Recent advances in the anode catalyst layer for proton exchange membrane fuel cells. *Renew. Sustain. Energy Rev.*, **2023**, *176*, 113182. https://doi.org/10.1016/j.rser.2023.113182

96. A. K. Mandal, S. Bisoi, S. Banerjee. Effect of phosphaphenanthrene skeleton in sulfonated polyimides for proton exchange membrane application. *ACS Appl. Polym. Mater.*, **2019**, *1*, 893. https://doi.org/10.1021/acsapm.9b00128

97. B. Ghanti, S. Banerjee. Fluorine-Free Sulfonated Poly (sulfone triazole) s with a Pendant Phosphaphenanthrene Moiety for Proton Exchange Membrane Applications. *Macromolecules*, **2025**. https://doi.org/10.1021/acs.macromol.5c00277

98. Z. Rui, J. Liu. Understanding of free radical scavengers used in highly durable proton exchange membranes. *Prog. Nat. Sci.: Mater. Int.*, **2020**, *30*, 732. https://doi.org/10.1016/j.pnsc.2020.08.013

99. B. Ghanti, R. Kamble, H. Komber, B. Voit, S. Banerjee. Synergistically Functionalized Pyridinyl-and Phosphine-Oxide-Based Semifluoro-Sulfonated Copolytriazole Membrane Preparation via "Click" Polymerization for Proton Exchange Membrane Applications. *Macromolecules*, **2024**, *57*, 4584. https://doi.org/10.1021/acs.macromol.4c00050

100. S. Roy, B. Ghanti, D. Ghosh, D. Pradhan, B. Voit, S. Banerjee. Sterically Hindered Pyridine-Linked Sulfonated Polytriazoles: Fabrication of Membranes and Investigation of Single Fuel Cell Performance. *ACS Appl. Polym. Mater.*, **2022**, *4*, 7450. https://doi.org/10.1021/acsapm.2c01189

101. B. Date, J. Han, S. Park, E. J. Park, D. Shin, C. Y. Ryu, C. Bae. Synthesis and morphology study of SEBS triblock copolymers functionalized with sulfonate and phosphonate groups for proton exchange membrane fuel cells. *Macromolecules*, **2018**, *51*, 1020. https://doi.org/10.1021/acs.macromol.7b01848

102. A. Abdolmaleki, K. Eskandari, M. R. Molavian. Sulfonated or phosphonated membranes? DFT investigation of proton exchange in poly (oxadiazole) membranes. *Polymer*, **2016**, *87*, 181. https://doi.org/10.1016/j.polymer.2016.02.011

103. S. Bano, Y. S. Negi, K. Ramya. Studies on new highly phosphonated poly (ether ketone) based promising proton conducting membranes for high temperature fuel cell. *Int. J. Hydrogen Energy*, **2019**, *44*, 28968. https://doi.org/10.1016/j.ijhydene.2019.09.067

104. T. Wei, Y. Zhao, Z. Ren, Y. Han, H. Zhang, Z. Shao. Facile and affordable synthesis of sulfonated and phosphonated poly (p-terphenyl perfluorophenyl) s for proton exchange membrane fuel cells. *Next Sustainability*, **2024**, *3*, 100021. https://doi.org/10.1016/j.nxsust.2023.100021

105. J. Parvole, P. Jannasch. Polysulfones grafted with poly (vinylphosphonic acid) for highly proton conducting fuel cell membranes in the hydrated and nominally dry state. *Macromolecules*, **2008**, *41*, 3893. https://doi.org/10.1021/ma800042m

106. N. Y. Abu-Thabit, S. A. Ali, S. J. Zaidi. New highly phosphonated polysulfone membranes for PEM fuel cells. *J. Membr. Sci.*, **2010**, *360*, 26. https://doi.org/10.1016/j.memsci.2010.04.041

107. H. Tang, K. Geng, Y. Hu, N. Li. Synthesis and properties of phosphonated polysulfones for durable high-temperature proton exchange membranes fuel cell. *J. Membr. Sci.*, **2020**, *605*, 118107. https://doi.org/10.1016/j.memsci.2020.118107

108. M. A. Hickner, H. Ghassemi, Y. S. Kim, B. R. Einsla, J. E. McGrath. Alternative polymer systems for proton exchange membranes (PEMs). *Chem. Rev.*, **2004**, *104*, 4587. https://doi.org/10.1021/cr020711a

109. A. Ghorai, S. Roy, S. Das, H. Komber, M. M. Ghangrekar, B. Voit, S. Banerjee. Chemically stable sulfonated polytriazoles containing trifluoromethyl and phosphine oxide moieties for proton exchange membranes. *ACS Appl. Polym. Mater.*, **2020**, *2*, 2967. https://doi.org/10.1021/acsapm.0c00443

110. T. Higashihara, K. Matsumoto, M. Ueda. Sulfonated aromatic hydrocarbon polymers as proton exchange membranes for fuel cells. *Polymer*, **2009**, *50*, 5341. https://doi.org/10.1016/j.polymer.2009.09.001

111. S. M. Ibrahim, E. H. Price, R. A. Smith. EI duPont de Nemours. *Proc. Electrochem. Soc.*, **1983**, 83.

112. R. Kamble, A. Ghorai, B. Ghanti, D. Pradhan, S. Banerjee. Fabrication of high proton conducting composite membranes from amino group functionalized MOF and semi-fluorinated sulfonated poly (arylene ether sulfone)s. *Eur. Polym. J.*, **2022**, *179*, 111574. https://doi.org/10.1016/j.eurpolymj.2022.111574

113. Z. Cui, E. Drioli, Y. M. Lee. Recent progress in fluoropolymers for membranes. *Prog. Polym. Sci.*, **2014**, *39*, 164. https://doi.org/10.1016/j.progpolymsci.2013.07.008

114. K. D. Kreuer. Ion conducting membranes for fuel cells and other electrochemical devices. *Chem. Mater.*, **2014**, *26*, 361. https://doi.org/10.1021/cm402742u

115. M. G. Dhara, S. Banerjee. Fluorinated high-performance polymers: Poly(arylene ether)s and aromatic polyimides containing trifluoromethyl

Banerjee and Ghanti

Innov. Chem. Mater. Sustain. **2025**, *2*(1), 032-073

groups. *Prog. Polym. Sci.*, **2010**, *35*, 1022. https://doi.org/10.1016/j.progpolymsci.2010.04.003

116. K. H. Lee, J. Y. Chu, A. R. Kim, D. J. Yoo. Facile fabrication and characterization of improved proton conducting sulfonated poly (arylene biphenylether sulfone) blocks containing fluorinated hydrophobic units for proton exchange membrane fuel cell applications. *Polymers*, **2018**, *10*, 1367. https://doi.org/10.3390/polym10121367

117. R. Devanathan. Recent developments in proton exchange membranes for fuel cells. *Energy Environ. Sci.*, **2008**, *1*, 101. https://doi.org/10.1039/b808149m

118. M. Kim, H. Ko, S. Y. Nam, K. Kim. Study on control of polymeric architecture of sulfonated hydrocarbon-based polymers for high-performance polymer electrolyte membranes in fuel cell applications. *Polymers*, **2021**, *13*, 3520. https://doi.org/10.3390/polym13203520

119. S. H. Mirfarsi, M. J. Parnian, S. Rowshanzamir, E. Kjeang. Current status of cross-linking and blending approaches for durability improvement of hydrocarbon-based fuel cell membranes. *Int. J. Hydrogen Energy*, **2022**, *47*, 13460. https://doi.org/10.1016/j.ijhydene.2022.02.077

120. C. H. Park, C. H. Lee, M. D. Guiver, Y. M. Lee. Sulfonated hydrocarbon membranes for medium-temperature and low-humidity proton exchange membrane fuel cells (PEMFCs). *Prog. Polym. Sci.*, **2011**, *36*, 1443. https://doi.org/10.1016/j.progpolymsci.2011.06.001

121. H. Hou, M. L. Di Vona, P. Knauth. Durability of sulfonated aromatic polymers for proton-exchange-membrane fuel cells. *ChemSusChem*, **2011**, *4*, 1526. https://doi.org/1002/cssc.201000415

122. L. Fu, G. Xiao, D. Yan. Sulfonated poly(arylene ether sulfone) s with phosphine oxide moieties: a promising material for proton exchange membranes. *ACS Appl. Mater. Interfaces*, **2010**, *2*, 1601. https://doi.org/10.1021/am1000739

123. J. Miyake, M. Watanabe, K. Miyatake. Sulfonated poly (arylene ether phosphine oxide ketone) block copolymers as oxidatively stable proton conductive membranes. *ACS Appl. Mater. Interfaces*, **2013**, *5*, 5903. https://doi.org/10.1021/am401625j

124. K. Umezawa, T. Oshima, M. Yoshizawa-Fujita, Y. Takeoka, M. Rikukawa. Synthesis of hydrophilic–hydrophobic block copolymer ionomers based on polyphenylenes. *ACS Macro. Lett.*, **2012**, *1*, 969. https://doi.org/10.1021/mz300290x

125. K. Si, R. Wycisk, D. Dong, K. Cooper, M. Rodgers, P. Brooker, D. Slattery, M. Litt. Rigid-rod poly (phenylenesulfonic acid) proton exchange membranes with cross-linkable biphenyl groups for fuel cell applications. *Macromolecules*, **2013**, *46*, 422. https://doi.org/10.1021/ma301875n

126. A. K. Mandal, A. Ghorai, S. Banerjee. Sulphonated polysilsesquioxane–polyimide composite membranes: proton exchange membrane properties. *Bull. Mater. Sci.*, **2020**, *43*, 1. https://doi.org/10.1007/s12034-020-02158-8

127. J. L. Jespersen, E. Schaltz, S. K. Kær. Electrochemical characterization of a polybenzimidazole-based high temperature proton exchange membrane unit cell. *J. Power Sources*, **2009**, *191*, 289. https://doi.org/10.1016/j.jpowsour.2009.02.025

128. J. Yang, H. Jiang, L. Gao, J. Wang, Y. Xu, R. He. Fabrication of crosslinked polybenzimidazole membranes by trifunctional crosslinkers for high temperature proton exchange membrane fuel cells. *Int. J. Hydrogen Energy*, **2018**, *43*, 3299. https://doi.org/10.1016/j.ijhydene.2017.12.141

129. Y. J. Huang, Y. S. Ye, Y. C. Yen, L. D. Tsai, B. J. Hwang, F. C. Chang. Synthesis and characterization of new sulfonated polytriazole proton exchange membrane by click reaction for direct methanol fuel cells (DMFCs). *Int. J. Hydrogen Energy*, **2011**, *36*, 15333. https://doi.org/10.1016/j.ijhydene.2011.08.093

130. S. Saha, S. Banerjee, H. Komber, B. Voit. Flexible diazide based sulfonated polytriazoles and their proton exchange membrane properties. *Macromol. Chem. Phys.*, **2017**, *218*, 1700070. https://doi.org/10.1002/macp.201700070

131. F. Liu, D. M. Knauss. Sulfonated poly (meta-phenylene isophthalamide)s as proton exchange membranes. *J. Polym. Sci. Part A: Polym. Chem.*, **2016**, *54*, 2582. https://doi.org/10.1002/pola.28136

132. Q. Yuan, P. Liu, G. L. Baker. Sulfonated polyimide and PVDF-based blend proton exchange membranes for fuel cell applications. *J. Mater. Chem. A*, **2015**, *3*, 3847. https://doi.org/10.1039/C4TA04910A

133. J. Fang, X. Guo, S. Harada, T. Watari, K. Tanaka, H. Kita, K. I. Okamoto. Novel sulfonated polyimides as polyelectrolytes for fuel cell application. 1. Synthesis, proton conductivity, and water stability of polyimides from 4, 4 '-diaminodiphenyl ether-2, 2'-disulfonic acid. *Macromolecules*, **2002**, *35*, 9022. https://doi.org/10.1021/ma020005b

134. J. M. García, F. C. García, F. Serna, J. L. de la Peña. High-performance aromatic polyamides. *Prog. Polym. Sci.*, **2010**, *35*, 623. https://doi.org/10.1016/j.progpolymsci.2009.09.002

135. P. W. Morgan. Synthesis and properties of aromatic and extended chain polyamides. *Macromolecules*, **1977**, *10*, 1381. https://doi.org/10.1021/ma60060a040

136. C. C. Lin, W. F. Lien, Y. Z. Wang, H. W. Shiu, C. H. Lee. Preparation and performance of sulfonated polyimide/Nafion multilayer membrane for proton exchange membrane fuel cell. *J. Power Sources*, **2012**, *200*, 1. https://doi.org/10.1016/j.jpowsour.2011.10.001

137. A. Ghosh, S. K. Sen, S. Banerjee, B. Voit. Solubility improvements in aromatic polyimides by macromolecular engineering. *RSC advances*, **2012**, *2*, 5900. https://doi.org/10.1039/C2RA20175E

138. S. Maji, S. Banerjee. Synthesis, characterization, and properties of novel fluorine containing aromatic polyamides. *J. Appl. Polym. Sci.*, **2008**, *108*, 1356. https://doi.org/10.1002/app.27831

139. N. Yamazaki, F. Higashi. Studies on reactions of the N-phosphonium salts of pyridines—VII: Preparation of peptides and active esters of amino acids by means of diphenyl and triphenyl phosphites in the presence of tertiary amines. *Tetrahedron*, **1974**, *30*, 1323. https://doi.org/10.1016/S0040-4020(01)97242-4

140. T. S. Jo, C. H. Ozawa, B. R. Eagar, L. V. Brownell, D. Han, C. Bae. Synthesis of sulfonated aromatic poly (ether amide)s and their application to proton exchange membrane fuel cells. *J. Polym. Sci. Part A: Polym. Chem.*, **2009**, *47*, 485. https://doi.org/10.1002/pola.23165

141. H. A. Every, G. J. Janssen, E. F. Sitters, E. Mendes, S. J. Picken. Performance analysis of sulfonated PPTA polymers as potential fuel cell membranes. *J. Power Sources*, **2006**, *162*, 380. https://doi.org/10.1016/j.jpowsour.2006.07.002

142. Y. Pérez-Padilla, M. A. Smit, M. J. Aguilar-Vega. Preparation and characterization of sulfonated copolyamides based on poly (hexafluoroisopropylidene) isophthalamides for polymer electrolytic membranes. *Ind. Eng. Chem. Res.*, **2011**, *50*, 9617. https://doi.org/10.1021/ie102409d

143. Y. Chang, Y. B. Lee, C. Bae. Partially fluorinated sulfonated poly (ether amide) fuel cell membranes: influence of chemical structure on membrane properties. *Polymers*, **2011**, *3*, 222. https://doi.org/10.3390/polym3010222

144. C. Wang, B. Shen, Y. Zhou, C. Xu, W. Chen, X. Zhao, J. Li. Sulfonated aromatic polyamides containing nitrile groups as proton exchange fuel cell membranes. *Int. J. Hydrogen Energy*, **2015**, *40*, 6422. https://doi.org/10.1016/j.ijhydene.2015.03.078

145. R. Sulub-Sulub, M. I. Loría-Bastarrachea, M. O. González-Díaz, M. Aguilar-Vega. Synthesis and characterization of block sulfonated amphiphilic aromatic copolyamides for cation conductive membranes. *Polym. Bull.*, **2023**, *80*, 429. https://doi.org/10.1007/s00289-022-04093-6

146. D. S. Kim, G. P. Robertson, Y. S. Kim, M. D. Guiver. Copoly(arylene ether)s containing pendant sulfonic acid groups as proton exchange membranes. *Macromolecules*, **2009**, *42*, 957. https://doi.org/10.1021/ma802192y

147. R. Mukherjee, S. Banerjee, H. Komber, B. Voit. Highly proton conducting fluorinated sulfonated poly (arylene ether sulfone) copolymers with side chain grafting. *RSC Advances*, **2014**, *4*, 46723. https://doi.org/10.1039/C4RA07291J

148. N. Li, D. W. Shin, D. S. Hwang, Y. M. Lee, M. D. Guiver. Polymer electrolyte membranes derived from new sulfone monomers with pendent sulfonic acid groups. *Macromolecules*, **2010**, *43*, 9810. https://doi.org/10.1021/ma102107a

149. R. N. Johnson, A. G. Farnham, R. A. Clendinning, W. F. Hale, C. N. Merriam. Poly(aryl ethers) by nucleophilic aromatic substitution. I. Synthesis and properties. *J. Polym. Sci. Part A: Polym. Chem.*, **1967**, *5*, 2375. https://doi.org/10.1002/pol.1967.150050916

150. F. Wang, M. Hickner, Q. Ji, W. Harrison, J. Mecham, T. A. Zawodzinski, J. E. McGrath. Synthesis of highly sulfonated poly(arylene ether sulfone) random (statistical) copolymers via direct polymerization. *Macromol. Symp.*, **2001**, *175*, 387. https://doi.org/10.1002/1521-3900(200110)175:1<387::AID-MASY387>3.0.CO;2-1

151. F. Wang, M. Hickner, Y. S. Kim, T. A. Zawodzinski, J. E. McGrath. Direct polymerization of sulfonated poly(arylene ether sulfone) random (statistical) copolymers: candidates for new proton exchange membranes. *J. Membr. Sci.*, **2002**, *197*, 231. https://doi.org/10.1016/S0376-7388(01)00620-2

152. C. Wang, D. W. Shin, S. Y. Lee, N. R. Kang, Y. M. Lee, M. D. Guiver. Poly(arylene ether sulfone) proton exchange membranes with flexible acid side chains. *J. Membr. Sci.*, **2012**, *405*, 68. https://doi.org/10.1016/j.memsci.2012.02.045

153. M. Oroujzadeh, S. Mehdipour-Ataei. Highly fluorinated poly(arylene ether)s containing sulfonated naphthol pendants with improved proton conductivity as a polymer electrolyte for proton exchange membrane fuel cells. *Renew. Energy*, **2025**, *240*, 122298. https://doi.org/10.1016/j.renene.2024.122298

154. L. Meng, M. Ju, J. Xu, X. Chen, P. Zhao, J. Lei, T. Lan, F. Chen, Z. Hu, Z. Wang. Achieving high efficient proton transport in sulfonated poly(arylene ether ketone sulfone)s containing fluorenyl groups by introducing bifunctionalized metal-organic frameworks. *Int. J. Hydrogen Energy*, **2023**, *48*, 40000. https://doi.org/10.1016/j.ijhydene.2023.07.148

155. J. Lei, L. Meng, P. Zhao, J. Wang, T. Lan, J. Xu. A simple strategy for synthesis of side-chain sulfonated poly(arylene ether ketone sulfone) constructing hydrophilic/hydrophobic phase separation structure. *J. Polym. Res.*, **2024**, *31*, 52. https://doi.org/10.1007/s10965-024-03894-9

156. Z. Zhao, D. Liu, J. Zhong, J. Li, Z. Lin, Z. Zhao, J. Pang. Poly(aryl ether sulfone ketone) with densely sulfonated structural units facilitate microphase separation to promote proton transport. *J. Membr. Sci.*, **2024**, *693*, 122319. https://doi.org/10.1016/j.memsci.2023.122319

157. X. Dong, H. Li, J. Xu, X. Wang, S. Wang, Y. Yin, C. L. Song, T. Lan, Z. Wang, Y. W. Yang. Cross-Linking of Bromo-Pillar-[5]-arenes and Sulfonated Poly(Aryl Ether Ketone Sulfone) Enhances Proton Conductivity of Membranes at Low Ion Exchange Capacity. *ACS mater. lett.*, **2024**, *6*, 4962. https://doi.org/10.1021/acsmaterialslett.4c01980

158. Y. Tan, K. Zhang, H. Liao, G. Xiao, Y. Yao, G. Sun, D. Yan. Trisulfonation approach: To improve the properties of poly (arylene thioether

Banerjee and Ghanti

Innov. Chem. Mater. Sustain. **2025**, *2*(1), 032-073

phosphine oxide)s based proton exchange membranes. *J. Membr. Sci.*, **2016**, *508*, 32. https://doi.org/10.1016/j.memsci.2016.02.020

159. C. Allam, K. J. Liu, J. E. McGrath, D. K. Mohanty. Preparation and properties of novel aromatic poly (thioethers) derived from 4, 4′-thiobisbenzenethiol. *Macromol. Chem. Phys.*, **1999**, *200*, 1854. https://doi.org/10.1002/(SICI)1521-3935(19990801)200:8<1854::AID-MACP1854>3.0.CO;2-9

160. S. J. Rodrigues, T. L. Reitz, T. D. Dang, Z. Bai, K. Bardua. Polyarylenethioethersulfone membranes for fuel cells. *J. Electrochem. Soc.*, **2007**, *154*, B960. https://doi.org/10.1149/1.2755881

161. Z. Bai, M. F. Durstock, T. D. Dang. Proton conductivity and properties of sulfonated polyarylenethioether sulfones as proton exchange membranes in fuel cells. *J. Membr. Sci.*, **2006**, *281*, 508. https://doi.org/10.1016/j.memsci.2006.04.021

162. K. B. Wiles, F. Wang, J. E. McGrath. Directly copolymerized poly(arylene sulfide sulfone) disulfonated copolymers for PEM-based fuel cell systems. I. Synthesis and characterization. *J. Polym. Sci. Part A: Polym. Chem.*, **2005**, *43*, 2964. https://doi.org/10.1002/pola.20744

163. X. Ma, L. Shen, C. Zhang, G. Xiao, D. Yan, G. Sun. Sulfonated poly(arylene thioether phosphine oxide)s copolymers for proton exchange membrane fuel cells. *J. Membr. Sci.*, **2008**, *310*, 303. https://doi.org/10.1016/j.memsci.2007.11.003

164. A. Kausar, S. Zulfiqar, M. I. Sarwar. Recent developments in sulfur-containing polymers. *Polym. Rev.*, **2014**, *54*, 185. https://doi.org/10.1080/15583724.2013.863209

165. S. J. Wang, Y. Z. Meng, A. R. Hlil, A. S. Hay. Synthesis and characterization of phthalazinone containing poly(arylene ether)s, poly(arylene thioether)s, and poly(arylene sulfone)s via a novel N− C coupling reaction. *Macromolecules*, **2004**, *37*, 60. https://doi.org/10.1021/ma030246z

166. J. P. Kim, W. Y. Lee, J. W. Kang, S. K. Kwon, J. J. Kim, J. S. Lee. Fluorinated poly (arylene ether sulfide) for polymeric optical waveguide devices. *Macromolecules*, **2001**, *34*, 7817. https://doi.org/10.1021/ma010439r

167. H. S. Chan, S. C. Ng. Synthesis, characterization and applications of thiophene-based functional polymers. *Prog. Polym. Sci.*, **1998**, *23*, 1167. https://doi.org/10.1016/S0079-6700(97)00032-4

168. S. Matsumura, N. Kihara, T. Takata. Properties of a few aromatic poly (thioether ketones) as sulfur-containing high-performance polymers. *J. Appl. Polym. Sci.*, **2004,** *92*, 1869. https://doi.org/10.1002/app.20169

169. Z. Bai, J. A. Shumaker, M. D. Houtz, P. A. Mirau, T. D. Dang. Fluorinated poly(arylenethioethersulfone) copolymers containing pendant sulfonic acid groups for proton exchange membrane materials. *Polymer*, **2009**, *50*, 1463. https://doi.org/10.1016/j.polymer.2009.01.028

170. L. Gui, C. Zhang, S. Kang, N. Tan, G. Xiao, D. Yan. Synthesis and properties of hexafluoroisopropylidene-containing sulfonated poly(arylene thioether phosphine oxide)s for proton exchange membranes. *Int. J. Hydrogen Energy*, **2010**, *35*, 2436. https://doi.org/10.1016/j.ijhydene.2009.12.137

171. J. Hou, S. Liu, X. Sun, Z. Xiao, H. Ding. Preparation and characterization of sulfonated poly (arylene thioether sulfone)/imino-containing phosphorylated silica particle composite proton exchange membranes. *High Perform. Polym.*, **2019**, *31*, 753. https://doi.org/10.1177/0954008318793932

172. D. Liu, H. Liao, N. Tan, G. Xiao, D. Yan. Sulfonated poly(arylene thioether phosphine oxide)/sulfonated benzimidazole blends for proton exchange membranes. *J. Membr. Sci.*, **2011**, *372*, 125. https://doi.org/10.1016/j.memsci.2011.01.057

173. H. Xu, K. Chen, X. Guo, J. Fang, J. Yin. Synthesis of novel sulfonated polybenzimidazole and preparation of cross-linked membranes for fuel cell application. *Polymer*, **2007**, *48*, 5556. https://doi.org/10.1016/j.polymer.2007.07.029

174. N. Tan, Y. Chen, G. Xiao, D. Yan. Synthesis and properties of sulfonated polybenzothiazoles with benzimidazole moieties as proton exchange membranes. *J. Membr. Sci.*, **2010**, *356*, 70. https://doi.org/10.1016/j.memsci.2010.03.028

175. H. Maekawa, K. Nakamura, H. Kudo. Synthesis and properties of highly thermally stable ultrathin films of fluorine-containing hyperbranched polybenzoxazoles. *J. Polym. Sci.*, **2024**, *62*, 1731. https://doi.org/10.1002/pol.20230659

176. R. Bouchet, E. Siebert. Proton conduction in acid doped polybenzimidazole. *Solid State Ion.*, **1999**, *118*, 287. https://doi.org/10.1016/S0167-2738(98)00466-4

177. R. He, Q. Li, G. Xiao, N. J. Bjerrum. Proton conductivity of phosphoric acid doped polybenzimidazole and its composites with inorganic proton conductors. *J. Membr. Sci.*, **2003**, *226*, 169. https://doi.org/10.1016/j.memsci.2003.09.002

178. J. A. Asensio, P. Gómez-Romero. Recent Developments on Proton Conduc-ting Poly (2, 5-benzimidazole)(ABPBI) Membranes for High Temperature Poly-mer Electrolyte Membrane Fuel Cells. *Fuel Cells*, **2005**, *5*, 336. https://doi.org/10.1002/fuce.200400081

179. S. Qing, W. Huang, D. Yan. Synthesis and characterization of thermally stable sulfonated polybenzimidazoles. *Eur. Polym. J.*, **2005**, *41*, 1589. https://doi.org/10.1016/j.eurpolymj.2005.02.001

180. S. Qing, W. Huang, D. Yan. Synthesis and properties of soluble sulfonated polybenzimidazoles. *React. Funct. Polym.*, **2006**, *66*, 219. https://doi.org/10.1016/j.reactfunctpolym.2005.07.020

181. J. A. Asensio, S. Borrós, P. Gómez-Romero. Sulfonated poly (2, 5-benzimidazole)(SABPBI) impregnated with phosphoric acid as proton conducting membranes for polymer electrolyte fuel cells. *Electrochim. Acta*, **2004**, *49*, 4461. https://doi.org/10.1016/j.electacta.2004.05.002

182. M. J. Ariza, D. J. Jones, J. Rozière. Role of post-sulfonation thermal treatment in conducting and thermal properties of sulfuric acid sulfonated poly(benzimidazole) membranes. *Desalination*, **2002**, *147*, 183. https://doi.org/10.1016/S0011-9164(02)00532-5

183. P. Staiti, F. Lufrano, A. S. Arico, E. Passalacqua, V. Antonucci. Sulfonated polybenzimidazole membranes—preparation and physico-chemical characterization. *J. Membr. Sci.*, **2001**, *188*, 71. https://doi.org/10.1016/S0376-7388(01)00359-3

184. X. Glipa, M. El Haddad, D. J. Jones, J. Rozière. Synthesis and characterisation of sulfonated polybenzimidazole: a highly conducting proton exchange polymer. *Solid State Ion.*, **1997**, *97*, 323. https://doi.org/10.1016/S0167-2738(97)00032-5

185. S. Kang, C. Zhang, G. Xiao, D. Yan, G. Sun. Synthesis and properties of soluble sulfonated polybenzimidazoles from 3, 3′-disulfonate-4, 4′-dicarboxylbiphenyl as proton exchange membranes. *J. Membr. Sci.*, **2009**, *334*, 91. https://doi.org/10.1016/j.memsci.2009.02.021

186. G. Wang, S. Yang, B. Y. Hua, M. X. Lu, J. Q. Kang, W. S. Tang, H. L. Wei, X. X. Liu, L. F. Cui, X. D. Chen. Soluble sulfonated polybenzimidazoles containing phosphine oxide units as proton exchange membranes. *New J. Chem.*, **2023**, *47*, 10613. https://doi.org/10.1039/d3nj00796k

187. N. Tan, G. Xiao, D. Yan, G. Su. Preparation and properties of polybenzimidazoles with sulfophenylsulfonyl pendant groups for proton exchange membranes. *J. Membr. Sci.*, **2010**, *353*, 51. https://doi.org/10.1016/j.memsci.2010.02.029

188. S. Mukhopadhyay, A. Das, T. Jana, S. K. Das. Fabricating a MOF material with polybenzimidazole into an efficient proton exchange membrane. *ACS Appl. Energy Mater.*, **2020**, *3*, 7964. https://doi.org/10.1021/acsaem.0c01322

189. Y. Wang, P. Sun, Z. Xia, Z. Li, H. Ding, Z. Fan, H. Guo. Anchoring highly sulfonated hyperbranched PBI onto oPBI: fast proton conduction with low leaching. *ACS Appl. Energy Mater.*, **2022**, *5*, 10802. https://doi.org/10.1021/acsaem.2c01491

190. S. Banerjee, M. K. Madhra, A. K. Salunke, G. Maier. Synthesis and properties of fluorinated polyimides. 1. Derived from novel 4, 4 ″-bis (aminophenoxy)-3, 3 ″-trifluoromethyl terphenyl. *J. Polym. Sci. Part A: Polym. Chem.*, **2002**, *40*, 1016. https://doi.org/10.1002/pola.10189

191. M. K. Madhra, A. K. Salunke, S. Banerjee, S. Prabha. Synthesis and properties of fluorinated polyimides, 2. Derived from novel 2,6-bis(3′-trifluoromethyl-p-aminobiphenyl ether)pyridine and 2,5-bis (3′-trifluoromethyl-p-aminobiphenyl ether) thiophene. *Macromol. Chem. Phys.*, **2002**, *203*, 1238. https://doi.org/10.1002/1521-3935(200206)203:9<1238::AID-MACP1238>3.0.CO;2-R

192. E. A. Mistri, A. K. Mohanty, S. Banerjee, H. Komber, B. Voit. Naphthalene dianhydride based semifluorinated sulfonated copoly (ether imide)s: Synthesis, characterization and proton exchange properties. *J. Membr. Sci.*, **2013**, *441*, 168. https://doi.org/10.1016/j.memsci.2013.03.015

193. S. K. Sen, S. Banerjee. Gas transport properties of fluorinated poly (ether imide) films containing phthalimidine moiety in the main chain. *J. Membr. Sci.*, **2010**, *350*, 53. https://doi.org/10.1016/j.memsci.2009.12.011

194. B. Dasgupta, S. K. Sen, S. Banerjee. Aminoethylaminopropylisobutyl POSS—Polyimide nanocomposite membranes and their gas transport properties. *Mater. Sci. Eng. B*, **2010**, *168*, 30. https://doi.org/10.1016/j.mseb.2009.10.006

195. V. Kute, S. Banerjee. Novel semi-fluorinated poly (ether imide) s derived from 4-(p-aminophenoxy)-3-trifluoromethyl-4′-aminobiphenyl. *Macromol. Chem. Phys.*, **2003**, *204*, 2105. https://doi.org/10.1002/macp.200350070

196. M. Ding. Isomeric polyimides. *Prog. Polym. Sci.*, **2007**, *32*, 623. https://doi.org/10.1016/j.progpolymsci.2007.01.007

197. K. Xie, J. G. Liu, H. W. Zhou, S. Y. Zhang, M. H. He, S. Y. Yang. Soluble fluoro-polyimides derived from 1,3-bis(4-amino-2-trifluoromethyl-phenoxy)benzene and dianhydrides. *Polymer*, **2001**, *42*, 7267. https://doi.org/10.1016/S0032-3861(01)00138-0

198. A. Ganeshkumar, D. Bera, E. A. Mistri, S. Banerjee. Triphenyl amine containing sulfonated aromatic polyimide proton exchange membranes. *Eur. Polym. J.*, **2014**, *60*, 235. https://doi.org/10.1016/j.eurpolymj.2014.09.009

199. A. K. Mandal, S. Bisoi, S. Banerjee, H. Komber, B. Voit. Sulfonated copolyimides containing trifluoromethyl and phosphine oxide moieties: synergistic effect towards proton exchange membrane properties. *Eur. Polym. J.*, **2017**, *95*, 581. https://doi.org/10.1016/j.eurpolymj.2017.08.050

200. A. G. Kumar, D. Bera, S. Banerjee, R. Veerubhotla, D. Das. Sulfonated poly(ether imide) with fluorenyl and trifluoromethyl groups: Application in microbial fuel cell (MFC). *Eur. Polym. J.*, **2016**, *83*, 114. https://doi.org/10.1016/j.eurpolymj.2016.08.009

201. C. Gao, J. Chen, B. Zhang, L. Wang. Effect of chemical structure and degree of branching on the stability of proton exchange membranes based on sulfonated polynaphthylimides. *Polymers*, **2020**, *12*, 652. https://doi.org/10.3390/polym12030652

Banerjee and Ghanti

Innov. Chem. Mater. Sustain. **2025**, *2*(1), 032-073

202. T. Rohilla, A. Husain, N. Singh, D. K. Mahajan. Atomistic simulation and synthesis of novel sulfonated Polyimide polymer electrolyte membranes with facile proton transport. *Chem. Eng. J.*, **2023**, *474*, 145727. https://doi.org/10.1016/j.cej.2023.145727

203. J. Yang, Y. Guo, L. Liu, L. Guo, Z. Sun, C. Wang. Preparation of proton exchange membrane with intrinsic micropores constructing efficient ion transport channels based on segmented copolymer (sulfonated polyimide). *J. Energy Storage*, **2023**, *72*, 108407. https://doi.org/10.1016/j.est.2023.108407

204. X. Wang, S. Zhao, S. Wang, X. Hou, J. Yang, C. Liang, Y. Zhao, L. Wang, C. Shen, N. Gao, L. Jia. Facile preparation of high-performance sulfonated polyimide proton exchange membrane by doping nano carbon sulfonic acid. *J. Membr. Sci.*, **2025**, *717*, 123605. https://doi.org/10.1016/j.memsci.2024.123605

205. E. J. Park, P. Jannasch, K. Miyatake, C. Bae, K. Noonan, C. Fujimoto, S. Holdcrof, J. R. Varcoe, D. Henkensmeier, M. D. Guiver, Y. S. Kim. Aryl ether-free polymer electrolytes for electrochemical and energy devices. *Chem. Soc. Rev.*, **2024**, *53*, 5704. https://doi.org/10.1039/D3CS00186E

206. G. A. Olah. Superelectrophiles. *Angew. Chem., Int. Ed. Engl.*, **1993**, *32*, 767. https://doi.org/10.1002/anie.199307673

207. G. A. Olah, G. Rasul, C. York, G. S. Prakash. Superacid-catalyzed condensation of benzaldehyde with benzene. Study of protonated benzaldehydes and the role of superelectrophilic activation. *J. Am. Chem. Soc.*, **1995**, *117*, 11211. https://doi.org/10.1021/ja00150a018

208. O. Hernández-Cruz, M. G. Zolotukhin, S. Fomine, L. Alexandrova, C. Aguilar-Lugo, F. A. Ruiz-Treviño, G. Ramos-Ortíz, J. L. Maldonado, G. Cadenas-Pliego. High-Tg functional aromatic polymers. *Macromolecules*, **2015**, *48*, 1026. https://doi.org/10.1021/ma502288d

209. M. K. Pagels, S. Adhikari, R. C. Walgama, A. Singh, J. Han, D. Shin, C. Bae. One-pot synthesis of proton exchange membranes from anion exchange membrane precursors. *ACS Macro Lett.*, **2020**, *9*, 1489. https://doi.org/10.1021/acsmacrolett.0c00550

210. M. R. Hibbs, C. H. Fujimoto, C. J. Cornelius. Synthesis and characterization of poly (phenylene)-based anion exchange membranes for alkaline fuel cells. *Macromolecules*, **2009**, *42*, 8316. https://doi.org/10.1021/ma901538c

211. J. Ahn, R. Shimizu, K. Miyatake. Sulfonated aromatic polymers containing hexafluoroisopropylidene groups: a simple but effective structure for fuel cell membranes. *J. Mater. Chem. A*, **2018**, *6*, 24625. https://doi.org/10.1039/C8TA09587F

212. Q. Wang, L. Sang, L. Huang, J. Guan, H. Yu, J. Zheng, Q. Zhang, G. Qin, S. Li, S. Zhang. Design and synthesis of comb-like bisulfonic acid proton exchange membrane with regulated microstructure. *Adv. Funct. Mater.*, **2024**, *34*, 2316506. https://doi.org/10.1002/adfm.202316506

213. C. Ba, S. Xu, C. G. Arges, J. H. Park, J. Park, M. Urgun-Demirtas. Design of non-fluorinated proton exchange membranes from Poly(Terphenyl fluorenyl isatin) with fluorene-linked sulfonate groups and microblock structures. *J. Membr. Sci.*, **2025**, *717*, 123551. https://doi.org/10.1016/j.memsci.2024.123551

214. T. Ryu, H. Jang, F. Ahmed, N. S. Lopa, H. Yang, S. Yoon, I. Choi, W. Kim. Synthesis and characterization of polymer electrolyte membrane containing methylisatin moiety by polyhydroalkylation for fuel cell. *Int. J. Hydrogen Energy*, **2018**, *43*, 5398. https://doi.org/10.1016/j.ijhydene.2017.12.164

215. H. Nederstedt, P. Jannasch. Poly(p-terphenyl alkylene)s grafted with highly acidic sulfonated polypentafluorostyrene side chains for proton exchange membranes. *J. Membr. Sci.*, **2022**, *647*, 120270. https://doi.org/10.1016/j.memsci.2022.120270

216. X. Yan, H. Zhang, Z. Hu, L. Li, L. Hu, Z. A. Li, L. Gao, Y. Dai, X. Jian, G. He. Amphoteric-side-chain-functionalized "ether-free" poly(arylene piperidinium) membrane for advanced redox flow battery. *ACS Appl. Mater. Interfaces*, **2019**, *11*, 44315. https://doi.org/10.1021/acsami.9b15872

217. H. Bai, H. Peng, Y. Xiang, J. Zhang, H. Wang, S. Lu, L. Zhuang. Poly(arylene piperidine)s with phosphoric acid doping as high temperature polymer electrolyte membrane for durable, high-performance fuel cells. *J. Power Sources*, **2019**, *443*, 227219. https://doi.org/10.1016/j.jpowsour.2019.227219

218. J. Guan, X. Sun, H. Yu, J. Zheng, Y. Sun, S. Li, G. Qin, S. Zhang. High conductive and dimensional stability proton exchange membranes with an all-carbon main chain and densely sulfonated structure. *J. Membr. Sci.*, **2024**, *700*, 122664. https://doi.org/10.1016/j.memsci.2024.122664

219. W. Li, R. Zhang, X. Zhao, Z. Yue, H. Qian, H. Yang. Highly proton conductive and stable sulfonated poly(arylene-alkane) for fuel cells with performance over 2.46 W cm^{-2}. *J. Mater. Chem. A*, **2023**, *11*, 4547. https://doi.org/10.1039/D2TA08911D

220. N. R. Kang, T. H. Pham, P. Jannasch. Polyaromatic perfluorophenylsulfonic acids with high radical resistance and proton conductivity. *ACS Macro Lett.*, **2019**, *8*, 1247. https://doi.org/10.1021/acsmacrolett.9b00615

221. Y. Liang, Z. Liu, K. Lin, W. Yin, Y. Zhu. High-performance poly(m-terphenyl fluorenyl)s containing long flexible side chains with dual 1,2,3-triazole and disulfonated units for proton exchange membranes. *J. Membr. Sci.*, **2025**, *718*, 123691. https://doi.org/10.1016/j.memsci.2025.123691

222. B. Xue, M. Z. Zhu, S. Q. Fu, P. P. Huang, H. Qian, P. N. Liu. Facile synthesis of sulfonated poly (phenyl-alkane) s for proton exchange membrane fuel cells. *J. Membr. Sci.*, **2023**, *673*, 121263. https://doi.org/10.1016/j.memsci.2022.121263

223. R. X. Yao, L. Kong, Z. S. Yin, F. L. Qing. Synthesis of novel aromatic ether polymers containing perfluorocyclobutyl and triazole units via click chemistry. *J. Fluor. Chem.*, **2008**, *129*, 1003. https://doi.org/10.1016/j.jfluchem.2008.04.012

224. G. Qiu, P. Nava, A. Martinez, C. Colomban. A tris(benzyltriazolemethyl)amine-based cage as a CuAAC ligand tolerant to exogenous bulky nucleophiles. *Chem. Commun.*, **2021**, *57*, 2281. https://doi.org/10.1039/D0CC08005E

225. M. C. Floros, J. F. Bortolatto, Jr O. B. Oliveira, S. L. Salvador, S. S. Narine. Antimicrobial activity of amphiphilic triazole-linked polymers derived from renewable sources. *ACS Biomater. Sci. Eng.*, **2016**, *2*, 336. https://doi.org/10.1021/acsbiomaterials.5b00412

226. X. Wang, X. Zhang, Y. Wang, S. Ding. IrAAC-based construction of dual sequence-defined polytriazoles. *Polym. Chem.*, **2021**, *12*, 3825. https://doi.org/10.1039/D1PY00718A

227. D. Huang, Y. Liu, A. Qin, B. Z. Tang. Nickel-Catalyzed Azide–Alkyne Click Polymerization toward 1, 5-Regioregular Polytriazoles. *Macromolecules*, **2023**, *56*, 10092. https://doi.org/10.1021/acs.macromol.3c02000

228. M. Li, X. Duan, Y. Jiang, X. Sun, X. Xu, Y. Zheng, W. Song, N. Zheng. Multicomponent polymerization of azides, alkynes, and electrophiles toward 1,4,5-trisubstituted polytriazoles. *Macromolecules*, **2022**, *55*, 7240. https://doi.org/10.1021/acs.macromol.2c00966

229. V. V. Rostovtsev, L. G. Green, V. V. Fokin, K. B. Sharpless. A stepwise huisgen cycloaddition process: copper (I)-catalyzed regioselective "ligation" of azides and terminal alkynes. *Angew. Chem., Int. Ed.*, **2002**, *41*, 2596. https://doi.org/10.1002/1521-3773(20020715)41:14<2596::AID-ANIE2596>3.0.CO;2-4

230. A. Ghosh, S. Banerjee. Sulfonated fluorinated-aromatic polymers as proton exchange membranes. *e-Polymers*, **2014**, *14*, 227. https://doi.org/10.1515/epoly-2014-0049

231. A. Ghorai, S. Roy, S. Das, H. Komber, M. M. Ghangrekar, B. Voit, S. Banerjee. Preparation of sulfonated polytriazoles with a phosphaphenanthrene unit via click polymerization: fabrication of membranes and properties thereof. *ACS Appl. Polym. Mater.*, **2021**, *3*, 4127. https://doi.org/10.1021/acsapm.1c00600

232. A. Ghorai, A. K. Mandal, S. Banerjee. Synthesis and characterization of new phosphorus containing sulfonated polytriazoles for proton exchange membrane application. *J. Polym. Sci.*, **2020**, *58*, 263. https://doi.org/10.1002/pol.20190030

233. A. Ghorai, S. Banerjee. Phosphorus-Containing Fluoro-Sulfonated Polytriazole Membranes with High Proton Conductivity: Understanding Microstructural and Thermomechanical Behaviors as a Function of Degree of Sulfonation. *Macromol. Chem. Phys.*, **2023**, *224*, 2200031. https://doi.org/10.1002/macp.202200031

234. R. Kamble, B. Ghanti, D. Pradhan, S. Banerjee. Fabrication of a High Proton-Conducting Sulfonated Fe-Metal Organic Framework-Polytriazole Composite Membranes: Study of Proton Exchange Membrane Properties. *Macromol. Rapid Commun.*, **2025**, 2401026. https://doi.org/10.1002/marc.202401026

235. A. Abdolmaleki, M. Zhiani, M. Maleki, S. Borandeh, K. Firouz. Preparation and evaluation of sulfonated polyoxadiazole membrane containing phenol moiety for PEMFC application. *Polymer*, **2015**, *75*, 17. https://doi.org/10.1016/j.polymer.2015.08.021

236. D. Zhao, J. Li, M. K. Song, B. Yi, H. Zhang, M. Liu. A durable alternative for proton-exchange membranes: Sulfonated poly(benzoxazole thioether sulfone)s. *Adv. Energy Mater.*, **2011**, *1*, 203. https://doi.org/10.1002/aenm.201000062

237. Z. Zhang, L. Wu, T. Xu. Synthesis and properties of side-chain-type sulfonated poly (phenylene oxide) for proton exchange membranes. *J. Membr. Sci.*, **2011**, *373*, 160. https://doi.org/10.1016/j.memsci.2011.03.002

238. G. Wang, S. Yang, N. Y. Kang, B. Hua, M. Lu, H. Wei, J. Kang, W. Tang, Y. M. Lee. Sulfonated polybenzothiazoles containing hexafluoroisopropyl units for proton exchange membrane fuel cells. *Macromolecules*, **2023**, *56*, 5546. https://doi.org/10.1021/acs.macromol.3c00301

239. G. Chao, Z. Zhang, Z. Lv, E. Yang, R. Gao, Q. Ju, H. Gao, C. Niu, H. Qian, K. Geng, N. Li. Copolymerized sulfonated poly (oxindole biphenylene) polymer electrolyte for proton exchange membrane fuel cells. *J. Membr. Sci.*, **2024**, *700*, 122674. https://doi.org/10.1016/j.memsci.2024.122674

240. K. F. Tadavani, A. Abdolmaleki, M. R. Molavian, S. Borandeh, E. Sorvand, M. Zhiani. Synergistic behavior of phosphonated and sulfonated groups on proton conductivity and their performance for high-temperature proton exchange membrane fuel cells (PEMFCs). *Energy Fuels*, **2017**, *31*, 11460. https://doi.org/10.1021/acs.energyfuels.7b01065

241. N. Y. Abu-Thabit, S. A. Ali, S. J. Zaidi, K. Mezghani. Novel sulfonated poly (ether ketone)/phosphonated polysulfone polymer blends for proton conducting membranes. *J. Mater. Res.*, **2012**, *27*, 1958. https://doi.org/10.1557/jmr.2012.145

242. B. Xue, S. Zhou, J. Yao, F. Wang, J. Zheng, S. Li, S. Zhang. Novel proton exchange membranes based on sulfonated-phosphonated poly(p-phenylene-co-aryl ether ketone) terpolymers with microblock structures for passive direct methanol fuel cells. *J. Membr. Sci.*, **2020**, *594*, 117466. https://doi.org/10.1016/j.memsci.2019.117466